A tale of six diatoms: an insight into the taxonomy of Arctic diatoms from different sea-ice communities and their physiological response to climate change

Simon Hasselø Kline

Thesis submitted for the degree of Master in Biosciences (Marine Biology and Limnology)
60 credits

Department of Biosciences
Section for Aquatic Biology and Toxicology
University of Oslo
September 2021

Simon Hasselø Kline
Simonhkline@hotmail.com
+47 95451199

Supervisors

Luka Supraha
Department of Biosciences, UiO/Norwegian Institute of Water Research
Luka.supraha@ibv.uio.no

Bente Edvardsen
Department of Biosciences, UiO
Bente.edvardsen@ibv.uio.no

Tom Andersen
Department of Biosciences, UiO
Tom.andersen@ibv.uio.no

This thesis is affiliated with the Nansen Legacy (Arven etter Nansen) research project, a collaboration between ten Norwegian research institutes aimed at gathering new knowledge on the Barents Sea and Arctic Basin as they undergo rapid changes. The University of Oslo is one of the participating institutes.

A tale of six diatoms: an insight into the taxonomy of Arctic diatoms from different sea-ice communities and their physiological response to climate change

http://www.duo.uio.no

Printed: Reprosentralen, University of Oslo

A tale of six diatoms: an insight into the taxonomy of Arctic diatoms from different sea-ice communities and their physiological response to climate change

Simon Hasselø Kline

UiO : University of Oslo

the Nansen LEGACY

Abstract

As a result of anthropogenic climate change, the Arctic region is warming at a much higher rate than the global average. One of the most pronounced and visible effects of this warming is on the dramatic decrease in Arctic sea-ice cover. While the effects of climate change on Arctic sea-ice and the Arctic region as a whole are well documented, the impacts on sea-ice algal communities, where diatoms dominate, remain understudied. As primary producers, sea-ice algae and phytoplankton in the Arctic form the basis of the food-chain, and any change in these communities could have cascading effects on the entire Arctic ecosystem.

In this thesis, I have examined the taxonomy (biodiversity) and physiology of six strains of Arctic diatom species (*Chaetoceros gelidus, Thalassiosira gravida, Nitzschia frigida, Synedropsis hyperborea, Nitzschia laevissima, and Nitzschia* sp.) from various sea-ice associated communities (surface, interior, and phytoplankton). My results have allowed me to answer two general questions about Arctic sea-ice diatom communities: what species are present and how will they respond to climate change?

I have isolated, amplified, and sequenced the variable D1 and D2 domain regions of the 28S rRNA gene. I used the obtained sequences to search the NCBI reference database using the BLAST tool and to create a maximum likelihood phylogenetic tree along with various reference sequences to check for phylogenetic relationships between the studied strains. I found that a lack of reference sequences available in genetic databases hinders our understanding of the genetic diversity found in these communities. I argue that the D1 and D2 domain regions of the 28S rRNA gene do not provide sufficient information to determine all species of Arctic diatoms, and that future studies should use multigene sequencing or genes with more variable and species-specific regions to explore the diversity of these diatom communities.

I examined morphological traits using light- and electron microscopy and described a potentially new species from the *Nitzschia* genus isolated from a melt pond. The phylogenetic analysis points to this species being closely related to *Nitzschia frigida*, but my morphological description shows that these species have distinctly different morphology. While the use of microscopy is a valuable tool in taxonomic characterizations of diatoms, I recommend that a closer examination into various adaptive traits such as the production of photoprotective molecules and ice-binding proteins, is necessary to gain an overview of how Arctic diatoms are adapted to their sea-ice communities.

I conducted two multistressor high-throughput growth experiments, testing various conditions of salinity, temperature, and light intensity on the growth rate of the diatom strains. I found temperature to be the dominating factor influencing the growth of Arctic diatoms, with all strains exhibiting a growth optimum between 4°C and 6°C, and higher temperatures negatively impacting the growth rates of sympagic (ice-associated) strains more than the planktonic strains. The species isolated from the plankton community, *Chaetoceros gelidus* and *Thalassiosira gravida*, exhibited the widest thermal tolerance, growing at temperatures up to 11°C and 15°C, respectively. This suggests that future warming of the Arctic and ice-free conditions may be conducive to phytoplankton growth.

Acknowledgements

I never anticipated that I would need to write my master's thesis in the middle of a global pandemic. While that experience has at times been stressful and wearing, I am thankful that both myself and those closest to me have escaped the worst effects of COVID, having stayed healthy and safe.

This thesis would not have been possible without algae. Both because they are vital to oxygen-requiring organisms such as ourselves, but also because there remains so much yet to discover when it comes to their diversity, their evolutionary history, and their ecological roles. To me, algae are fascinating and mysterious, and the more I learn about them, the more curious I become. My interest in algae is very much due to the lectures by Stein Fredriksen, Wenche Eikrem and Bente Edvardsen in the biodiversity course I had during my bachelor's degree. Their fascination of algae was infectious, and when it came time to choose which topic I wanted for my master's thesis, I had no doubt that I wanted to write about algae.

Thank you to my supervisors, Luka Supraha, Bente Edvardsen, and Tom Andersen. My experience as a master's student would not have been the same without them. They guided me in all the practical and theoretical aspects associated with designing and executing this thesis and supported me continuously throughout the last two years, for which I am deeply grateful. Their passion and hard work as scientists have inspired me to push myself and think critically around this thesis, and I could not have had better supervisors. Thank you especially to Bente and Luka for giving me the opportunity to go on two Arven etter Nansen research cruises to the Arctic. I feel enormously privileged that you both placed that level of trust in me, and my experiences on those cruises have been defining in my wish to continue a career in Arctic research. An additional thank you to Antje Hofgaard, Karoline Saubrekka, and Jan Heuschele for all the help they have provided me in the making of this thesis.

Thank you to my family: Mamma, Pappa, Stian, Dadda, Thea, Olivia, Tante Tina, Uncle Mike, Patrick, and Lyn. The constant support, affection, and encouragement I have gotten from them since my childhood to be curious and appreciative of my surroundings, has shaped me well into my adult life. Og tusen takk til deg Bestemor, for at du har støttet og elsket meg som bare en bestemor kan. Det er ingen som deg og for det er jeg ubeskrivelig takknemlig! Thank you to my friends for supporting and motivating me (especially my office buddies, Jessica and Ida-Camilla).

Thank you to my partner, and best friend, Anette. Thank you for always challenging me when I'm wrong and indulging me when I'm right. I am beyond grateful to have you with me for this ride and the ones to come. Your intelligence and humility keep me grounded and inspired, and there is no one I would rather explore and discover the world with than you.

This thesis marks an end to the last five years I have spent at the University of Oslo as a student. I can't wait to see what the next chapter of my life will bring.

Preface

My first introduction to the Arctic came when I was a child reading a book recounting Roald Amundsen's diary from his Gjøa expedition in the early 20th century. The book provided pictures and excerpts, describing the first expedition to fully explore the Northwest Passage, the route through the Arctic connecting the Atlantic and Pacific Oceans. I remember Amundsen's words, and the image that they painted for me at a young age. To me, the Arctic became a resilient, mystical place, full of ice and snow, harsh and impervious to change. At the time of the Gjøa expedition, the Arctic was considered enduring, immutable, and unmapped. As I later in life became a biologist, I began to understand that while the Arctic ecosystem is defined by extreme conditions, it is dynamic, and it is vulnerable. Even though the Arctic still has many inaccessible areas in need of further study, we now recognize that it is an exposed region, susceptible to change. The sea-ice in the Arctic is quickly disappearing, and it is possible that the entire region will become unrecognizable within the lifetime of the current generation.

Science is a communal effort, and my hope is that this thesis builds upon the work done by the polar researchers that came before me, and maybe plays a small role in laying the foundation for the ones yet to come.

TERMINOLOGY

Annulus
Hyaline ring on the interior of valves found in some centric diatoms and the silica first formed during valve formation.

Araphid
Pennate diatoms lacking a raphe system.

Areolae
Pores that can be found on the valves of diatoms.

Central nodule
The heavily silicified region found between the raphe ends in raphid diatoms.

Costae
Elongated thickening of a diatom valve.

Cribrum
Type of velum that has pores.

Epiphytic
Organisms that grow on the surface of plants or algae.

Fibulae
Internal structures of silica in the valve that support the raphe canal.

Frustule
The silicified cell wall found in diatoms.

Fultoportula (Strutted Process)
Tubular processes passing through the valve.

Girdle (Cingulum)
The silicified bands that attach the two diatom valves.

Halocline
Boundary between two water masses created by a density gradient due to salinity differences.

Helictoglossa
Terminal end of a raphe, often in the shape of lips when viewed internally.

High-throughput
Technique that allows multiple experiments to run simultaneously.

Hyaline
Area of a diatom valve that is unornamented, lacking pores or other structures.

TERMINOLOGY

Keel
The thickened silica that contains and elevates the raphe within the raphe canal system, found in raphid diatoms.

Multistressor
Technique that tests multiple parameters and interactions.

Proximal Raphe
The portion of the raphe near the central nodule.

Pycnocline
Boundary between two water masses created by a density gradient. Includes the halocline.

Sympagic
Ice-associated organisms.

Raphe
Structure in many pennate diatoms, often raised in a canal system and aids in movement.

Raphid
Pennate diatoms with a raphe system.

Rimoportula (Labiate Process)
Tubular process found in some diatoms that penetrates the valve and can have the shape of lips when viewed internally.

Rostrate
A beak-like cell shape found in some diatoms.

Setae
Spine-like extensions of the diatom valve, found in *Chaetoceros* species.

Sigmoid
An S-like cell shape found in some diatoms.

Stellate
Colonies that are formed in the shape of a star.

Sternum
The thickened silicified region first developed in pennate diatoms during valve formation.

Stria
Row of areolae on diatom valves.

Velum
Thin layer of silica that can cover areolae.

Table of Contents

1. Introduction

1.1 The Arctic

While a common definition of the Arctic is the polar region north of the Arctic circle at approximately 66° North Latitude (Doel et al., 2014), it is more often defined in scientific literature by its climatic conditions. This includes a summer isotherm, where the Arctic is determined to be the region where the average temperature for its warmest month is below 10°C (Weller, 2019). The differences between the two definitions can be seen in Figure 1, but for the remainder of this study, the presence of a July isotherm will be the definition used when referring to the Arctic region. This region is defined by extreme contrasts in seasons and photoperiods. During the winter months, the sun remains permanently below the horizon, while during the summer months the sun remains permanently above the horizon (Hawley et al., 2017).

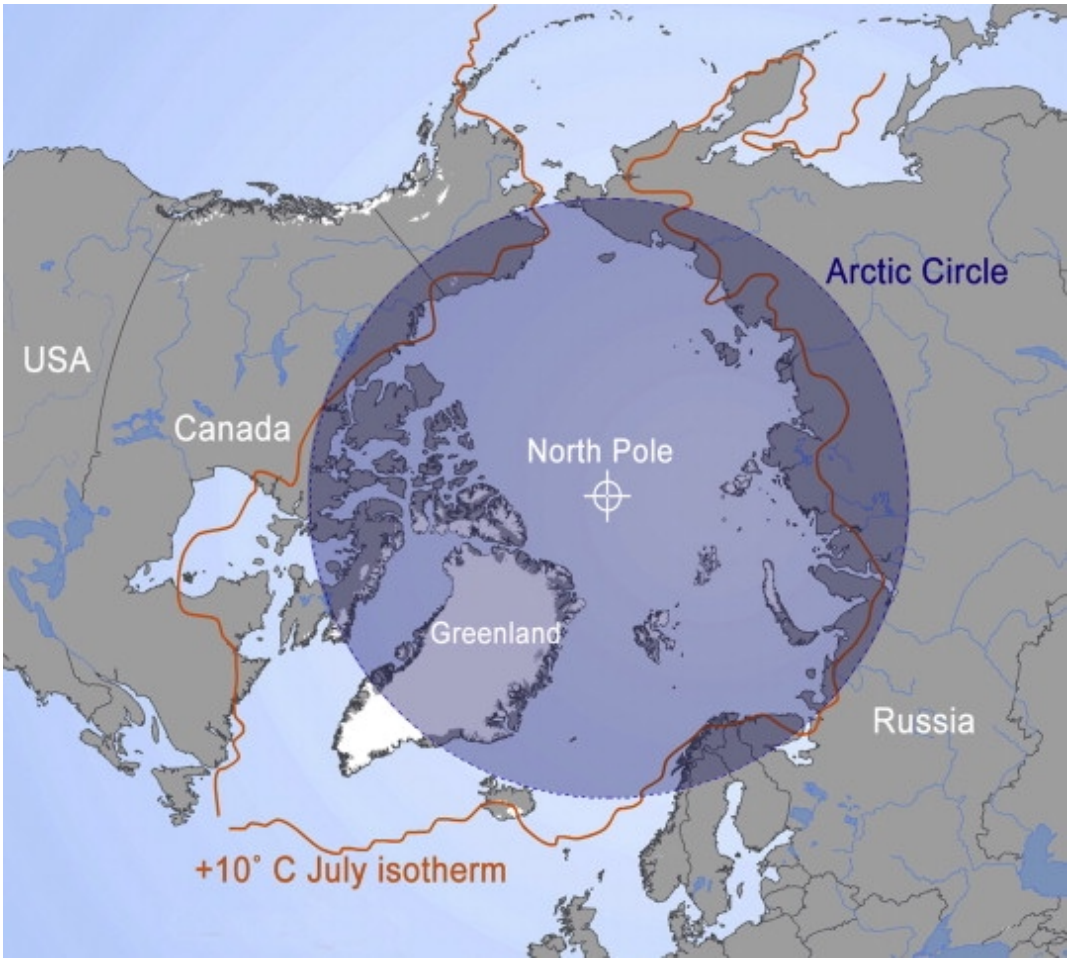

Figure 1: *Common definitions of the Arctic region include the area north of the Arctic circle at approximately 66° North Latitude (visualized in the figure as the shaded region) or as the region with a 10°C July isotherm (visualized in the figure as the region within the jagged red line). Figure from Doel et al. (2014).*

INTRODUCTION

While the Arctic Ocean occupies much of the Arctic region, encompassing ~14 million km^2, it is the smallest ocean on Earth (von Friesen & Riemann, 2020). It is a shallow ocean with an average depth of 1201 meters (Jakobsson, 2002), connected both to the Atlantic and the Pacific Ocean. The exchange of water between the Arctic and Atlantic Ocean especially is vital in maintaining the global thermohaline circulation (Eldevik & Nilsen, 2013), which in turn has dramatic effects on global climate systems.

The Arctic Ocean consists of approximately three layers of water masses: cold polar surface water, warm intermediate water originating from the Atlantic Ocean, and deep bottom water (Shu et al., 2019). The pycnocline (the boundary created due to density differences) between the cold surface water and the warm intermediate layer is driven by shifts in both salinity and temperature (Melling & Lewis, 1982; Fer, 2009).

The Arctic sea-ice is one of the most defining characteristics of the region, and its composition, its presence, and its abundance throughout the seasons and over time, have dramatic consequences on the Arctic ecosystem as well as the global climate (Smith et al., 2003). The development of sea-ice on the continental shelves is one of the main forces behind the formation and preservation of the Arctic pycnocline. During the fall and winter months, as seawater on the continental shelves freezes and sea-ice is formed, cold and highly saline water is produced and transported to the central Arctic Ocean (Figure 2) (Aagaard et al., 1981). During the spring and summer months, the sea-ice begins to melt, ensuring that the sea surface temperature is close to zero (Rudels et al., 1991) and that the pycnocline is maintained throughout the year.

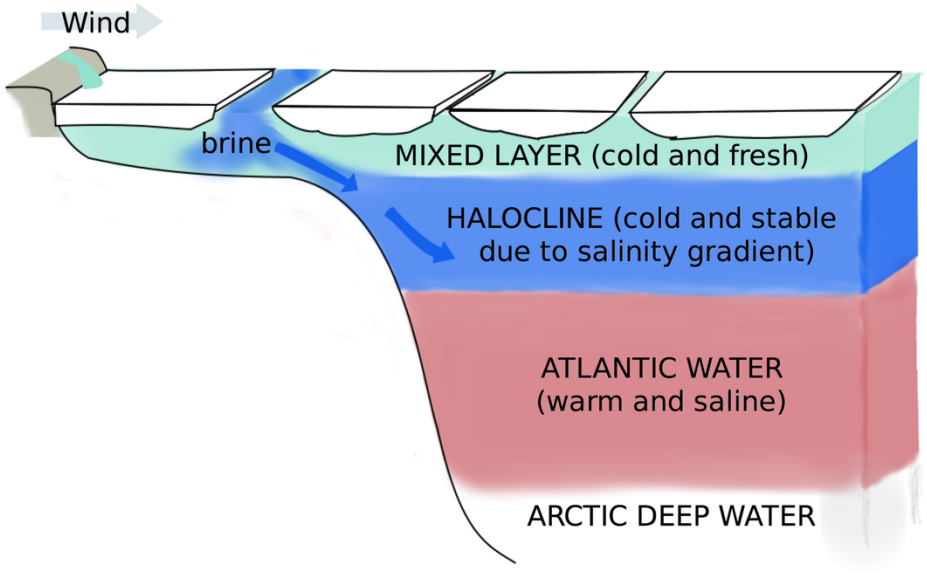

Figure 2: *In the process of freezing during the winter, the salt in seawater is released as brine, which due to a higher density sinks and creates the halocline above the Atlantic water mid layer. The ice created at the continental shelves is transported by wind towards the central Arctic Ocean. Figure from Metzner et al. (2020).*

Typically, Arctic sea-ice reaches its seasonal maximum extent in March and its seasonal minimum extent in September (Petty et al., 2018). The sea-ice can roughly be divided into two zones: the perennial ice zone, where there is ice cover during the entire year, and the seasonal ice zone, where there is ice cover depending on the season. While much of the perennial ice zone is composed of multiyear ice which has survived more than one melt season, the seasonal ice cover is mainly composed of first year ice (Comiso, 2012).

1.2 The loss of sea-ice

As a result of human driven climate change, the Arctic region is underdoing dramatic change at a much more rapid pace than any other environment on the planet. This includes changes to the hydrological cycle, shifting animal distributions, increased runoff and discharge from land, and higher air surface temperatures (Box et al., 2019). This is coupled with consequential changes in the Arctic sea-ice cover conditions, with the Arctic on track to experiencing ice-free conditions during the summer months in the future (Stroeve et al., 2012). The increase in sea surface temperature and decrease in sea-ice concentration the Arctic has experienced over the last three decades is shown in Figure 3. While much of the sea-ice loss has occurred during the summer months and in the seasonal ice zone, there appears to be a shift towards rapid ice loss during all seasons, including the winter months (Onarheim et al., 2018).

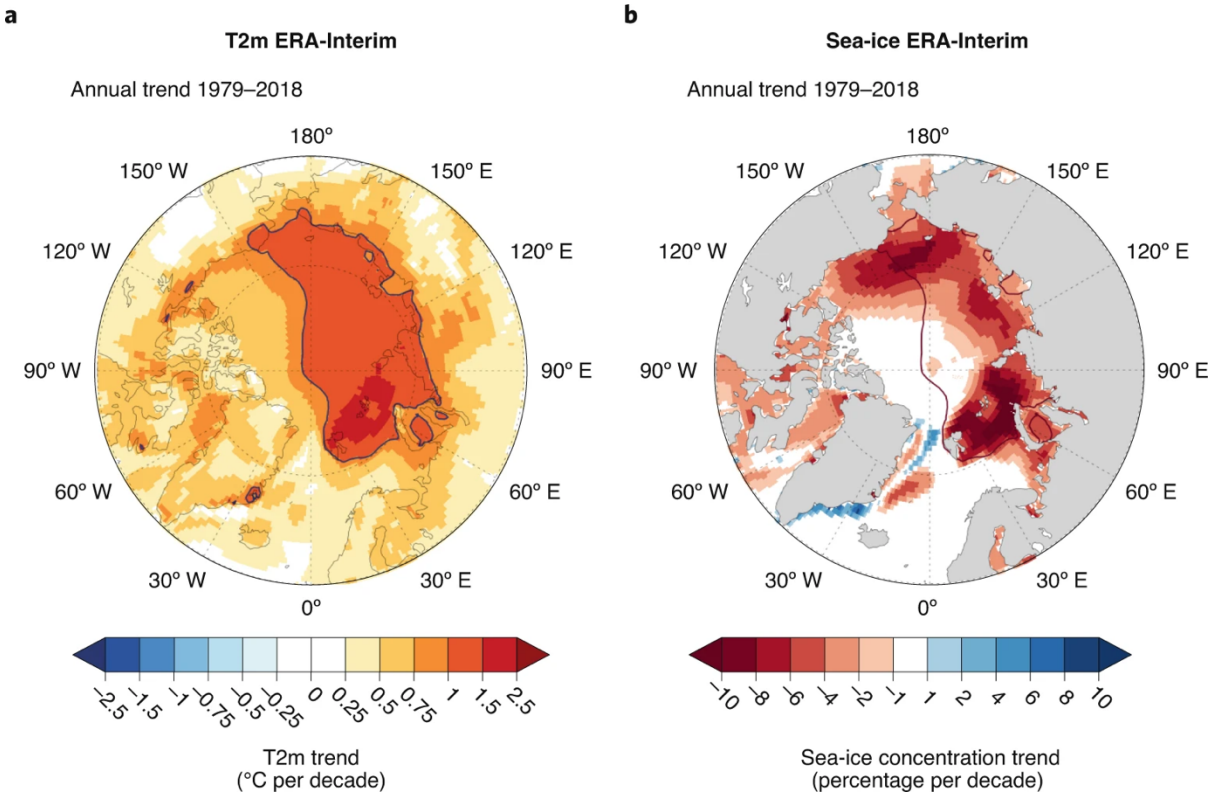

Figure 3: *Changes in average surface air temperature and sea ice concentration in the Arctic over time. (A) Near-surface air temperature trends showing average change between 1979 and 2018. (B) Sea-ice concentration trend showing average change between 1979 and 2018. The contour lines show the area with greater than 1 °C near surface air temperature increase per decade. Figure from Jansen et al. (2020).*

In addition to a general decrease in sea-ice cover in the Arctic, the sea-ice is getting thinner (Kwok & Rothrock, 2009), and the oldest areas of the sea-ice have essentially disappeared (Maslanik et al., 2007). The loss of sea-ice cover is therefore accompanied by a shift in the composition of the sea-ice that remains towards sea-ice that is thinner, younger, and more fragile. These changes in sea-ice also contribute to a positive feedback mechanism: the reduction of sea-ice results in a reduction in planetary albedo, which in turn leads to a higher absorption of solar radiation and an increase in the global temperature, amplifying the negative effects on the sea-ice (Miller et al., 2010).

1.3 Life in the sea-ice

Arctic sea-ice itself hosts multiple communities, including various meiofauna species such as copepods, flat worms, polychaetes, juvenile polar cod, and nauplius larvae (Bluhm et al., 2017). Many vertebrate species of fish, mammals, and birds also depend on sea-ice for foraging, reproduction and resting (Post et al., 2009).

Additionally, the sea-ice interface supports various communities of phytoplankton and sympagic (ice-associated) algae (Figure 4), which together represent the primary producers in the Arctic. Together, these communities account for 57% of the total annual primary production that occurs in the Arctic Ocean (Gosselin et al., 1997) and serve as the basis of the Arctic marine food web.

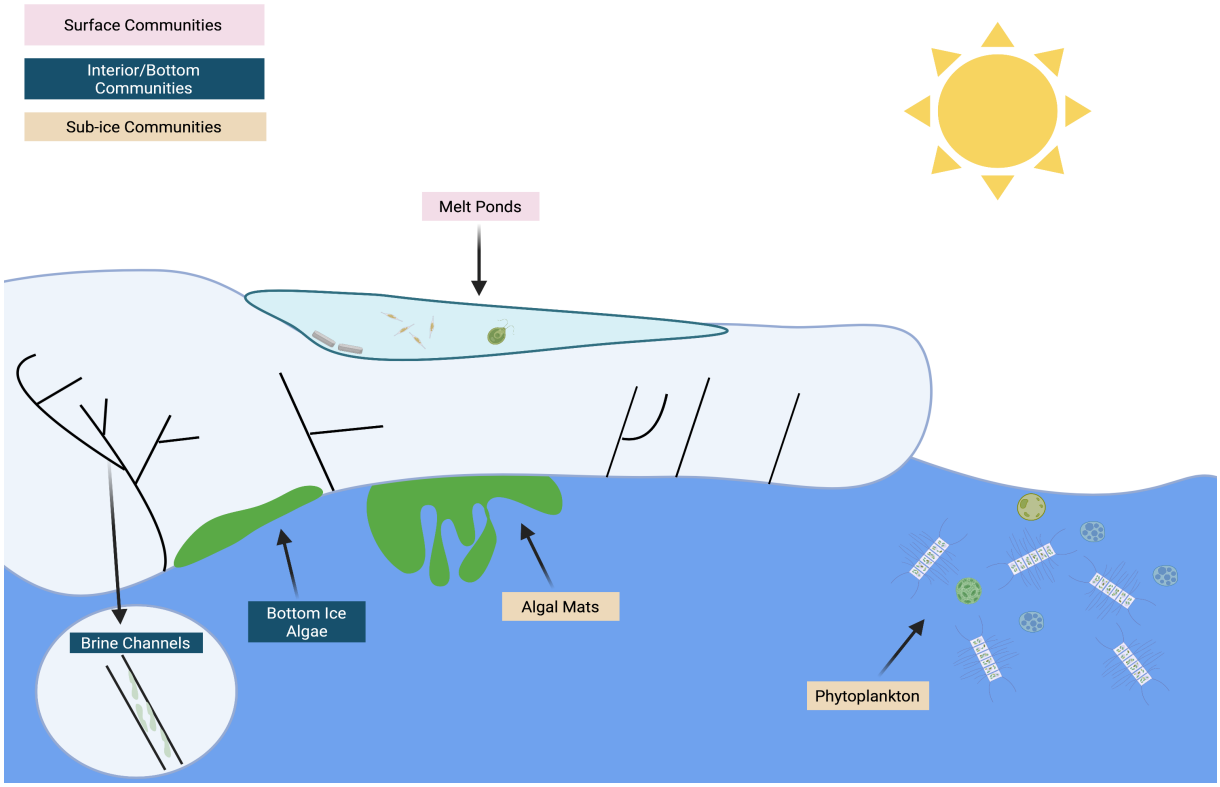

Figure 4: *Illustration of the various sea-ice algal communities, which can be divided into three approximate layers: surface communities, interior/bottom communities, and sub-ice communities. Figure created with Biorender.com.*

The ice algae communities can be divided into three approximate habitats: a surface layer, interior/bottom layer, and sub-ice layer (Horner et al., 1992) (Figure 4). Diatoms appear to dominate the sea-ice algal communities (Szymanski & Gradinger, 2016), accounting for more than 90% of the diversity (Arrigo, 2017). Diatoms are an ecologically rich and important lineage in marine and freshwater systems worldwide, with an estimated 200,000 species (Mann & Droop, 1996), and are responsible for over 20% of global carbon fixation (Kale & Karthick, 2015). They are characteristically defined by the presence of silica cell walls, known as frustules (Figure 5), with pores that are arranged either radially (centric diatoms) or bipolarly (pennate diatoms). Diatoms have a complex phylogeny, and although the pennate and centric diatoms diverged relatively recently (90 million years ago), they share only approximately 60% of their genes (Bowler et al., 2008).

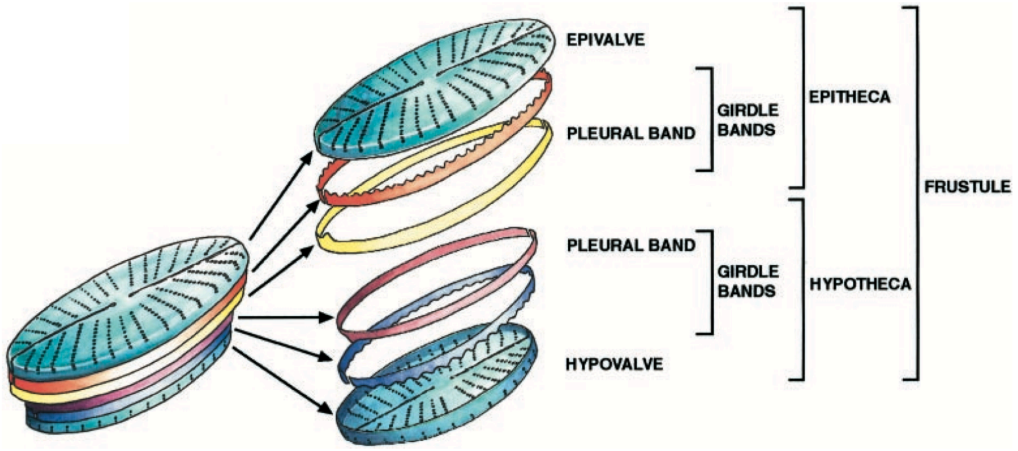

Figure 5: *Typical morphology of a diatom cell. The silica cell walls are known as frustules, which are in turn composed of the epitheca and hypotheca. The illustrated diatom cell is a pennate diatom, with a bipolar radiation of pores on the frustules. Figure from Zurzolo & Bowler (2001).*

Surface communities

As the snow and sea-ice surface begins to melt during the melt season, the meltwater produced can accumulate in characteristic melt ponds that can cover up to 60% of the sea-ice floes (Fetterer & Untersteiner, 1998). The composition of the sea-ice additionally influences the production of melt ponds, with higher melt pond production found on first-year ice than multiyear ice (Perovich et al., 2011). Melt ponds are traditionally characterized into either open or closed ponds. Open ponds are dark blue in color and are connected to the water mass below and therefore have a seawater environment, while closed ponds are light blue and are largely freshwater (Lee et al., 2011) (Figure 6).

Diatoms have been found to play a role in both open and closed melt ponds, although the community composition in open and saline melt ponds is mostly marine and brackish species (Gradinger, 2002), while the closed freshwater melt ponds generally have a higher concentration of freshwater algal species (Melnikov et al., 2002; Zhang et al., 2019).

Figure 6: *A typical view of an ice floe late in the melting season, showing both dark blue open melt ponds (seawater) (yellow arrow) and light blue closed melt ponds (freshwater) (black arrow). Photo was taken on the Nansen Legacy JC2-1 research cruise (12-29th July 2021) at approximately 82° N.*

The ice algal communities in the melt ponds on the surface of sea-ice are subjected to various extreme conditions, especially high light irradiance from solar radiation and reflection by the sea-ice surface (Mundy et al., 2011). Many ice algal species found in melt ponds may therefore exhibit adaptations to high light intensity, including the production of photoprotective pigments (Leu et al., 2010) such as mycosporine-like amino acids (MAAs) (Belzile et al., 2000) which act as a natural UV protective sunblock (Řezanka et al., 2004), and quenching of photosynthetic pigments (Katayama & Taguchi, 2013).

Interior and bottom communities

As sea-ice forms, much of the highly saline brine produced is trapped and a system of brine channels are created in the interior of the ice, which Wakatsuchi & Kawamura (1987) describe as taking "the form of a tree; the channels consist of large vertical tubes attended by smaller tributary tubes". These channels and pockets throughout the sea-ice filled with brine can account for up to 30% of the ice volume (Krembs et al., 2001), and they have a widely known role as a habitat for sympagic algae (Horner et al., 1988; Spindler, 1994). The algal communities inhabiting the brine channels and interior of the sea-ice have a mixed community structure consisting mostly of pennate and centric diatoms (Stoecker et al., 2000; Krembs et al., 2001).

These brine channels can pose challenges to the ice algal communities inhabiting them, as they can have especially variable salinity conditions and can be redistributed as the sea-ice goes through melting and freezing phases (Cottier et al., 1999). Temperature conditions can also vary dramatically throughout the interior of the sea ice and in brine channels (down to -20° C) (Thomas & Dieckmann, 2002) and the extreme salinity and temperature gradients could possibly explain why the interior sea ice communities have a relatively low productivity (Lizotte, 2001).

Most of the biomass in the interior of the sea-ice is concentrated in the bottom 20 cm, at the ice/water interface (Sullivan & Palmisano, 1981), possibly due to the more stable temperature and salinity conditions as well as the availability of nutrients from the water column (Arrigo, 2014). The bottom section of the interior of the sea ice is dominated by pennate diatoms (Hsiao, 1980), and the productivity of the bottom section of the sea-ice can often be the most productive ice algae community (Hsiao, 1980; Hoshiai & Fukuchi, 1981).

Sub-ice communities

Under sea-ice, thick mats of a brownish algae can grow and form tendrils that flow in the water column. These mats are an important part of the sub-ice algal community, and are formed by *Melosira arctica*, a centric diatom species that almost exclusively uses the sea-ice underside as substrate (Figure 7) (Syvertsen, 1991; Torstensson et al., 2021). It is also common to find multiple species of diatoms growing epiphytically on *Melosira arctica* aggregates. Poulin et al. (2014) found species from the genera *Chaetoceros*, *Synedropsis*, and *Pseudogomphonema* as *M. arctica* epiphytes, as well as multiple species of raphid pennate diatoms present gliding on the surface of *M. arctica* colonies.

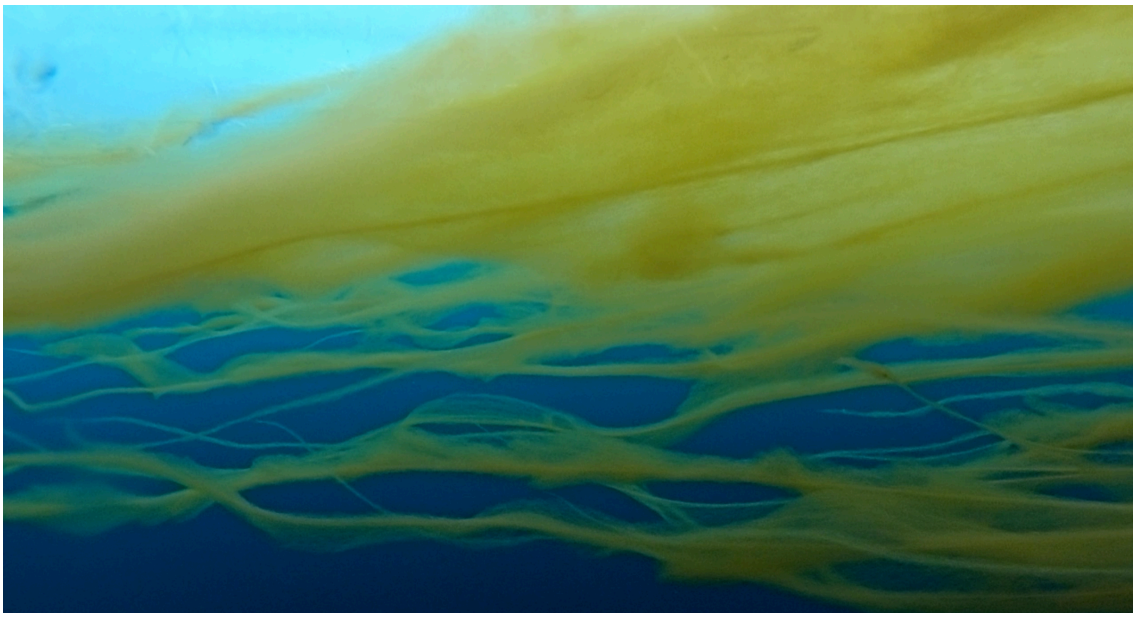

Figure 7: *Melosira arctica filaments growing on the underside of sea-ice. Forming long chains with mucilage, this centric diatom forms colonies that additionally have multiple other diatom species as epiphytes and potential symbionts. Photo from Oliver Müller (University of Bergen) taken during the MOSAiC expedition.*

In addition to the large aggregations of *M. arctica* growing on the underside of the sea ice, the sub-ice algal community consists of phytoplankton below the ice. The prevalence and importance of phytoplankton below the sea-ice is somewhat discussed, with Syvertsen (1991) speculating that planktonic algal species are more abundant in the southern edge of the Arctic Ocean where there is an influx of Atlantic water, while the planktonic sub-ice community in the north of the Arctic Ocean is likely ice algae suspended in the water column. However, phytoplankton blooms in the Arctic Ocean below the sea-ice by various diatom species have previously been reported (Booth & Horner 1997; Arrigo et al., 2012).

The presence of phytoplankton in the sub-ice community is potentially controlled by a variety of sea-ice factors, including its thickness (Syvertsen, 1991; Arrigo et al., 2012), the presence of melt ponds on the surface which increases the photosynthetic active radiation in the water column (Perovich et al., 1998) and meltwater from sea-ice forming a shallow pycnocline (Strass & Nöthig, 1996).

1.4 Ice algae in bloom and their role as trophic links

The Arctic is an extreme environment, even for species adapted to Arctic conditions. The growth of sympagic algae is limited by the strong seasonality of light, nutrients, temperature, and salinity (Cota et al., 1991; Harrison & Cota, 1991). In general, sea-ice algae begin to grow in the late winter and into spring, with maximum production in the late spring, while phytoplankton below ice generally have highest productivity during the summer (Hsiao, 1988). The ability of sea-ice algae to initiate the growth season during the late winter is due to their highly efficient photosynthetic pigments, allowing them to begin to grow with as little as 0.01% surface irradiance (Cota, 1985). This is a beneficial adaptation to have, as it extends the growth season and allows them to achieve a spring bloom as soon as there is a seasonal change in the photoperiod. The below ice phytoplankton on the other hand, are light limited until the melting season begins, as they require higher irradiance than sympagic ice algae (Kvernvik et al., 2021).

While light is generally the limiting factor controlling the start of the sympagic and phytoplankton blooms in the Arctic, nutrient availability is the limiting factor determining the accumulated biomass in the blooms (Smith et al., 1993). While silicon is an important nutrient for diatom growth, it appears that nitrogen is most commonly the nutrient limiting the growth of algal blooms in the Arctic (Smith et al., 1997; Campbell et al., 2016).

Although ice algae in the Arctic have an uneven distribution (Gutt, 1995; Rysgaard et al., 2001), the onset of the blooms both in the sea-ice and in the pelagic layer below, have important ecological effects on the Arctic ecosystem. Although the total primary productivity of the various sea-ice algal communities is relatively low with an estimated 15 g C m^{-2} $year^{-1}$ (Gosselin et al., 1997), they contribute to the biogeochemical cycle in the Arctic Ocean (Søreide et al., 2006) and are the main source of carbon for higher trophic levels during bloom conditions (Søreide et al., 2010).

The separate sympagic algae and phytoplankton blooms coincide with varying life stages of grazers, meaning that different life stages utilize the separate blooms (Søreide et al., 2010). In addition, ice algae (especially sub-ice algae) and phytoplankton are important links between the pelagic and benthic systems, serving as an important energy source for organisms in both systems (McMahon et al., 2006; Boetius et al., 2013).

1.5 Ice algae in a changing environment

With the Arctic experiencing dramatic increases in both air and ocean temperature leading to a consequential loss of sea-ice (Walsh et al., 2011), an important question that arises is: How will the sea-ice algal communities and the Arctic ecosystem as a whole respond to a reduction in sea-ice or ice-free conditions? The answer to this question is difficult to predict, especially when taking into consideration that any change of algal productivity in the Arctic will have reverberating effects on the remaining food chain.

One of the most widely predicted future scenarios is a shift in bloom dynamics of sympagic and pelagic microalgae in the Arctic. While a reduction in sea-ice cover will potentially enhance primary productivity in the Arctic Ocean as a whole, this is due to a shift in community structures towards conditions more favorable to phytoplankton species (Arrigo et al., 2008).

As the composition of Arctic sea-ice changes, trending towards thinner and less prevalent sea-ice, the interval between the sympagic and phytoplankton blooms will shorten. While a reduction in sea-ice may lead to a longer phytoplankton growth period (Arrigo et al., 2008; Arrigo & van Dijken, 2011), the shift in the time between the sympagic and pelagic blooms could lead to a mismatch between when the primary producers are present in the ice and water column, and the consumers that are adapted to graze on the different blooms (Søreide et al., 2010; Ji et al., 2013). This alteration in bloom dynamics and the ensuing mismatch with consumers, could then cause further mismatches between prey-predator relationships throughout the Arctic Ocean (Asch et al., 2019).

While certain phytoplankton species could take advantage of changes in sea-ice and snow composition that increases irradiation levels in the Arctic Ocean, many sympagic algae adapted to lower light conditions could experience photoinhibition and damaged photosystems as a result of large changes in irradiance (Juhl & Krembs, 2010). Although the increase in light irradiation could cause conditions preferable to phytoplankton blooms, the intensifying sea-ice melt causing an influx of freshwater in the euphotic zone could reduce the nutrients available for phytoplankton growth (Lee et al., 2012) and generate a shift in phytoplankton community structure towards picoplankton dominance, which in turn could negatively impact the Arctic food chain as a whole (Li et al., 2009).

The Arctic region is undergoing rapid change, and it is reasonable to expect that the loss of sea-ice has had and will continue to have effects on the sympagic algal communities, with a possible loss of algal biodiversity in the Arctic if sea-ice algae are unable to adapt to new conditions. However, this requires much more research and there exists a large gap in the understanding between the biodiversity of sea-ice algal communities and how they will respond to a changing Arctic with possible ice-free conditions.

1.6 Bridging the gap: Aims of the thesis

While it is generally well known that diatoms dominate the algal biomass in the Arctic, much research remains on their biodiversity within various sea-ice associated communities and new species of diatoms are encountered in the Arctic relatively frequently (von Quillfeldt, 1997; Werner et al., 2007; Różańska et al., 2008; Lund-Hansen et al., 2020). There appears to be very few studies that examine the molecular assemblages of protists in sea-ice (Mock & Thomas, 2005) and the exact number of Arctic phytoplankton and sympagic algae species remains to be determined (Poulin et al., 2011). Additionally, there is a high degree of uncertainty involved in how sympagic and phytoplankton communities in the Arctic will respond to climate change. Especially lacking in earlier research on Arctic algae have been the effects of multiple parameters and their interactions on algal growth rates (Young & Schmidt, 2020).

This thesis attempts to contribute to bridging the knowledge gap between the sea-ice diatom communities present in the Arctic and how they might respond to varying environmental conditions associated with climate change. I have used six strains of Arctic diatoms to attempt to answer two essential questions (including sub-questions) about Arctic sea-ice communities and their potential response to a changing Arctic:

1. **What** diatom species are present in the sea-ice communities?

    - What are the taxonomic identities of the sea-ice diatoms studied based on molecular and morphological approaches?

    - What morphological traits do we find in the sea-ice diatoms studied from the different sea-ice associated communities?

2. **How** will they respond to changes?

    - What is the effect of various environmental conditions on the growth rates of the studied sea-ice diatoms?

    - Which potential morphological and physiological traits observed in the various sea-ice diatoms could influence their ability to adapt to a changing Arctic?

In attempting to answer these questions, this thesis is organized into two parts. Part one uses molecular, morphological, and phylogenetic analyses to attempt to answer the first question. Part two uses two multistressor high-throughput growth experiments to attempt to answer the second question.

While this thesis may be divided into two parts, they are intrinsically connected: to be able to know **how** a community might respond to environmental change, it is vital to know **what** organisms are present.

1.7 Hypotheses and a step into the future

This thesis hopefully contributes to a glimpse both into what is present in the vital diatom communities associated with Arctic sea-ice, but also how these communities may adapt and respond to a changing ecosystem. With that objective in mind, I have made the following hypotheses on what the results of this thesis could potentially show:

Hypothesis one: The ice diatoms isolated from exposed melt ponds will be able to tolerate higher fluctuations in environmental conditions than ice diatoms isolated from sheltered habitats inside and under the sea ice.

Hypothesis two: There will be a clear relationship between the morphological and phylogenetic analyses done on the selected ice diatom species with the results of the growth experiments: species closely related phylogenetically will have similar growth responses to the tested environmental parameters.

2. Materials and Methods

In this section, I will begin by presenting the strains of diatoms I used throughout this thesis. I then describe the methods for part one and part two of this thesis in detail.

2.1 Algal Strains: The Group of Six

The foundation of this thesis are six strains of diatom species isolated from Arctic research cruises and kept in culture at the Institute of Biosciences (University of Oslo). The information on these strains can be seen in Table 1. The stock cultures were grown in 15 mL borosilicate tubes containing the half-defined algal medium IMR ½ + Si (Eppley et al., 1967) with salinity 30. The cultures were kept in a temperature-controlled room at 4°C with white fluorescent illumination and some natural light. The cultures were transferred to new medium every 6-8 weeks.

Table 1: *Background information on the diatom strains included in this study including information on where the strains were originally isolated.*

Strain ID	Species	Habitat	Date of Isolation	Latitude	Longitude	Cruise
HE492-7	*Thalassiosira gravida*	Plankton	05-09-2017	78.97N	9.49E	AWI cruise HE492
AeN707-15	*Chaetoceros gelidus*	Plankton	05-09-2018	83.15N	31.46E	The Nansen Legacy cruise 707
AeN707-42	*Nitzschia laevissima*	Melt Pond	06-09-2018	83.15N	31.46E	The Nansen Legacy cruise 707
AeN707-94	*Synedropsis hyperborea*	Ice Core	16-08-2018	83.32N	29.46E	The Nansen Legacy cruise 707
AeN706-04	*Nitzschia frigida*	Ice Core	18-09-2018	81.91N	29.11E	The Nansen Legacy cruise 706
AeN706-17	*Nitzschia* sp.	Melt Pond	18-09-2018	81.53N	30.97E	The Nansen Legacy cruise 706

The six strains of diatoms used were originally isolated from three separate sea-ice associated communities: *Chaetoceros gelidus* and *Thalassiosira gravida* from the plankton, *Nitzschia laevissima* and *Nitzschia* sp. from melt ponds on the surface of sea-ice, and *Nitzschia frigida* and *Synedropsis hyperborea* from ice cores in the interior of sea-ice (Figure 8).

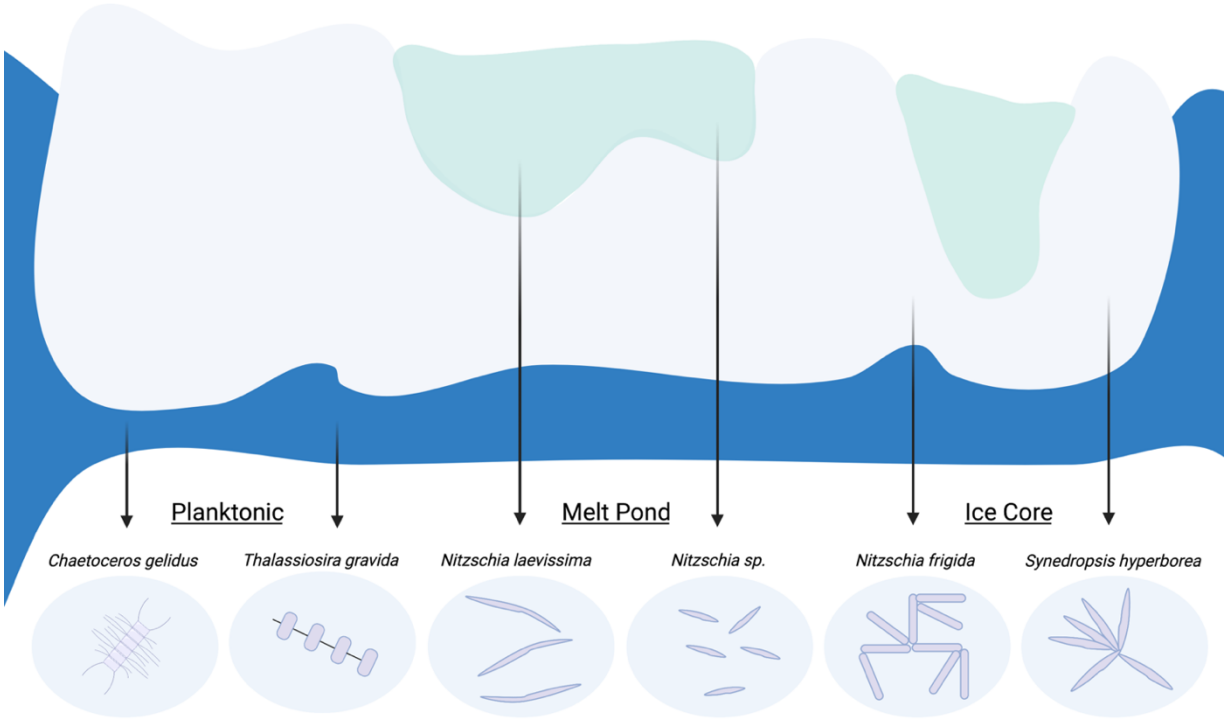

Figure 8: *A schematic presentation of the six strains of Arctic diatoms used in this thesis, and the sea-ice associated community they were originally isolated from. Figure created with Biorender.com.*

Since sea-ice hosts dynamic and distinct habitats, it was important to choose species isolated from various communities for further study in this thesis. Choosing which six strains to use in this thesis required taking into consideration the health of the cultures, how representative the species were for Arctic sea-ice communities, and their abundances from previously reported Arctic research.

The strains I have used are all isolated from the Arctic Ocean, and a map of their geographic sampling locations can be seen in Figure 9.

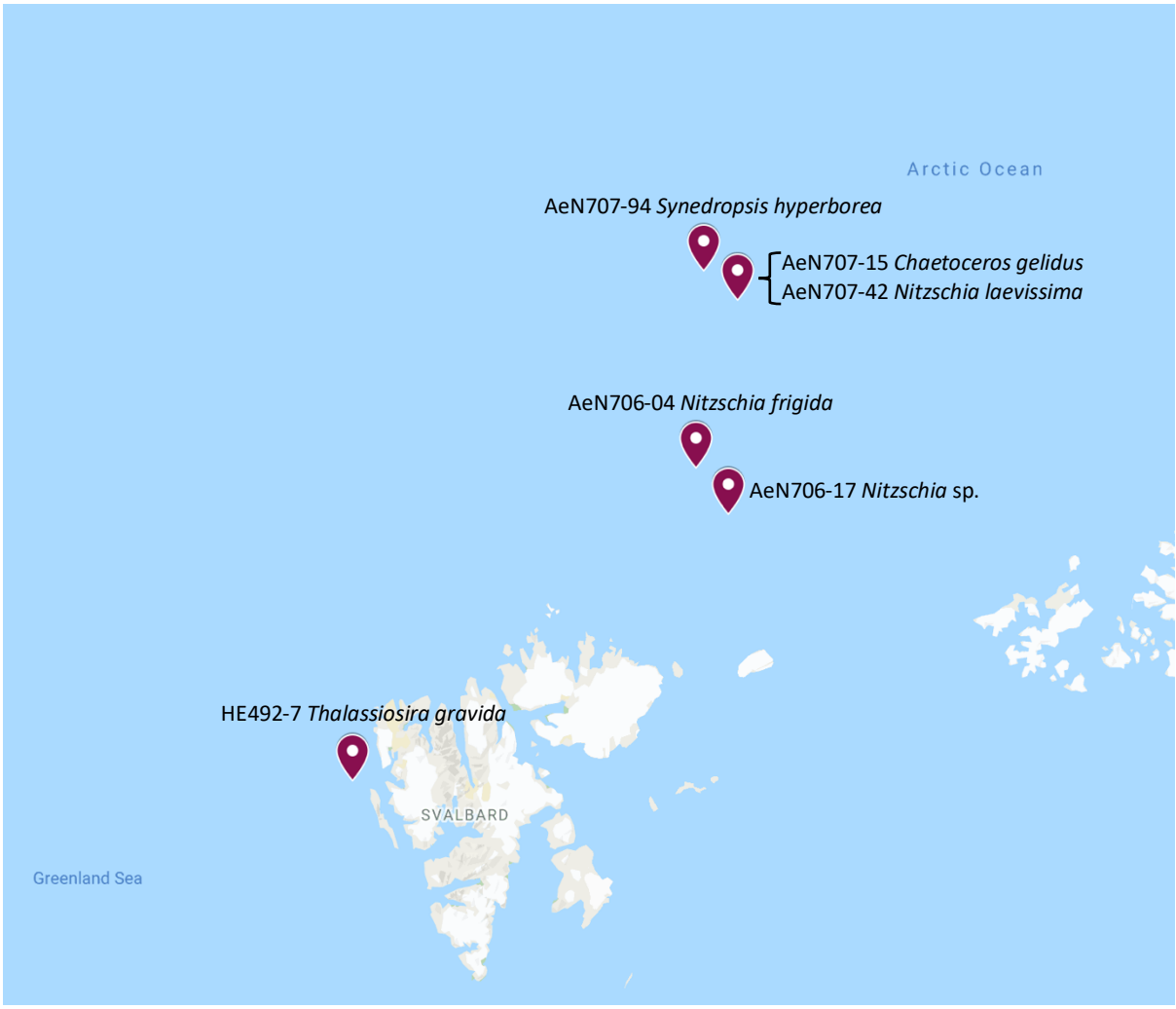

Figure 9: *Sampling map of where the various strains originate, based on the coordinates of the sampling stations provided in Table 1.*

2.2 Part One: Molecular, Phylogenetic, and Morphological Analyses

Part one of this thesis starts with molecular, phylogenetic, and morphological analyses on the six strains of diatoms (Figure 10). By isolating and sequencing DNA, I have been able to produce a phylogenetic tree showing the evolutionary relationship of the strains used in this thesis. Additionally, by examining the strains under light and electron microscopy, morphological and physiological traits have been characterized.

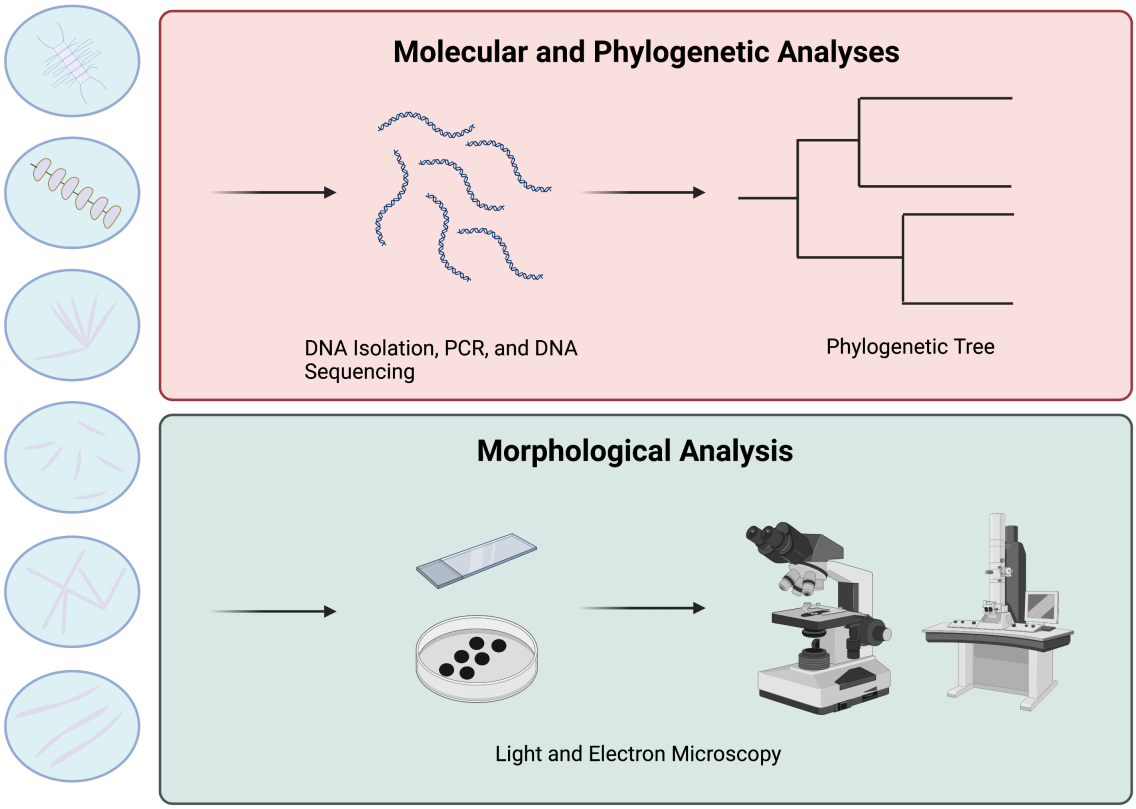

Figure 10: *Schematic representation of part one of this thesis, which involved isolating, amplifying, and sequencing DNA, and assembling a phylogenetic tree. Additionally, the strains were prepared for light and electron microscopy and examined morphologically. Figure created with Biorender.com.*

2.3 Molecular and Phylogenetic Analyses

2.4 DNA Isolation

The strains of *Thalassiosira gravida* (HE492-7), *Nitzschia laevissima* (AeN707-42), *Chaetoceros gelidus* (AeN707-15), and *Synedropsis hyperborea* (AeN707-94) were previously sequenced with ribosomal DNA and the sequences were already available for analysis.

DNA from the strains collected on the AeN706 cruise, *Nitzschia frigida* (AeN706-04) and *Nitzschia* sp. (AeN706-17) was extracted in the lab using the Qiagen DNeasy Blood and Tissue Kit (Qiagen, Germany). The protocol in the kit was followed, with some small modifications.

Samples from the cultures were kept frozen in 1.5 ml centrifuge vials. To ensure efficient extraction of DNA from the diatom cells, the frozen cultures were kept at room temperature for a few minutes until evenly thawed before the molecular work was begun. In each vial AL lysis buffer was added, a chaotropic agent that ensures that the cellular membranes are lysed and that proteins are denatured, releasing the DNA into the solution. Proteinase K was added into the solution, digesting any proteins. This cellular solution was then vortexed (Lab Dancer S40, IKA, Germany) and incubated at 56°C (Grant QBD2 Block Heater, Grant Instruments, United Kingdom).

Ethanol was added to the solution, promoting DNA precipitation. The solution was vortexed again and pipetted into a DNeasy Mini spin column which was placed into a collection tube. The collection tube with the spin column and solution were centrifuged at 8000 rotations per minute (rpm) (Centrifuge 5424 R, Eppendorf, Germany). The collection tube with the flow through solution was discarded, and the spin column was added to a new collection tube. The AW1 washing buffer was added to the filter in the spin column, washing out contaminating proteins, salt, inhibitors, and molecules on the filter. The collection tube with spin column was then placed in the centrifuge again at 8000 rpm. The collection tube with flow through solution was discarded, and the spin column was placed in a new collection tube.

A new washing buffer, AW2, was added to the filter in the spin column, and the collection tube with spin column was centrifuged at 14000 rpm. The collection tube with flow through was discarded, and the spin column was added to a new and final collection tube. An elution buffer, AE, was added to the filter on the spin column, with seperates the DNA molecules from the filter. The spin column and collection tube were incubated at room temperature, and then centrifuged at 8000 rpm. To maximize the DNA yields, the collection tube was not discarded after this step and a second round of AE buffer and centrifuging was done. Following the second centrifuge, the spin column was discarded and an Eppendorf tube with extracted DNA was labeled and kept in a -20°C freezer.

2.5 DNA Quantification

To ensure that a sufficient amount of DNA was extracted to use for PCR and sequencing, the isolated DNA was quantified using a Qubit fluorometer quantification machine (Invitrogen Qubit 3.0 fluorometer, Thermo Fisher Scientific, USA). To prepare the extracted DNA for quantification using the Qubit fluorometer, a high sensitivity qubit kit was used (Qubit dsHS Assay Kit, Invitrogen, Thermo Fisher Scientific, USA) and the manufacturer's protocol was followed. By using this method, a reagent acting as a fluorophore was added and attached to the DNA molecules in the samples. This was then measured by the fluorometer, which emits a light and estimates the amount of DNA present based off the fluorescence.

The kit contains two standard solutions (S1 and S2) with known DNA concentration values, and the DNA quantification makes a calibration curve based on these standard solutions. These standard solutions were taken out of the fridge and kept at room temperature for an hour prior to use, while the DNA samples were taken out of the freezer and thawed on ice. After the DNA samples were thawed, they were vortexed and spun down.

A master mix of buffer and fluorophore reagent was made, with the amount of each varying based on how many DNA samples were being quantified (Table 2).

Table 2: *Contents of Qubit master mix, containing buffer and reagent, with volumes varying based on how many DNA samples were being tested.*

Components	Volume
Qubit Buffer DNA Samples	x*199 µl (x= number of DNA samples + 1 extra)
Qubit Buffer Standard DNA solutions	2*190 µl
Qubit reagent (fluorophore)	x*1 µl (x=number of DNA samples + 2 standard DNA solutions)

Qubit tubes that followed with the kit were taken out, with one for each DNA sample and one for each standard. Master mix was added into each Qubit tube, followed by standard solutions and DNA samples in their respective tubes. Each Qubit tube was then vortexed and spun down and incubated at room temperature for 5 minutes. After incubation, each Qubit tube was measured using the fluorometer, giving the DNA concentration in ng/µl.

2.6 PCR (Polymerase Chain Reaction) DNA Amplification

The PCR done in this thesis aimed to amplify a part of the 28S nuclear ribosomal large subunit rRNA gene, a conserved eukaryotic gene that also contains variable regions. A solution containing PCR master mix (GoTaq Green Master Mix, Promega Biotech, USA), primers, and nuclease-free MilliQ water was made. The manufacturer's protocol was followed for PCR. The components in the PCR master mix can be found in Table 3, along with volumes of each component.

The GoTaq Green master mix in the solution contained DNA Taq-polymerase, dNTP (deoxyribonucleotide triphosphate), $MgCl_2$, and stabilizers.

Table 3: *Contents of the PCR master mix, with the volumes of each component varying based on the number of DNA samples being amplified.*

Components	Volume (x= number of samples + 1 blank/negative control + 2 extra)
GoTaq Green Master Mix	x*12.5 µl
MilliQ H_2O	x*7 µl
Forward primer	x*1.5 µl
Reverse primer	x*1.5 µl

For the DNA polymerase in the kit to be able to attach to the DNA strands, complementary forward and reverse primers were needed. For the 28S rRNA gene, the DiR-F forward primer and D2C-R reverse primer were used (Scholin et al., 1994) (Table 4). These primers amplify the hypervariable D1 and D2 domain regions.

Table 4: *Oligonucleotide primers used for PCR and sequencing of the D1 and D2 domain regions 28S rRNA gene. Sd = synthesis direction: F = forward; R = reverse.*

Code	PCR	Sequencing	Sd	Nucleotide sequence 5´ to 3´
DIR-F	LSU	LSU	F	ACCCGCTGAATTTAAGCATA
D2C-R	LSU	LSU	R	CCTTGGTCCGTGTTTCAAGA

PCR tubes were prepared, with solutions consisting of both DNA sample and the PCR master mix. A negative control of MilliQ H_2O was included in one of the tubes. The PCR tubes were then placed in a PCR thermocycler (Mastercycler EP Gradient S, Eppendorf, Germany) and amplified with the program found in Table 5.

Table 5: *The PCR program used for amplifying the partial 28S rRNA gene.*

Temperature	Time	Number of Repeated Cycles
94°C	3 minutes and 30 seconds	
94°C	50 seconds	35
55°C	50 seconds	35
72°C	80 seconds	35
72°C	10 minutes	
8°C	Hold	

This program was based on repeated cycles of DNA denaturation at 94°C, annealing of primers at 55°C, elongation of DNA strands at 72°C and a hold stage at 8°C.

2.7 Agarose Gel Electrophoresis

The PCR products were run through a gel electrophorese on 0.8% agarose gel to test for yield and purity.

The agarose gel was made using 0.8 grams of agarose powder added to 100 ml of 1X TAE buffer. The agarose solution was heated for 2 minutes in a microwave to ensure that the reagents mixed. Once the mixture cooled to approximately 55°C, 4 µl of GelRed (Nucleic Acid Gel Stain, Biotium, USA) was added, and the solution was poured into an electrophoresis cast with combs and left for 30 minutes to set. The PCR products were mixed with 6X loading buffer (Abgene, New Hampshire, USA) and loaded onto the gel, along with 6 µl of the DNA ladder 1 kb (New England Biolabs, Massachusetts, USA) for size reference. The gel was then run in the electrophoresis machine (Electrophoresis Power Supply-EPS 301, Bio-Science AB, Sweden) at 100 V for 30-45 minutes and eventually studied using a UV transilluminator (Gene Genius Bioimaging System, Syngene, UK).

2.8 PCR Product Cleanup and Processing for Sequencing

Before the PCR products can be sent off for sequencing, they need to be purified and cleaned of any remaining free primers, enzymes, nucleotides, and buffer components. To clean the PCR products, I used the USB ExoSAP-IT PCR Product Cleanup kit (Thermo Fisher Scientific, USA) and followed the protocol in the kit.

A mixture containing 2.0 µl of PCR product and 2 µl of ExoSAP-IT reagent was made and incubated at 37°C for 15 minutes to degrade the primers and nucleotides, and then 80°C for 15 minutes to inactivate the reagent (Grant QBD2 Block Heater, Grant Instruments, United Kingdom).

For each cleaned DNA sample, 0.5 µl was added to two separate vials. Into each vial 4.5 µl of H_2O was added, as well as 5 µl of primer (each vial received a separate primer: one vial with LSU DiR-F, and one vial with LSU D2C-R). The total volume in each vial was 10 µl, and these vials were then sent for DNA sequencing at Eurofins using the Light Run tube service (Eurofins Genomics, Germany).

2.9 Construction of Phylogenetic Trees

Phylogenetic trees were assembled to reflect the evolutionary relationship between the strains and place them taxonomically. A consensus tree was assembled using the 28S rRNA genetic sequences from the six strains of diatoms along with reference sequences of other diatom strains.

The sequences were first run through the BLAST (Basic Local Alignment Search Tool) algorithm, which compares the sequences used for analysis with other sequences in the NCBI

database (National Center for Biotechnology Information, National Institute of Health, United States).

The BLAST algorithm produces a table giving information on the sequences obtained when compared to the sequences in the database, finding similar sequences and regions with high similarity and calculating statistical significance.

Before constructing the phylogenetic trees, the sequences were edited and aligned with other reference sequences, along with an outgroup sequence. This was done in the software Geneious Prime (version 2021.1.1, Biomatters Ltd, New Zealand), using the alignment function, and selecting "MAFFT alignment". The full alignment can be seen in Appendix C: Supplementary Results, Table S13. The RAxML function was used to construct a maximum likelihood phylogenetic tree, placing the obtained sequences in relation to the reference sequences with the outgroup as a root. This tree included the bootstrap values.

2.10 Morphological Analysis

2.11 Microscopy

The six strains were examined under both light and scanning electron microscopy (SEM).

An inverted light microscope (Zeiss Axio Vert.A1, Carl Zeiss AG, Germany) with Differential Interference Contrast (DIC) objectives was used, with an attached camera (Leica MC170 HD, Leica Biosystems, Germany) and imaging program (LAS EZ Digital Imaging System, Leica Biosystems, Germany) to capture images.

The strains were prepared for electron microscopy as described below and then examined using a scanning electron microscope (S-4800, Hitachi High-Tech, Japan). Many of the unique morphological features of diatoms are in the structures of their silica frustules. To be able to properly examine the frustules in detail, it is necessary to use an electron microscope. A scanning electron microscope works by focusing an electron beam through magnetic lenses and apertures, scanning the sample, and producing secondary electrons on the surface of the sample which are used to form an image.

2.12 Acid Cleaning of Diatom Cells

It is necessary to first clean the diatom samples of organic compounds, proteins, lipids, cellular contents, and other contaminating molecules that cover the silica frustules and can interfere with the quality of the electron imaging.

To effectively clean the samples of diatoms and prepare them for electron microscopy, I followed the protocol as originally described by Hasle and Fryxell (1970). This entailed using strong acids to clean the samples, removing the organic material, leaving only the frustules in the solution. The acid cleaning process took approximately two days. The first day involved transferring 10 ml of diatom culture into separate 100 ml Erlenmeyer flasks. Working under the fume hood, 2 ml of sulfuric acid (5.9 M H_2SO_4) and 10 ml of saturated potassium

permanganate (0.41 M $KMnO_4$) were added to each flask (Figure 11, A). The flasks with the solution were left under the fume hood for 24 hours and stirred 3-8.

After 24 hours, the cleaning process continued. The flasks were stirred one final time, and 2 ml of oxalic acid (2.2 M $C_2H_2O_4$) was added into each flask, causing the solution in the flasks to bubble. Another 3 ml of oxalic acid was added into the flasks, which caused a color change in the solution (Figure 11, B). The flasks were gently shaken to ensure even mixing, and a few more ml of oxalic acid were added to the solutions that were not yet completely transparent. No more than 10 ml of oxalic acid was added into one flask, as this will increase the risk of crystallization. For each sample, two centrifuge tubes were prepared, and once the solutions in the flask were translucent, 5 ml of sample was removed and added to each centrifuge tube.

The aim of the following process is to ensure that the acids are removed from the samples, that the frustules are thoroughly cleaned, and that the frustules are concentrated into a smaller volume. Once the samples are transferred to two centrifuge tubes, they were placed in the centrifuge (Centrifuge 5810R, Eppendorf, Germany) at spun at 4000 rpm at 22°C for 5 minutes. Meanwhile, a peristaltic pump (Ismatec, Switzerland) was placed under a fume hood and prepared by choosing the setting with a pump speed of 400 ml/min.

After the centrifuging process was finished, the centrifuge tubes were placed under the fume hood with the peristaltic pump. A glass pipette was attached to the pump tube, and the supernatant in each centrifuge tube was removed, until approximately 2 ml of sample was left (Figure 11, C). Between each sample a new glass pipette was used to avoid contamination.

The remaining contents of the Erlenmeyer flasks were transferred between the two centrifuge tubes for each sample and placed in the centrifuge with the same settings as before. Once the centrifuge was finished, the supernatant was again removed using the peristaltic pump until approximately 2 ml of the sample was left. The two centrifuge tubes of each sample were combined into one centrifuge tube with the acid cleaned product.

The remaining cleaning process used distilled H_2O to rinse the samples. This involved adding 5 ml of distilled H_2O into each centrifuge tube with sample, centrifuging, and removing the supernatant with the peristaltic pump. This process was repeated four times, ensuring that the samples are thoroughly rinsed, cleaned, and concentrated.

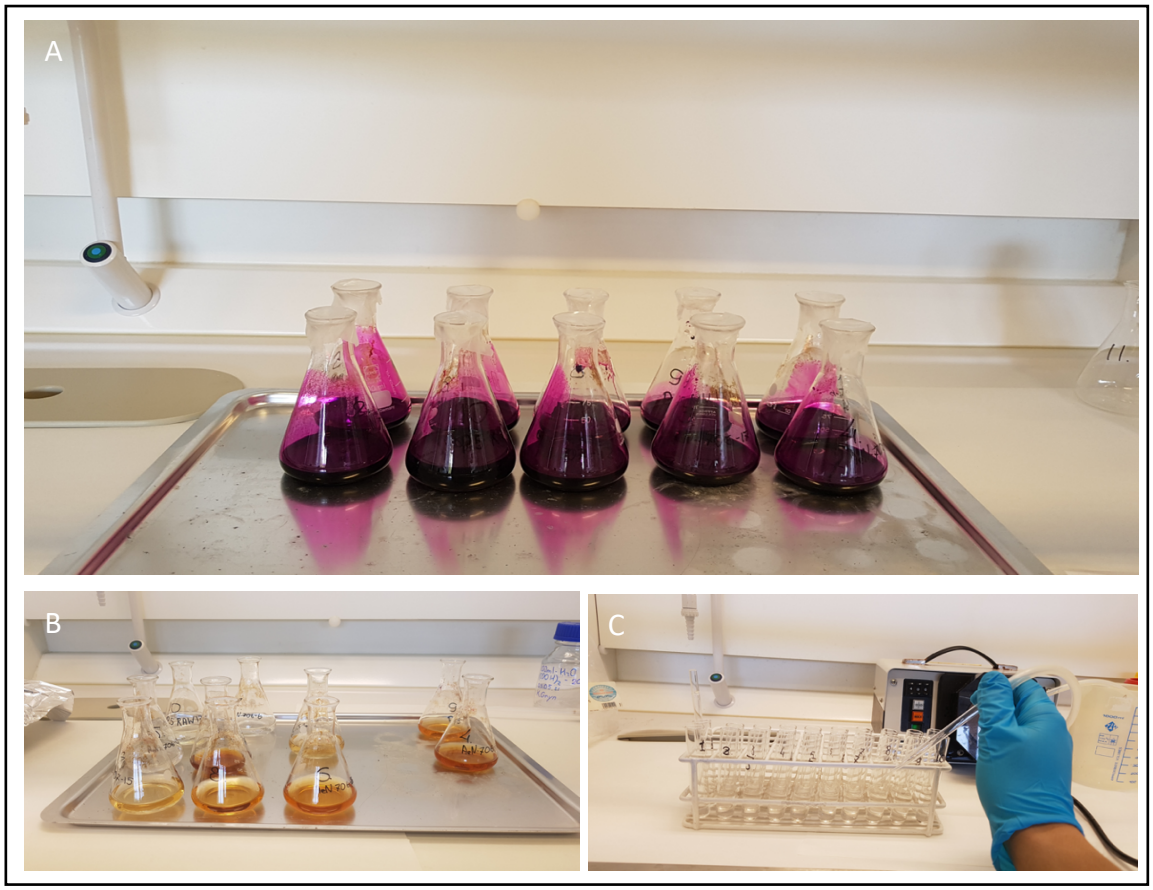

Figure 11: *(A) The Erlenmeyer flasks containing a sample of the diatom cultures, sulfuric acid, and saturated potassium permanganate. These flasks were left under the fume hood for 24 hours. (B) The Erlenmeyer flasks after the addition of oxalic acid, which causes a color change. The solution in each flask eventually became translucent. (C) Using the Ismatec peristaltic pump, the supernatant is removed after each centrifuging. This ensures that the solution becomes more concentrated with diatoms frustules after each step.*

To prepare the cleaned samples for SEM, a double-sided sticker (9mm Carbon Adhesive Tabs, Electron Microscopy Sciences, USA) was placed on a stub (Aluminum Mount, Electron Microscopy Sciences, USA). Polylycin glue was added to the stub, on which a drop of acid cleaned sample was placed. This was left to dry, and then sputter coated with layer of gold-palladium by thermal evaporator (Cressington 308R, Cressington Scientific Instruments, UK). The samples were then examined under SEM.

2.13 Part Two: Growth Experiments

Part two of this thesis consists of two multistressor high-throughput growth experiments on the six strains of diatoms (Figure 12). These novel growth experiments, testing various conditions of salinity, light intensity, and temperature on the growth of the tested strains over time, have allowed me to test multiple combinations of environmental parameters simultaneously and relatively quickly. The data from these growth experiments was then analyzed through biostatistics, allowing me to visualize growth curves and determine growth rates of each strain.

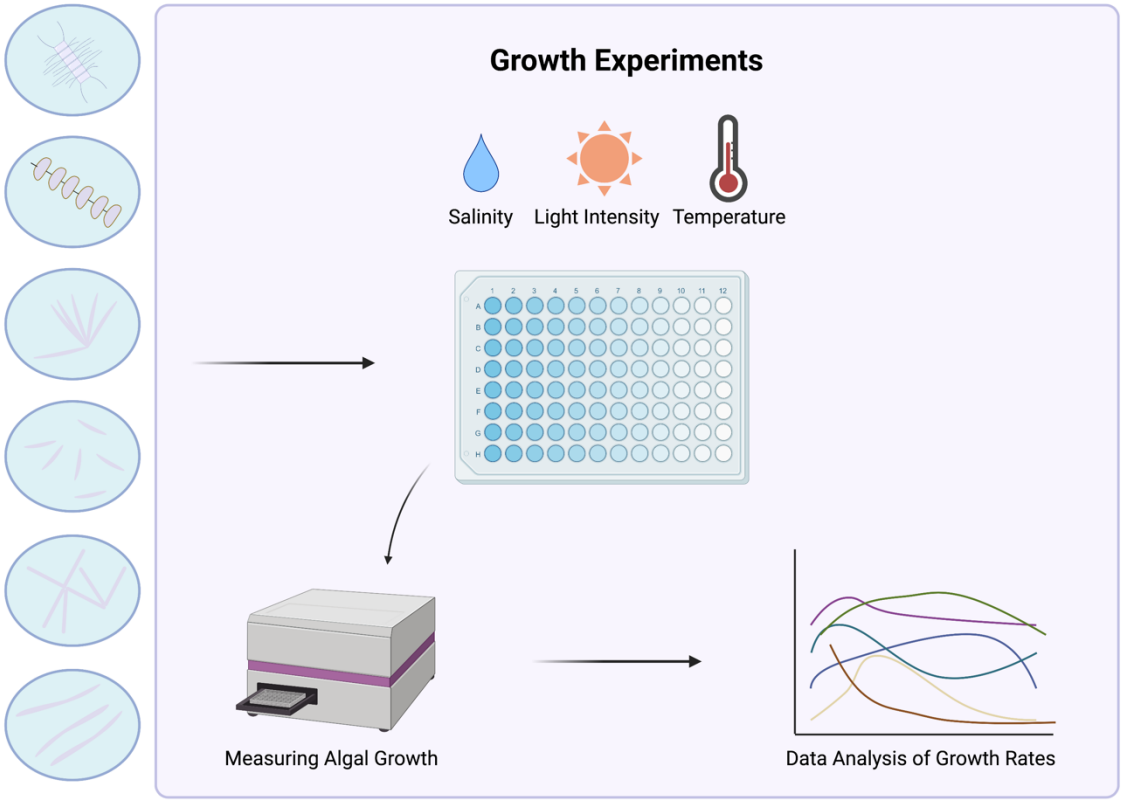

Figure 12: *Schematic representation of part two of this thesis, which involved two multistressor high-throughput growth experiments. This entailed testing various concentrations of salinities, light intensities, and temperatures on the diatom strains, measuring their growth and analyzing their growth rates. Figure created with Biorender.com.*

I will briefly discuss why each parameter was chosen, and how they are projected to influence algal growth rates.

Salinity

As salinity deviates from seawater values, the photosynthetic efficiency and growth rates of sea-ice algae are reduced (Ryan et al., 2004; Krell et al., 2007). While sea-ice algae can adapt changes in salinity (Grant & Horner, 1976), it appears that sea-ice algae have a salinity optimum at around 30 PSU (Bates & Cota, 1986). As sea-ice melts and freshwater is expelled into the Arctic Ocean, climate change will cause a significant freshening of the water mass (Shu et al., 2018) which then in turn should impact the productivity of sea-ice algal communities.

Four salinities were chosen for the growth experiments: 34 PSU (practical salinity unit) (approximately ambient seawater values), 30 PSU, 25 PSU and 22 PSU. The salinity gradient reflects the future scenario of a freshening Arctic Ocean.

Temperature

Although an increase in temperature has been shown to increase growth (Werner et al., 2007) and photosynthesis rates (Mock & Hoch, 2005) in sea-ice algae, this only occurs up to the level at which proteins begin to denature (Rothschild & Mancinelli, 2001). Previous experiments have shown that higher temperatures up to 10°C led to lower biomass and chlorophyll a concentration in Arctic phytoplankton, as well as a shift in the community structure towards smaller phytoplankton groups (Coello-Camba et al., 2014). Although sea-ice algae over time can adapt to a range of thermal conditions (Mock & Hoch, 2005), the expected rise in oceanic and atmospheric temperatures in the Arctic is expected to impact both the structure and productivity of sea-ice algal communities.

Four temperatures were chosen for the growth experiments: 4°C, 6°C, 11°C and 15°C. These temperatures reflect the range that most microalgae are currently accustomed to, the future temperature conditions the Arctic will experience (Hassol, 2004), and a hypothetical extreme condition, respectively.

Light Intensity

Sea-ice associated algal communities tolerate extreme light intensity conditions. Communities on the surface of the sea-ice can experience potentially damaging levels of light and UV radiation, and the surface communities have therefore adapted by developing various photoprotective strategies (Elliott et al., 2015). The interior and sub-ice communities on the other hand are adapted to low light irradiance conditions (Hancke et al., 2018). Experiments have shown that certain ice-algal species can rapidly adjust to light levels between 10 and 100 µmol photons m^{-2} s^{-1}, depending on which community they are associated with (Galindo et al., 2017). As sea-ice continues to disappear, creating thinner ice and ice-free conditions, many algal communities will be subjected to higher light irradiance levels than they are currently acclimated to (Nicolaus et al., 2012).

Four light intensities were tested in the second growth experiment: 12, 25, 35, and 50 µmol photons m^{-2} s^{-1}. This reflects a gradient of increasing light intensities above the current conditions that particularly interior and below ice communities experience (Suzuki et al., 1997) and could thus be indicative of future irradiance conditions in an ice-free Arctic.

2.14 Making of Algal Medium

For the two growth experiments, the diatom strains were grown in medium with different salinities. The medium used was IMR ½ (Eppley et al., 1967) and growth media with PSU of 34, 30, 25 and 22 were made.

The base for algal medium is natural seawater, which for our media was seawater collected from approximately 40 meters depth from the Oslo fjord outside of Drøbak. This seawater had a PSU of 34, which was checked using a refractometer (Handheld Refractometer N-8, Atago CO LTD., Japan). The seawater was filtered through GF/C glass fiber filters (Whatman Glass Microfiber Filters Grade GF/C, Cytiva Lifesciences, USA) Distilled H_2O was added to the natural sea water, with the amount added depending on which PSU was desired (lower PSUs will need to have higher amounts of distilled H_2O added to the natural seawater). The salinity level of the diluted sea water was checked using the refractometer.

Once the desired salinity was achieved, the stock solutions were added. This included nitrate, phosphate, selenite, and silicate solutions, as well as B vitamins. Together, these are all required for diatom growth. A solution of trace metals was also added, which contained both trace metals necessary for growth, as well as chelators which detoxify heavy metals and ensure the medium has a low level of reactive trace metals.

The media were then autoclaved (HS 6610EC-1 Autoclave, Getinge, Sweden) with the program PO3 for wet autoclaving at 121°C for 20 min. The media was stored in a temperature room at 14°C.

2.15 First Growth Experiment

The first growth experiment tested four salinity conditions (22, 25, 30 and 34 PSU) and four temperature conditions (4°C, 6°C, 11°C, and 15°C). The first growth experiment utilized 96-well plates (Nunc 96-well MicroWell Plates, Thermo Fisher Scientific, USA) and the setup of the plates can be seen in Figure 13. The six strains of diatoms were arranged on the plates with 16 wells each.

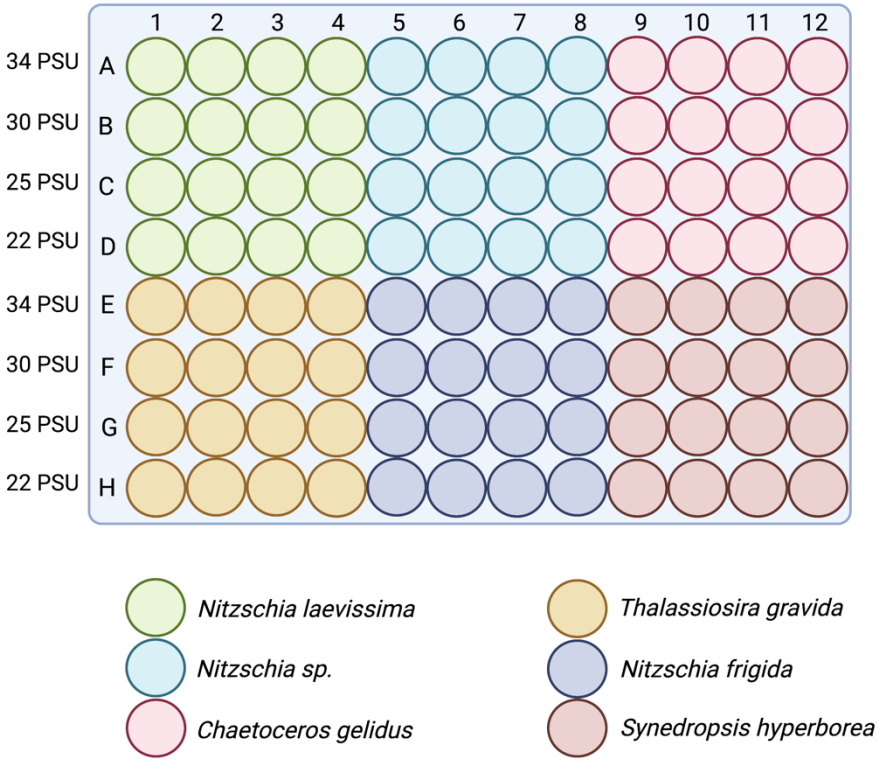

Figure 13: *The plate setup used for the first growth experiment. The setup shows the arrangement of the six strains of diatoms used, as well as the salinity (measured in PSU) of the media used in each row. Figure created with Biorender.com.*

Translucent 96-well plates were used, and in each well there was 270 µl of algal growth medium (IMR ½ + Si) and 30 µl of diatom sample inoculate. For this experiment, I made four replicates of the 96-well plates, with the same arrangement of strains and media. These were then placed into separate temperature rooms. Each temperature room had one 96-well plate placed into it, and the plates were labeled and covered with the plate lid.

All plates received the same irradiance level (approximately 10 µmol photons m^{-2} s^{-1}), emitted from a plant growth light bulb with a photoperiod of 16 hours on and 8 hours off setting.

The 96-well plates were left in the temperature rooms over a period of 18 days. The algal growth was measured approximately every second day, using a plate reader (Synergy Mx Monochromator-based multi-mode microplate reader, Biotek, USA) (see Figure 14). The plate reader estimates algal growth through fluorescence, emitting a blue light (wavelength ~450nm) that is absorbed by the chlorophyll a pigment in the diatoms and is reemitted as a red light (wavelength ~660nm). This is used as a proxy for cell concentration and the plate reader records these measurements automatically, uploading them to the connected computer.

When transporting the plates out of the temperature rooms for measurements, they were kept on ice to maintain a cooler temperature and to prevent the strains from experiencing thermal shock.

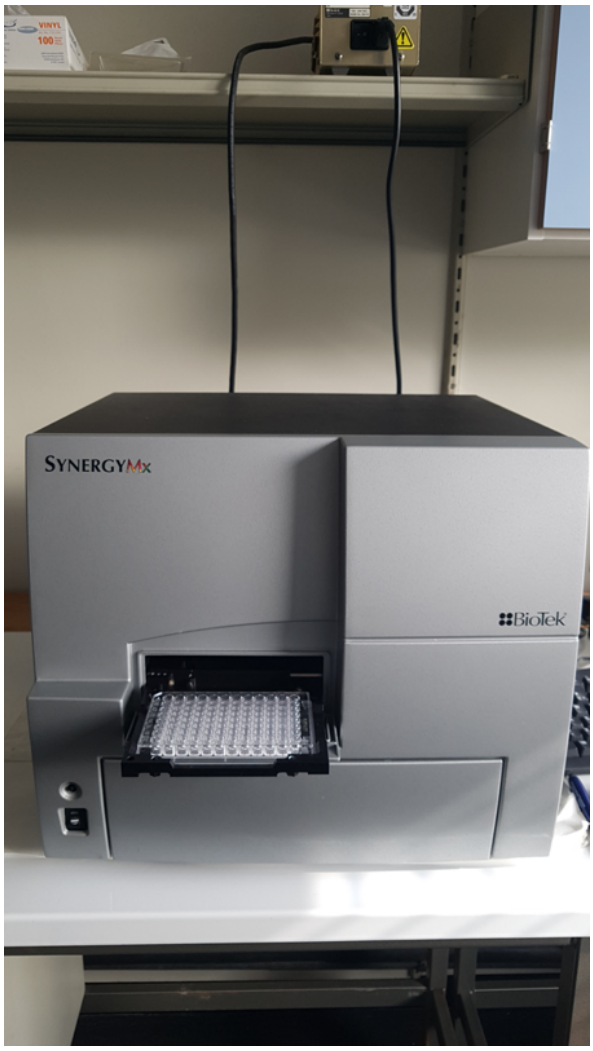

***Figure 14**: The Synergy Mx plate reader used to measure algal growth through fluorescence.*

2.16 Second Growth Experiment

The second growth experiment tested four salinity conditions (22, 25, 30 and 34 PSU), four temperature conditions (4°C, 6°C, 11°C, and 15°C) and four light intensities (12, 25, 35 and 50 µmol m^{-2} s^{-1}).

Experimental Setup

The main difference between the first and second growth experiment was the introduction of light intensity as a new parameter. The 96-well plate setup for the second growth experiment was the same as in the first growth experiment (Figure 15) with regards to the arrangement of media and diatom strains. The amount of medium and algal strain in each well for the second growth experiment varied based off the results from the first growth experiment. The method for calculating medium and algal strains inoculate volumes can be found in Appendix A: Supplementary Methods.

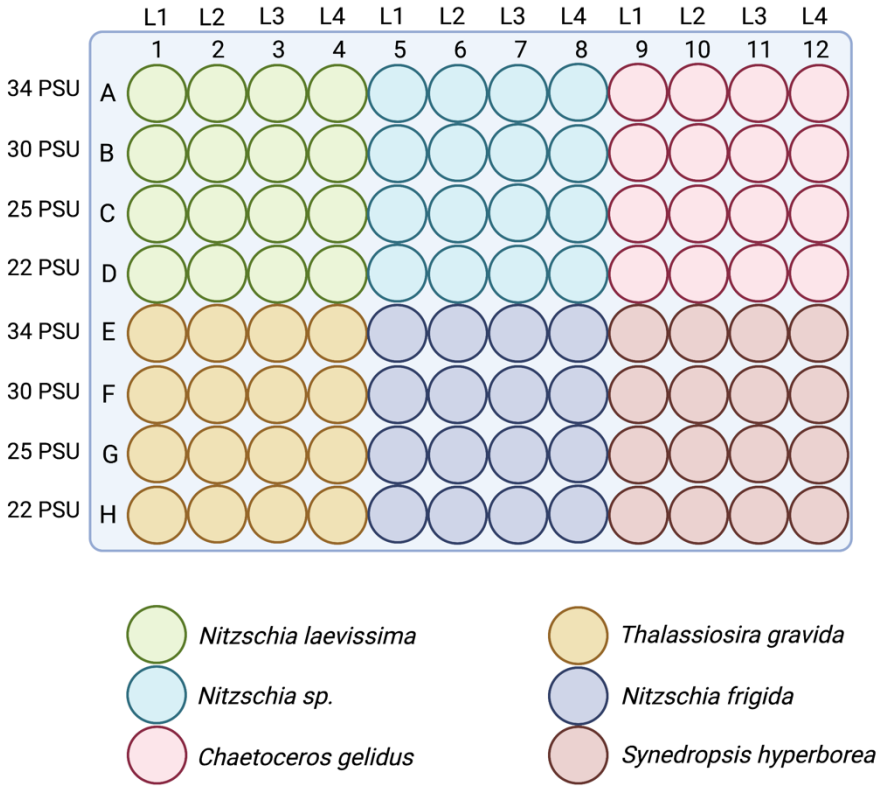

Figure 15: *The plate setup used in the second growth experiment. This experiment introduced light intensity as a new parameter, and the light intensity tested on each column is shown: L1 (12 µmol m^{-2} s^{-1}), L2 (25 µmol m^{-2} s^{-1}), L3 (35 µmol m^{-2} s^{-1}) and L4 (50 µmol m^{-2} s^{-1}). Figure created with Biorender.com.*

Additionally, the final growth experiment had replicate plates for each condition, meaning that there were in total eight 96-well plates tested.

White 96-well plates (Nunc 96-well MicroWell Plates, Thermo Fisher Scientific, USA) were used for the second growth experiment. The translucent plates from the first growth experiment were deemed insufficient, as too much light would flow between the wells.

To be able to test four different light intensities on the same 96-well plates, 96-well light panels were used (96-well RGB LED microplate light panels, Maplebear Electronics, USA) (*https://www.tindie.com/products/Maplebear/96-and-384-well-rgb-led-microplate-light-panels/*) (Figure 16, A). With replicates and in total eight 96-well plates, eight light panels were used. These light panels had 96 LED light sources that each could be programmed individually, allowing flexibility in applying the desired irradiances. The light panels were programmed with the experimental conditions, ensuring that white light was emitted, and with a plate setup as shown in Figure 15.

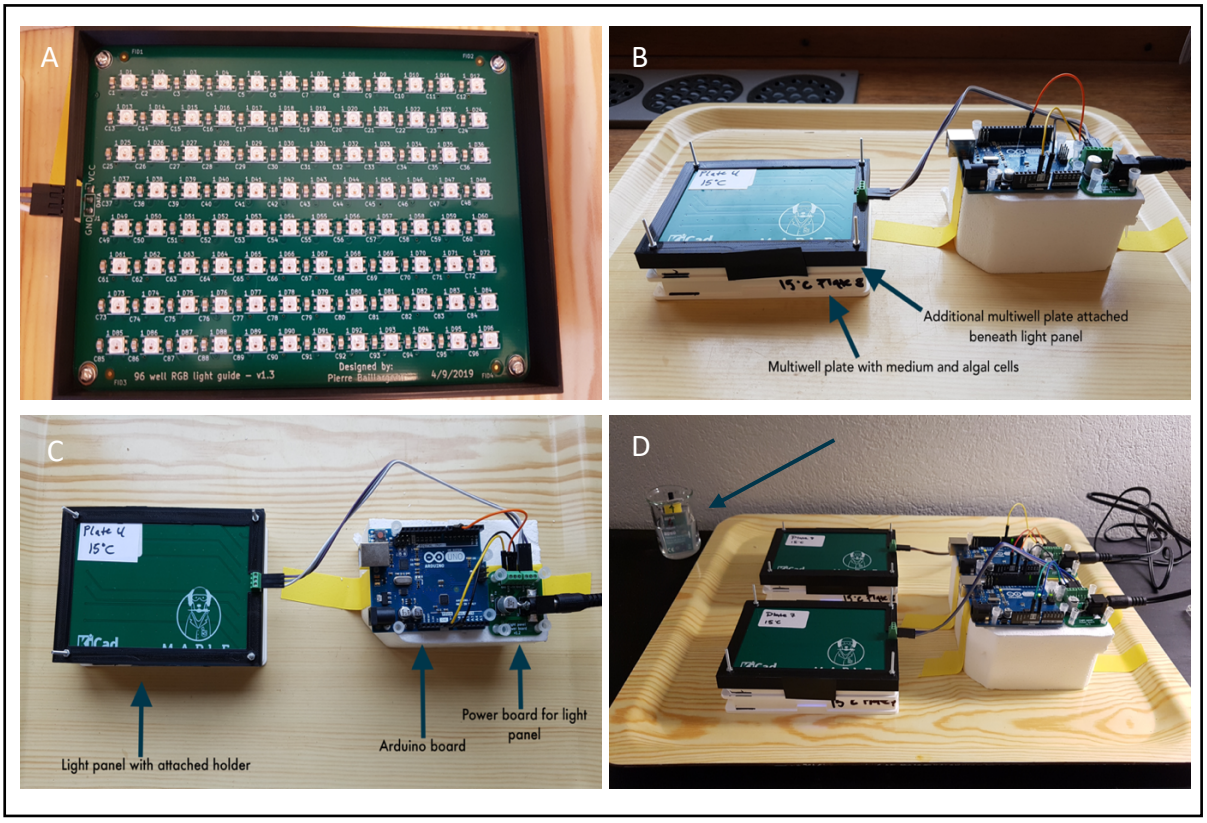

Figure 16: *(A) The 96 well RGB light panels used for the second growth experiment. These light panels were programmed to test four different light intensities on each 96-well plate concurrently. (B) The experimental setup for the final growth experiment, showing the arrangement of the 96-well plates and light panels. The light panels were held in place by a 3D printed holder, and an empty 96-well plate was placed between the light panel and plates with medium and algal cells. (C) The arrangement of the light panels and 96-well plates, the Arduino programming boards, and the power boards for the light panel. (D) Showing the finished setup of the second growth experiment, with two replicates on a tray. Four trays were made in total, each placed in a separate temperature condition. A temperature logger (arrow) was included in each temperature room to monitor that the correct temperature was maintained.*

To see how the light panels were programmed, see Appendix A: Supplementary Methods. The programming of the light panels used an Arduino Uno board (Arduino UNO Microcontroller Board, Arduino, Italy) and these boards transmitted the information with the light intensities to the light panels and were connected to the light panels throughout the entirety of the growth experiment (Figure 16, C). To provide sufficient power supply, each light panel had an accompanied 5-volt power board (96 and 384 well RGB light panel power-board v1.2, Maplebear Electronics, USA) (*https://www.tindie.com/products/Maplebear/96-and-384-well-rgb-light-panel-power-board/*) (Figure 16, C).

To reduce the risk of overheating the diatoms strains, and to efficiently channel the light into the individual wells on the multiwell plates, an empty 96-well plate was attached to each light panel. The attached 96-well plates had the plastic membrane underneath removed, and a hole on the side was made to ensure that the light panel fit properly on the plate (Figure 16, B).

On the 96-well plates with the diatom cells and growth media, a clear sealing tape (BarSeal sealing tape for 96 wells microplate, Pekema, Denmark) was adhesively added on the top of the plates. This tape ensured that the solution with medium and algal cells did not evaporate, while still allowing for diffusion of necessary gases for algal growth.

A 3D-printed holder was created for each light panel, securing the light panels and plates together (Figure 16, B). The holder and light panels were attached using screws.

The experimental setup of the second growth experiment phase can be seen in Figure 16, D. On a tray, the light panels with the associated 96-well plates, as well as the Arduino boards and the light panel power boards were arranged. The Arduino and power boards were placed on a piece of styrofoam and held in place with pipette tips. The light panels were attached to the power boards using insulated copper electrical wires and screwed into place. To see how the light panels, Arduino boards, and power supplies connect, see Appendix A: Supplementary Methods, Figure S3.

Each tray therefore had two setups with 96-well plates, light panels, Arduino boards and light panel power boards, and was placed in a separate temperature room. Additionally, for this experiment, a temperature logger was placed in a beaker filled with 34 PSU medium along with the trays to record whether there were any noticeable temperature fluctuations that could impact the results of the growth experiment.

The light panel power boards were plugged into electrical outlets with a mechanical timer that allowed for the same photoperiod cycle as was used in the first growth experiment, with 16 hours on and 8 hours off.

The plates were left in the temperature rooms for 28 days. The process of measuring the algal growth in the 96-well plates was the same as for the first growth experiment, by transporting the plates on ice and using the Synergy plate reader (Figure 14). The growth was measured daily for the first 18 days, and then intermittently for the remaining period.

2.17 Data Analysis

The same data analyses were done on the results from both growth experiments. This involved composing growth curves of the experiments and calculating growth rates. These analyses were done using the R programming software (R version 3.6.2 GUI 1.70, R Foundation for Statistical Programming, United States) as well as RStudio (RStudio 1.2.5033, R Foundation for Statistical Programming, United States).

The data files from the growth experiments were imported into R as .csv files, with information on the plate variables. This file included the unique ID of each well (composed of row letter and column number), as well as the species, salinity of medium and light intensity (only included in the .csv file for the second growth experiment) of each well.

The full script used in R for composing growth plots and calculating growth rates of the results from the growth experiments can be found in Appendix B: Scripts. It will therefore only be shortly presented in the following sections.

Growth Curves

Once the required packages were loaded and the .csv files of the plate data was imported into RStudio, the data was arranged into a "Tibble" data frame. The parameters of the experiments (salinity, temperature, and light intensity) were defined, as well as the unique IDs of the 96-well plates. This was done to ensure that RStudio understood the information in each well, which was included in the plate variable file uploaded.

After the plate information was defined, the contaminated wells were removed from the data file, ensuring more reliable growth curves. The utilized ggplot2 package allowed me to create plots visualizing the growth curves with the log in vivo fluorescence (Chlorophyll a) concentrations on the y axis and the number of days passed on the x axis, across the varying tested parameters. These growth curves were created through estimating the specific growth rate (μ), which is the rate of biomass production per unit biomass concentration per unit time. This nullified the effect of initial biomass concentration and explains how the specific growth rate (μ) is the relative change of biomass per unit time. It is therefore equal to the slope of the exponential growth phase in the growth curves of log in-vivo fluorescence against time and gives insight into the growth properties of the tested diatom strains. While these growth curves assume the log in-vivo fluorescence measurements by the plate reader to be the log chlorophyll a concentration, the fluorometer plate readers measures the amount of fluorescence. Although the emitted wavelengths of ~450 nm by the fluorometer correspond to the absorption peak of the chlorophyll a pigment, it is possible other pigments become excited and that the measurements are not necessarily the same as the actual concentration of chlorophyll a in the wells.

The script for these plots allowed for filtering out and creating growth curves, for example for each individual species or a specific 96-well plate.

Growth Rates

The growthrates-package (*https://tpetzoldt.github.io/growthrates/doc/Introduction.html*) by Thomas Petzoldt served as the basis of calculating and visualizing growth rates from the growth experiments. Once this was done, the defined data from the growth curves was loaded. Here we also included a filter for time passed, which can be seen in the full scripts in Appendix B: Scripts. A "spar" value was defined, essentially defining how well the growth rate lines need to fit the data.

The growthrates-package has many options for determining the growth rates within multiple data sets. In this thesis, the growthrates::all_splines function was used. This function uses a curve fitting technique, fitting smoothing splines to the individual growth rates based on the log-transformed in-vivo fluorescence measurements. The first derivative, which indicates the slope of the curve, is then estimated for each spline, and the largest first derivative of the splines then represents the maximum growth rate (μmax). This is the maximum growth rate achieved after passing the lag-phase, but before reaching the stationary-phase of the growth cycles. The maximum growth rates were used to create plots to visualize the growth. For all the plots, the goodness of fit R^2 value was defined at 0.5, removing all the well data that had results with R^2 below this value.

The script used allowed for flexibility in visualizing the growth rates. The plots visualizing growth rates could be filtered by individual species or parameters, enabling multiple growth rate plots to be composed.

3. Results

3.1 Part One: Molecular, Phylogenetic, and Morphological Analyses

3.2 Molecular Analysis

A part of the 28S ribosomal RNA gene coding for the large subunit (LSU) was sequenced from the six diatom strains used in this study. The sequenced part was ca 670 bp long and consisted of the D1 and D2 variable domain regions. The sequences were first edited to remove errors and then compared with reference sequences in the gene database NCBI by the BLAST algorithm (Table 6 shows the results from BLAST analyses of the analyzed strains, with their best matching DNA sequence in the NCBI nucleotide database, their pairwise similarity, and the query cover). The pairwise similarity (in %) gives an indication as to how similar the sequenced strains are to their best matching DNA sequence in the NCBI database. A higher percentage indicates a higher sequence match, and potentially how closely related the matched strains are. The query cover provides information on how much overlap there is between the obtained sequence and the reference sequence. A table with the three best NCBI database matches can be found in Appendix C: Supplementary Results, Table S12.

Table 6: *The six strains of diatoms used in this study with their respective highest BLAST results matches of the 28S rRNA gene. The description of their highest match, the pairwise ID % and the accession number of their highest match is included.*

Species	Strain ID	BLAST LSU NCBI	Pairwise ID %	Query Cover %	Accession Number
Thalassiosira gravida	HE492-7	Thalassiosira gravida voucher Iceland1 28S ribosomal RNA gene, partial sequence	100	89.01	JX069343
Nitzschia laevissima	AeN707-42	Nitzschia frustulum isolate kd92 large subunit ribosomal RNA gene, partial sequence	93.7	97.89	KX839245
Nitzschia sp.	AeN706-17	Nitzschia lecointei strain 5-21 large subunit ribosomal RNA gene, partial sequence	96.6	99.30	AF417667
Chaetoceros gelidus	AeN707-15	Chaetoceros gelidus clone D8 28S ribosomal RNA gene, partial sequence	100	94.28	KF219703
Nitzschia frigida	AeN706-4	Nitzschia lecointei strain 5-21 large subunit ribosomal RNA gene, partial sequence	96.8	100	AF417667
Synedropsis hyperborea	AeN707-94	Fragilariaceae SB-2012 strain MALINA_FT42.3PG3 28S ribosomal RNA gene, partial sequence	98.9	87.87	JQ995394

3.3 Phylogenetic Analysis

After the BLAST sequence search was completed, an alignment was constructed using the sequences from the strains in this study, reference sequences that provide phylogenetic information to the tree, and an outgroup. The phylogenetic analysis maximum likelihood was then performed. Figure 17 shows the phylogenetic tree with *Bolidomonas pacifica* (Accession number AB430658.1), an algal species closely related to diatoms, as an outgroup. The tree was constructed using 200 bootstraps, indicating the number of iterations the tree was resampled in the algorithm. The bootstrap values can be seen on Figure 17 as numerical values between the nodes. These values represent the number of times the nodes are recovered through resampling, which denotes the likelihood of the shown branching pattern. The branch lengths of the tree can be compared with the scale bar, which gives an estimation of approximately 0.09 nucleotide substitutions per site, calculated through the number of substitutions divided by the length of the sequences.

The sequences from this study do not have accession numbers as they have not yet been submitted to a genetic sequence database. The sequences will be submitted to the GenBank (NCBI) database at a later point.

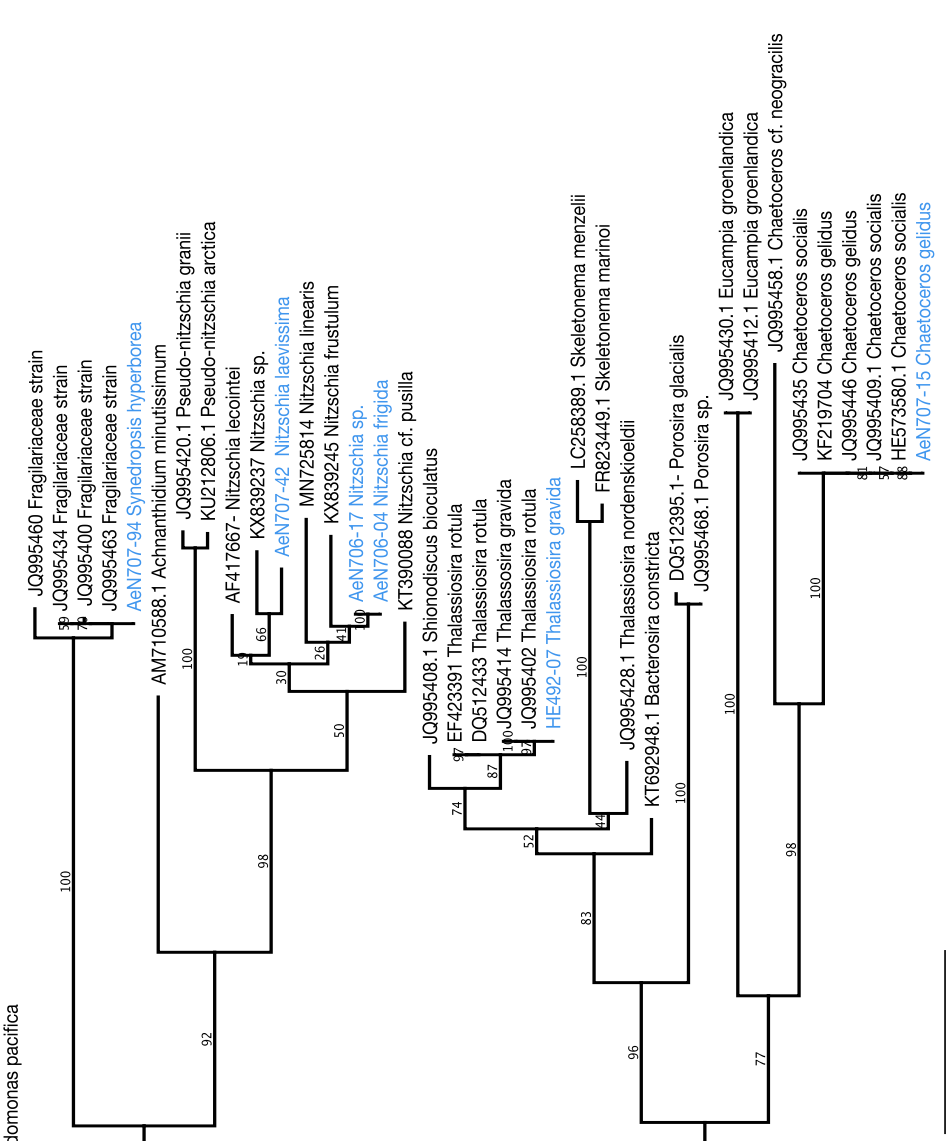

Figure 17: *Maximum likelihood (RAxML) phylogenetic tree based on the 28S rRNA gene from the strains used in this study. Sequences of reference species with varying taxonomy were added to indicate possible evolutionary relationships and taxonomic placement. The tree was constructed with 200 bootstraps, and the strains used in this study are indicated in blue. The scale-bar of the tree is a genetic distance of 0.09 base pairs, indicating the number of nucleotide substitutions per site. The outgroup for this phylogenetic tree is AB430658.1 Bolidomonas pacifica.*

3.4 Morphological Analysis

3.5 *Nitzschia laevissima*

The AeN707-42 *Nitzschia laevissima* strain (Table 1) is a pennate diatom isolated from a melt pond on the surface of the sea-ice (Figure 18).

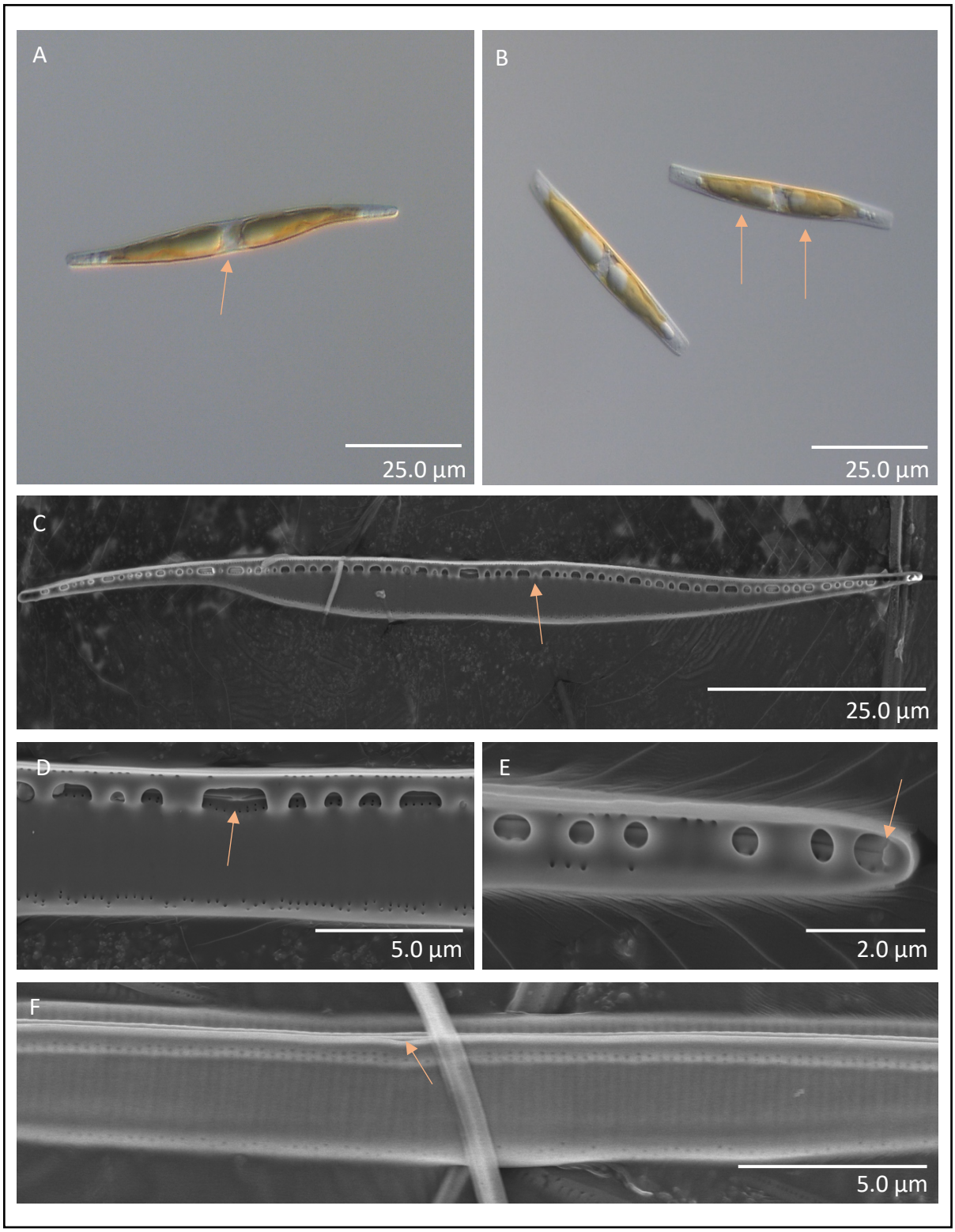

Figure 18: *Strain AeN707-42 Nitzschia laevissima Differential Interference contrast (DIC) LM (A-B); SEM (C-E). (A) Single cell from valve view, showing the typical sigmoid cellular shape and the nucleus (arrow). (B) Single cell from girdle view, showing the two chloroplasts within each cell (arrows). (C) Inside view of a valve, showing the stria with areolae concentrated at the valve's edge and a large hyaline region. Fibulae structures (arrow) can be seen running along the length of the valve. (D) Inside view of a valve, showing the central nodule (arrow) and the canal raphe system. (E) The apex end of the valve is rounded, and the helictoglossa (arrow) can be seen, with the raphe behind in the raphe canal. (F) Outer view of the valve, showing the central nodule (arrow) with the associated proximal raphe ends in the keel, the elevated ridge containing the raphe.*

The strain in culture was found to be a solitary species, with no observations of colony formation. The cells of *N. laevissima* are typically 70-90 µm long and have a characteristic sigmoid shape (Figure 18, A), with each cell containing two large chloroplasts (Figure 18, B). The inside view of a valve shows that *N. laevissima* has relatively few areolae, all concentrated on the edge of the valve, with a dominating hyaline area (Figure 18, C). This hyaline area lacks pores and is otherwise unornamented silica. The stria containing areolae run along the upper and lower edges of the valve (Figure 18, C and D). Both the central nodule (Figure 18, D), the densely silicified region by the proximal raphe ends, and the eccentrically placed raphe, are contained in a raphe canal system. The raphe, the slit in the siliceous valve that aids in the cell's motility, is contained within a keel, a raised structure that elevates the raphe (Figure 18, F). This is supported by silica branches called fibulae (Figure 18, C, D and E) running along the entirety of the valve to the apex ends. *N. laevissima* has rounded apex valve ends, and the helictoglossa, the termination of the raphe at the apex can be seen (Figure 18, E).

The AeN707-42 *Nitzschia laevissima* strain had a 93.7% similarity in the 28S rRNA gene with a *Nitzschia frustulum* (Accession number KX839245) strain isolated from Malaysia (Table 6) and a 93.5% similarity in the 28S rRNA gene with a *Nitzschia cf. pusilla* (Accession number KT390088) (Table S12, Appendix C: Supplementary Results) strain isolated from the South China Sea. The phylogenetic tree did not place *N. laevissima* into a clade with either of these matches, instead placing it into a clade with a *Nitzschia* sp. (Accession number KX839237) isolated from Malaysia (Figure 17). This clade had relatively low support, having a bootstrap value of 66.

3.6 *Nitzschia frigida*

The AeN706-4 *Nitzschia frigida* strain (Table 1) is a benthic pennate diatom isolated from the sea-ice core (Figure 19).

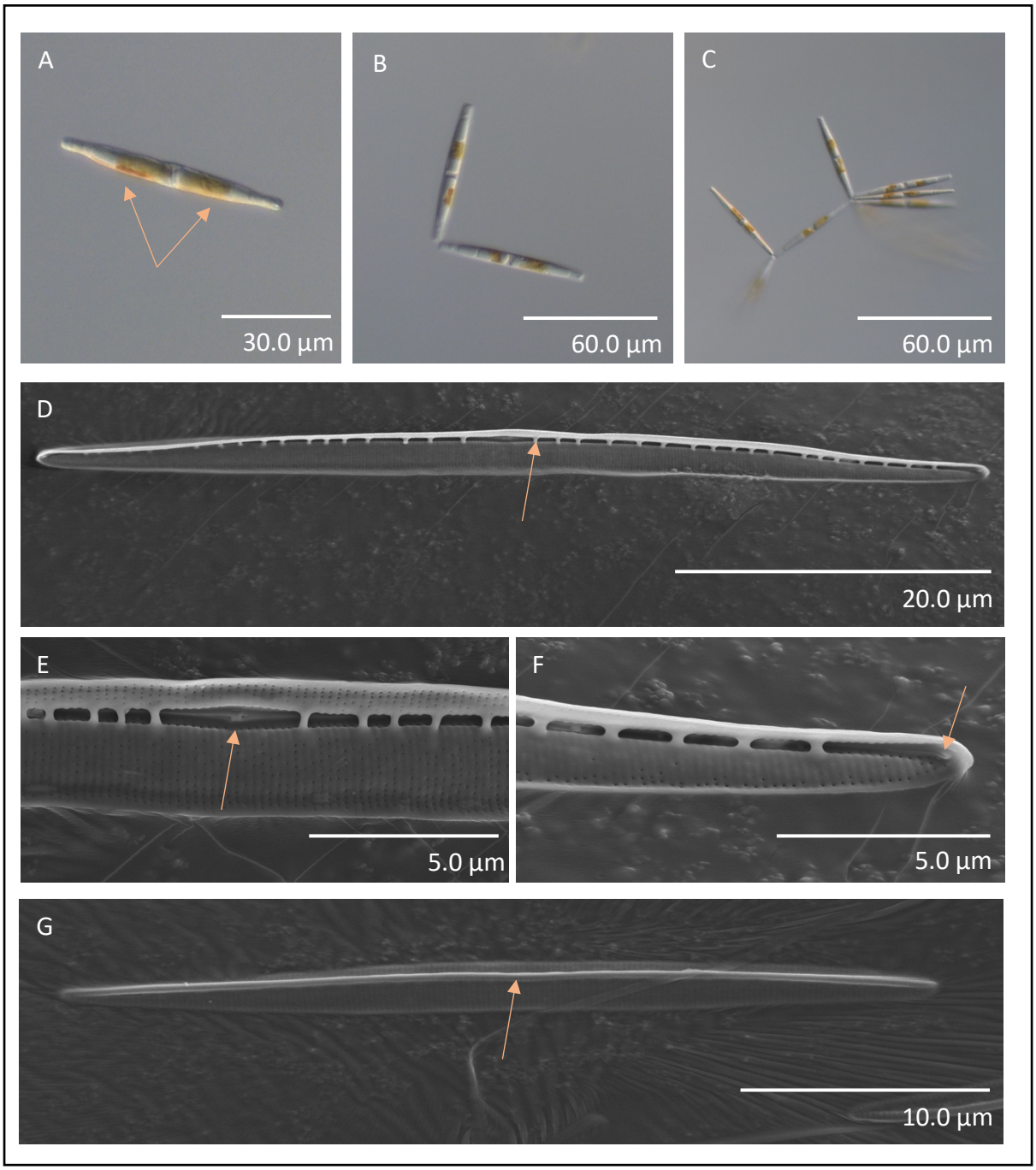

Figure 19: *Strain AeN706-4 Nitzschia frigida Differential Interference contrast (DIC) LM (A-C); SEM (D-G). (A) Single cell from valve view, showing the two chloroplasts present in each cell (arrows). (B) Single cells from the girdle view. (C) Colony of N. frigida with the typical stepping pattern shape. (D) Inside view of an elliptically shaped valve, with parallel running striae, containing intermittently placed pores. Fibulae structures (arrow) can be seen running along the length of the valve, with a wide space at the apex ends of the valve and by the central nodule. (E) Inside view of a valve, showing the central nodule (arrow) and the canal raphe system. (F) The apex end of the valve is rounded, and the helictoglossa (arrow) can be seen, with the raphe behind in the raphe canal. (G) Outer view of the valve showing the keel (arrow), the elevated ridge containing the raphe.*

The strain in culture was observed to make typical *N. frigida* colonies with a stepping formation, connecting at the ends of their individual frustules (Figure 19, C). This was common in the observed strain, with multiple separate colonies forming. Single cells of *N. frigida* were also commonly seen, having an elliptical shape, and containing two large chloroplasts (Figure 19, A). The cells were typically 80-100 µm in length. The keel, a thick silica structure containing the raphe within a canal, can be seen in the interior of the valves (Figure 19, G). The keel is supported by an intermittently placed system of fibulae (Figure 19, D). At the rounded apex end of the valve, there is no fibulae and the termination of the raphe, the helictoglossa, can be seen (Figure 19, D). The central nodule, the heavily silicified region between the proximal raphe ends, was observed in the interior view of the valves (Figure 19, E). The fibulae surrounding the central nodule region had a wider separation than the remaining fibulae. The striae along the interior of the valve consist of parallel running areolae (Figure 19, D), which appeared to be sporadically placed.

The AeN706-4 *Nitzschia frigida* strain shared a 96.8% similarity in the 28S rRNA gene with a *Nitzschia lecointei* (Accession number AF417667) strain isolated from the Antarctic Ross Sea (Table 6), but these did not form a clade in the phylogenetic tree (Figure 17). The AeN706-4 *Nitzschia frigida* strain formed a solid clade with the AeN706-17 *Nitzschia* sp. strain used in this study, with a bootstrap value of 100 (Figure 17). These strains of *Nitzschia frigida* and *Nitzschia* sp. formed a clade with a *Nitzschia frustulum* (Accession number KX839245) (Table S12, Appendix C: Supplementary Results) strain isolated from Malaysia, which shared a 96.2% similarity in the 28S rRNA gene with *N. frigida*.

3.7 *Chaetoceros gelidus*

The AeN707-15 *Chaetoceros gelidus* strain (Table 1) is a planktonic centric diatom isolated from the plankton community (Figure 20).

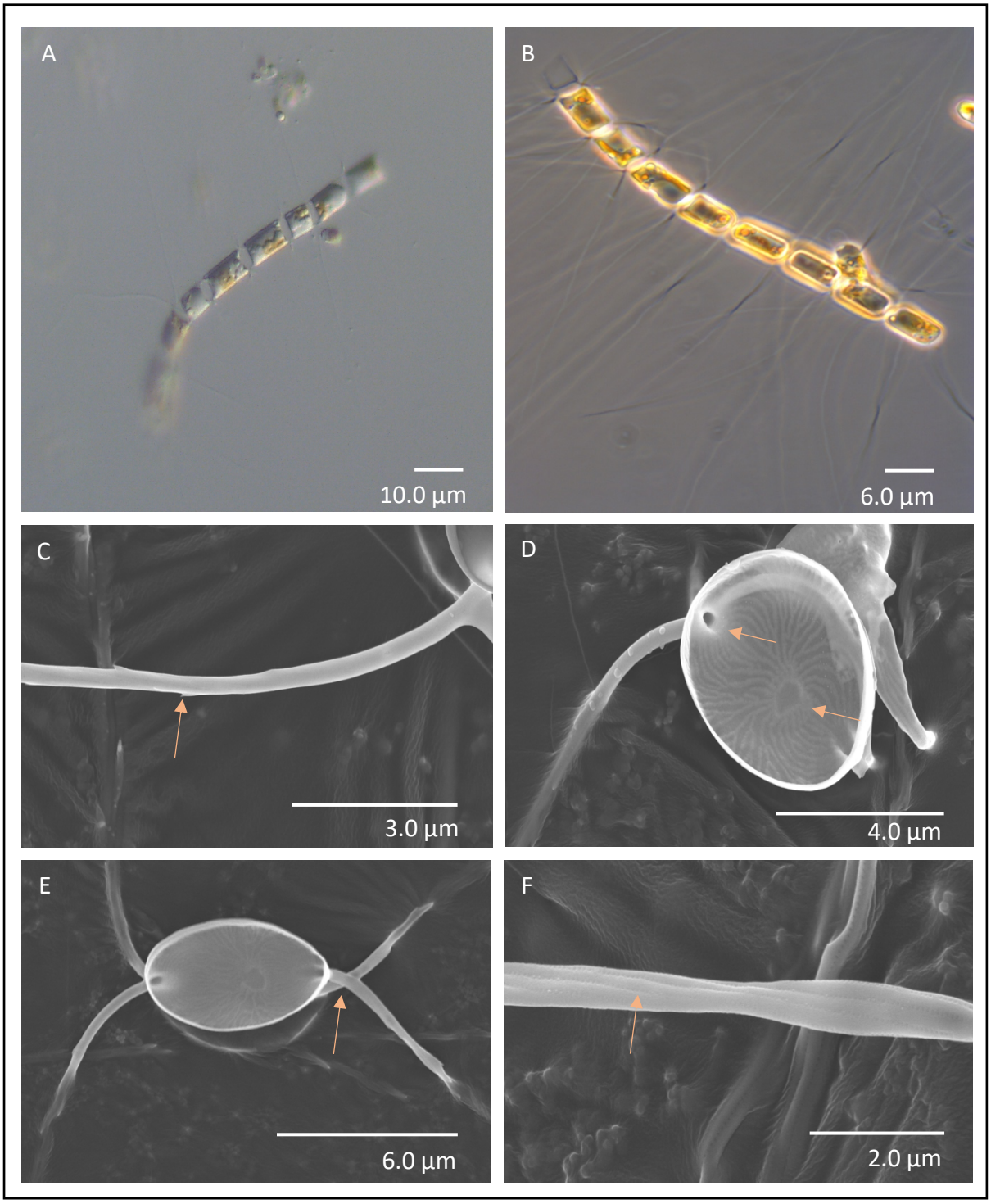

Figure 20: *Strain AeN707-15 Chaetoceros gelidus Differential Interference contrast (DIC) LM (A); Phase Contrast LM (B); SEM (C-G). (A-B) Single chains from girdle view, showing elongated cells that are longer than they are wider. The cells have three shorter setae and one longer seta. Between each cell in a chain there is a somewhat elliptically shaped aperture (arrow). (C) The shorter setae have spirally arranged spines (arrow). (D) Inside view of a valve, with the indicated pore (arrow) at the base of the setae. The annulus (arrow) was observed, with branching costae. (E) Inside view of a valve, showing the four setae. Two of the setae cross-over each other (arrow) and the pores at the base of each pair of setae are shown. (F) The longer smooth setae, seen to have no spines and spirally arranged pores (arrow).*

The strain in culture was observed to make colonies in a mucilage matrix, with individuals joining together through the aid of their setae. The setae were observed to branch from the edge of the valve (Figure 20, E) and some setae were also observed to cross over at the base (Figure 20, E). The setae were observed to have spirally arranged pores (Figure 20, F), with the shorter setae having spines (Figure 20, C) while the longer setae were mostly smooth (Figure 20, F). The longer setae had a small number of spines at the terminal ends but remained mostly spineless. The pore on the interior of the valve at the base of the branching setae was close to the valve edge (Figure 20, D). The annulus, the silica that is first formed during cellular division among centric diatoms, can be observed on the interior of the valve with branching costae (Figure 20, E). The cell shape of *C. gelidus* is rectangular, with elongated cells (Figure 20, A and B) each containing one chloroplast. The aperture windows between the cells were small (Figure 20, A and B) and had an elliptical shape.

The AeN707-15 *Chaetoceros gelidus* strain shared a 100% similarity in the 28S rRNA gene with a *Chaetoceros gelidus* (Accession number KF219703) strain isolated from Denmark (Table 6), as well as a 100% similarity in the 28S rRNA gene with a *Chaetoceros socialis* (Accession number JQ995411) (Table S12, Appendix C: Supplementary Results) isolated from the Arctic. These sequences were not included in the phylogenetic tree. The AeN707-15 *Chaetoceros gelidus* strain formed a solid clade with the other *C. gelidus* and *C. socialis* strains included, forming a monophyletic group with a bootstrap value of 100 (Figure 17). This clade also formed a monophyletic group with the *Chaetoceros cf. neogracilis* (Accession number JQ995458.1) strain, with a bootstrap value of 98 (Figure 17).

3.8 *Thalassiosira gravida*

The HE492- 7 *Thalassiosira gravida* strain (Table 1) is a planktonic centric diatom isolated from the plankton community (Figure 21).

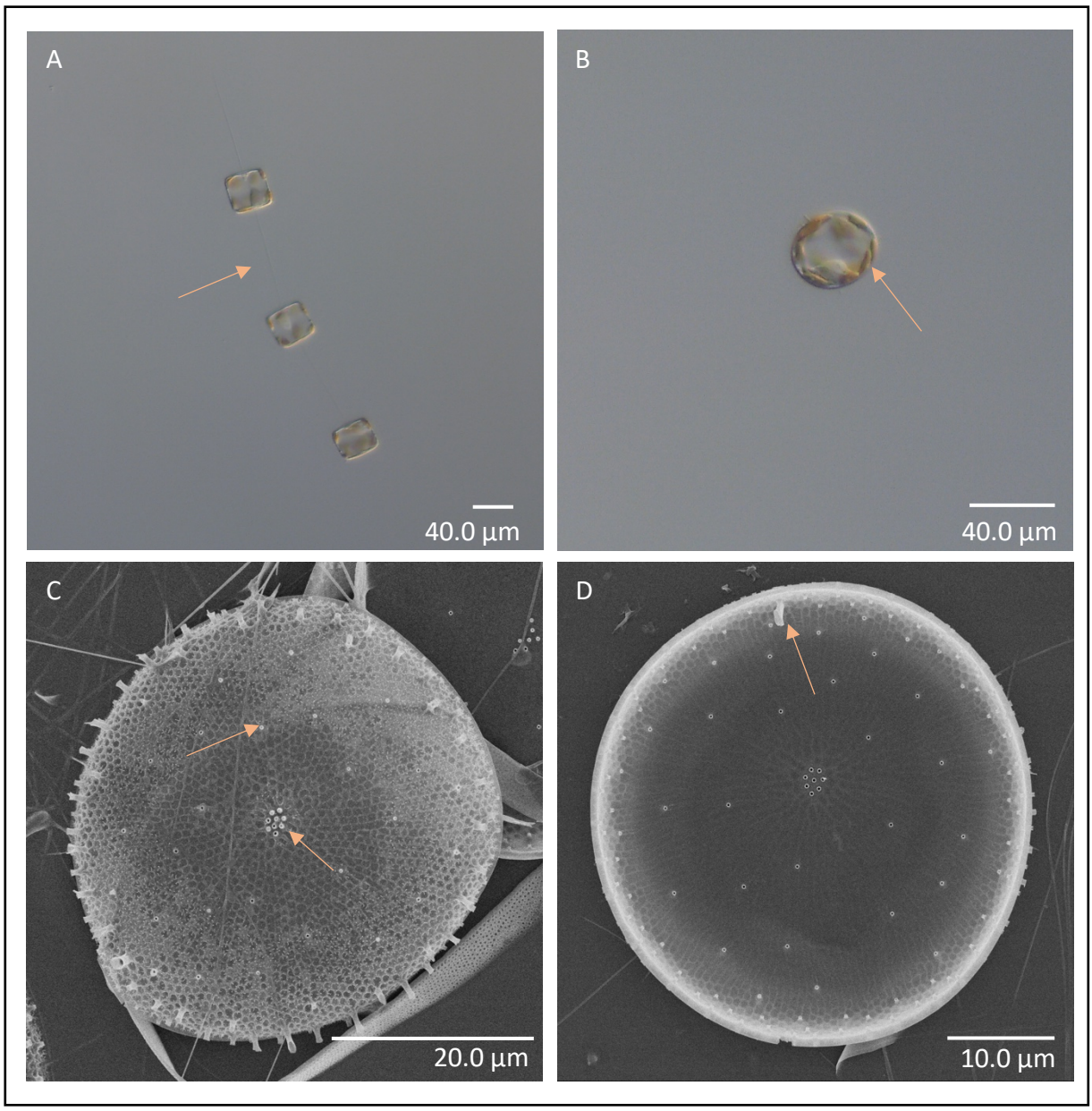

Figure 21: *Strain HE492-7 Thalassiosira gravida Differential Interference contrast (DIC) LM (A-B); SEM (Photos by Luka Supraha) (C-D). (A) Single chain from girdle view, with rectangular shaped cells connected by organic threads (arrow) at the valve margins. (B) Single cell from valve view, containing multiple lobe shaped chloroplasts (arrow). (C) Exterior valve view showing the multiple fultoportulae processes across the valve (arrow), as well as the central cluster of fultoportulae (arrow). The exterior opening of the single rimoportula can also be seen. (D) Interior valve view, showing the single rimoportula opening (arrow). Note also the interior view of the fultoportulae across the valve, including the central cluster of fultoportulae. Surrounding the central fultoportulae is the annulus, with the branching costae extending across the valve.*

The strain in culture was observed to make colonies with multiple cells in a chain (Figure 21, A) connected with organic threads between the cells. *T. gravida* has rectangularly shaped cells (Figure 21, A) when seen from the girdle view, and each cell contains multiple lobe shaped chloroplasts (Figure 21, B). The organic threads connecting the cells in a chain are extruded from a collection of centrally located fultoportulae (Figure 21, C), processes passing through the valve. The valves are approximately 40-50 µm in diameter. Spread across the valves are additional fultoportulae (Figure 21, C and D), as well as a single rimoportula (Figure 21, C and D) which also secretes organic compounds. Surrounding the central fultoportulae is the annulus (Figure 21, D), the silica first formed in the valve during cellular division, and the system of branching costae (Figure 21, D) which creates the radially arranged areolae in the valve. Each areola is additionally covered with a cribrum velum, a thin layer of silica with pores.

The HE492-7 *Thalassiosira gravida* strain shared a 100% similarity in the 28S rRNA gene with a *Thalassiosira gravida* (Accession number JX069343) strain isolated from Iceland (Table 6), as well as a 99.5% similarity in the 28S rRNA gene with a *Thalassiosira rotula* (Accession number JX069335) strain (Table S12, Appendix C: Supplementary Results). These strains were not included in the phylogenetic tree. Instead, other reference sequences of various *T. gravida* and *T. rotula* strains were included, which together with the HE492-7 *Thalassiosira gravida* strain, formed a monophyletic group with a bootstrap support of 87 (Figure 17).

3.9 *Nitzschia* sp.

The AeN706-17 *Nitzschia* sp. strain (Table 1) is an unidentified species likely belonging to the *Nitzschia* genus. It is a pennate diatom isolated from a melt pond on the surface of the sea-ice (Figure 22).

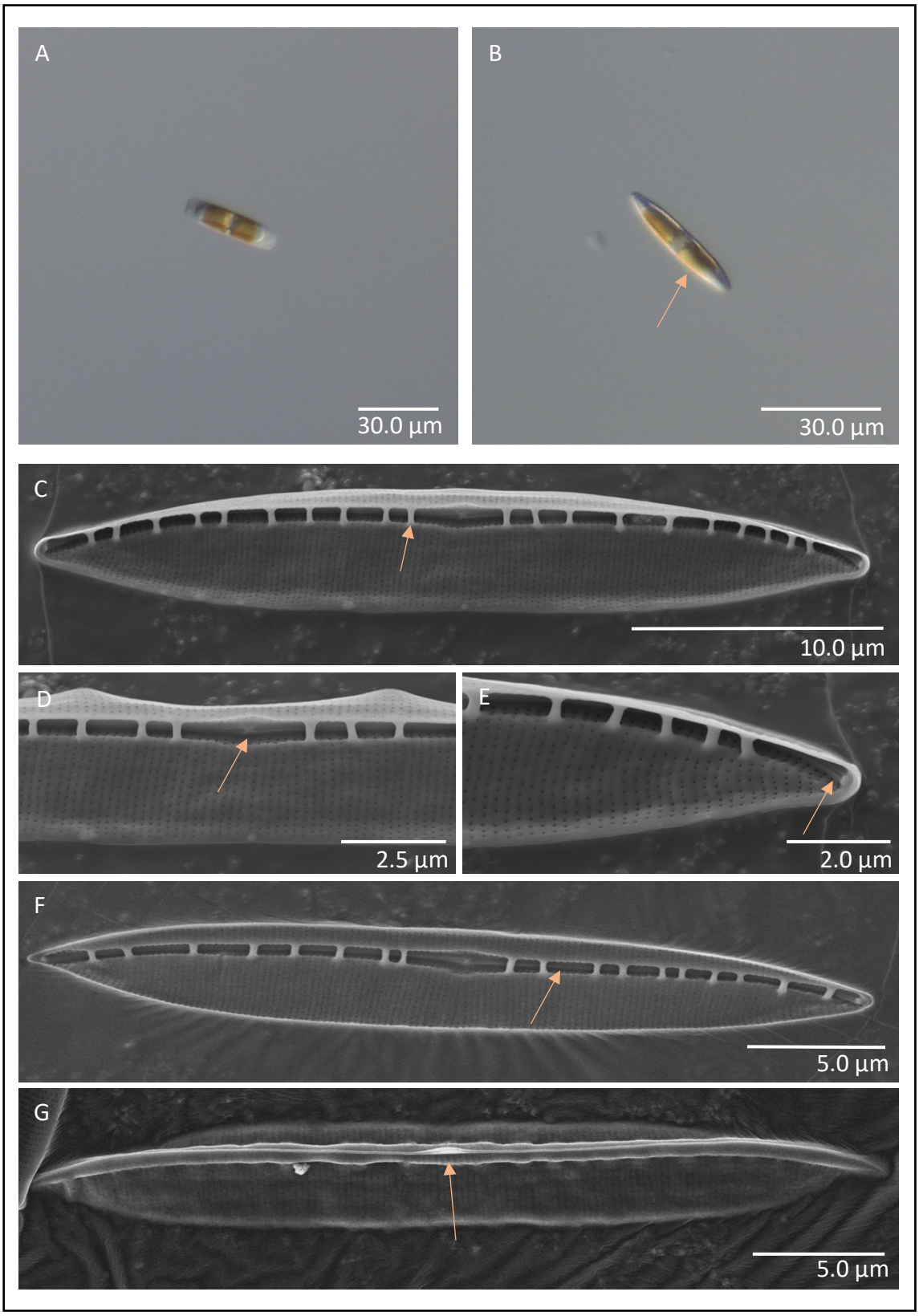

Figure 22: *Strain AeN706-17 Nitzschia sp. Differential Interference contrast (DIC) LM (A-B); SEM (C-G). (A) Single cell from girdle view. (B) Single cell from valve view, showing the two chloroplasts within each cell (arrow). (C) Inside view of an elliptically shaped valve, with fibulae (arrow) running along the entirety of the valve supporting the raphe canal system. Note also the parallel stria with areolae ornamenting the entirety of the valve. (D) Inner view of valve, magnified to show the central nodule (arrow) with the proximal raphe ends on each side, and the wide space between the fibulae by the central nodule. (E) Apex end of a valve, showing the helictoglossa (arrow). (F) Inside view of valve, showing clearly the interior view of the raphe canal system (arrow), where the raphe is elevated by the heavily silicified keel. (G) Exterior valve view, showing the canal raphe system with the central nodule (arrow), the keel, and the elevated raphe running along the outside of the valve.*

While the strain in culture was observed to make ribbon forming colonies, solitary cells dominated (Figure 22, A and B). The cells contain two large chloroplasts (Figure 22, B) and are approximately 30-40 µm long with an elliptical cell shape when seen from the valve view (Figure 22, B). From the girdle view, the cells are rectangular in shape (Figure 22, A). The interior of the valve shows that the strain is a raphid diatom, with a canal raphe system (Figure 22, C). Similar to the strains of *Nitzschia frigida* and *Nitzschia laevissima* examined in this study, the *Nitzschia* sp. strain has a heavily silicified keel that elevates the raphe (Figure 22, C, F and G), supported by a system of fibulae (Figure 22, C and F) running along the interior of the valve. Surrounding the central nodule (Figure 22, D), the heavily silicified area between the proximal raphe ends, the fibulae are more widely spaced. The apex ends of the valves are rounded (Figure 22, E) and the end of the raphe, the helictoglossa, can be seen (Figure 22, E). The valves have parallel running stria with areolae (Figure 22, C). These areolae are continuously placed along the entirety of the valve, and there are appeared to be no dominating hyaline regions.

The AeN706-17 *Nitzschia* sp. strain shared a 96.6% similarity in the 28S rRNA gene with a *Nitzschia lecointei* (Accession number AF417667) strain isolated from the Antarctic Ross Sea (Table 6). The phylogenetic tree placed the AeN706-17 *Nitzschia* sp. strain in a monophyletic group with the AeN706-4 *Nitzschia frigida* strain used in this study, with a bootstrap value of 100 indicating strong support for an evolutionary relationship (Figure 17).

3.10 *Synedropsis hyperborea*

The AeN707-94 *Synedropsis hyperborea* strain (Table 1) is a benthic pennate diatom isolated from a sea-ice core (Figure 23).

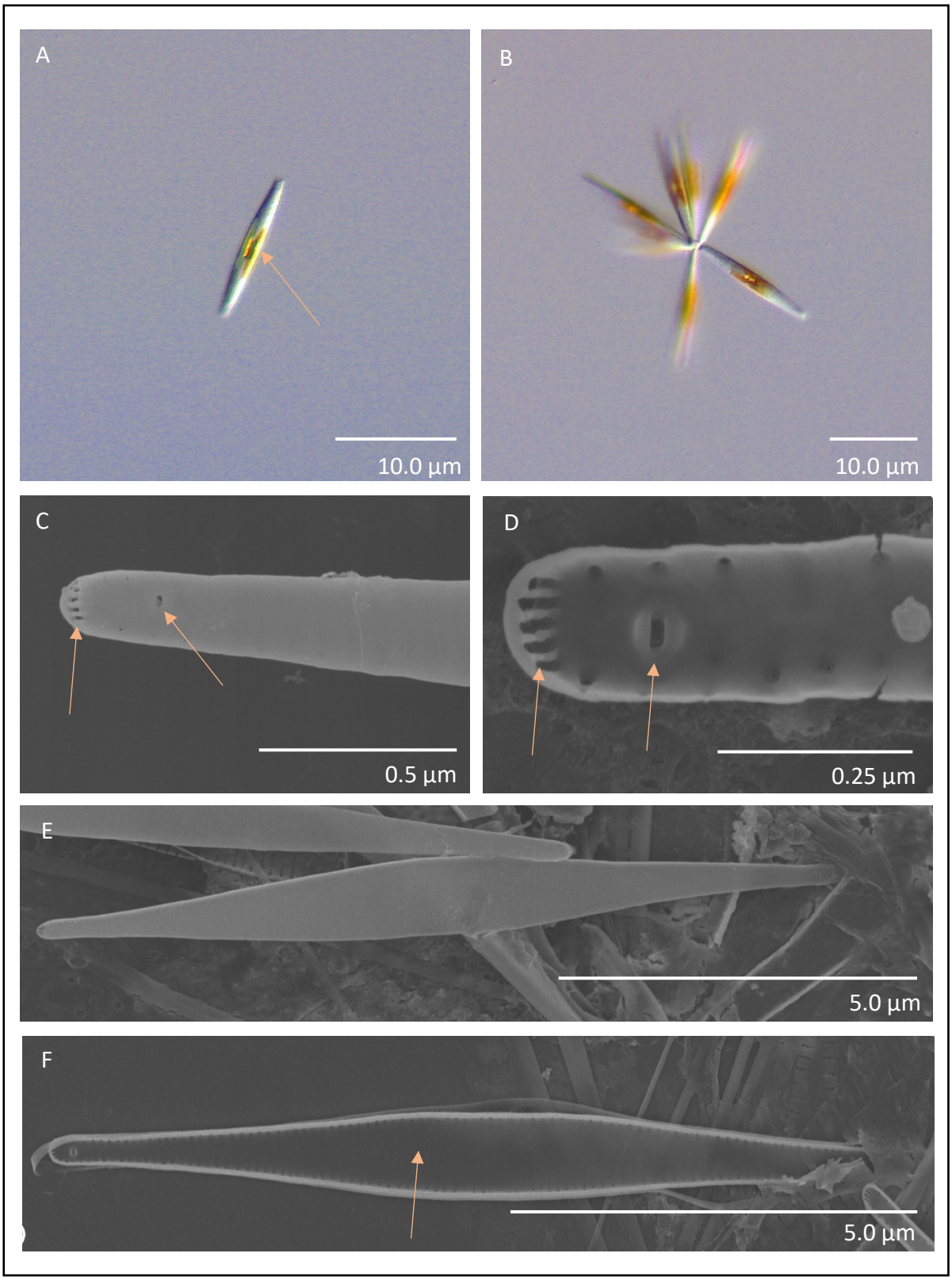

Figure 23: *Strain AeN707-94 Synedropsis hyperborea Differential Interference contrast (DIC) LM (A-B) (Photos by Luka Supraha); SEM (C-F) (Photos by Luka Supraha). (A) Single cell from valve view, showing the rostrate shape and the two plate like chloroplasts (arrow). (B) Colony formation of S. hyperborea, with the typical stellate pattern. (C) Exterior view of the apex end of the valve. Note the 5 apical slits (arrow) as well as the labiate process (arrow). (D) Interior view of the apex end of a valve, with the apical slits (arrow) and the labiate process (arrow). (E) Exterior view of entire valve, note lack of raphe and ornamentation. (F) Interior view of entire valve, showing the uniseriate striae placed at the edge of the valve and the hyaline sternum (arrow) which occupies almost the entirety of the valve.*

The strain has a rostrate cell shape (Figure 23, A), although this varied among the cells. The cells each have two plate like chloroplasts (Figure 23, A) and were approximately 10-15 µm in length. The strain in culture was observed to commonly make stellate colony formations (Figure 23, B) with cells adjoining at the apex ends of the frustules. *S. hyperborea* is an araphid diatom, lacking a raphe system. This can be seen when examining the unornamented valve, with the hyaline sternum, the thickened silicate region first developed in pennate diatoms during cellular division, dominating the valve face (Figure 23, E and F). The areolae are arranged in uniseriate striae (Figure 23, F), which are placed at the valve margin. At the rounded apex ends of the valves, there are 5 apical slits (Figure 23, C and D) and a single labiate process (Figure 23, C and D), a hollow tube of silica perforating the valve.

The AeN707-94 *Synedropsis hyperborea* strain shared a 98.9% similarity in the 28S rRNA gene with an unidentified Fragilariaceae strain (Accession number JQ995394) isolated from the Arctic (Table 6). This sequence was not included in the phylogenetic tree. The phylogenetic tree showed *S. hyperborea* forming a monophyletic clade with various other Fragilariaceae strains, which had a strong bootstrap support value of 100 (Figure 17).

3.11 Part Two: Growth Experiments

Two growth experiments were conducted in this study testing the effects of salinity, temperature, and light intensity on the growth of six species of Arctic diatoms.

3.12 First Growth Experiment: Salinity and Temperature Responses

The first growth experiment tested four different salinities (22, 25, 30 and 34 PSU) and four temperatures (4°C, 6°C, 11°C, and 15°C) on the strains of diatoms. This growth was measured in log transformed chlorophyll a concentration, which is summarized in Figure 24.

These growth curves (Figure 24) are visualizations of the specific growth rates in response to salinities and temperature, with log chlorophyll concentration as a function of time.

The maximum growth rate (μmax) is the maximum growth rate achieved during the exponential phase of the growth period in each well across the entire growth experiment. These are plotted with a fitted curve in Figure 25, showing how the maximum growth rate changes across the parameter combinations.

Across all habitats associated with sea-ice (plankton, ice cores, and melt ponds), it appears that the lowest temperature and salinity combinations are most conducive to diatom growth (Figure 25).

Each salinity and temperature combination had four replicate points, as represented in Figure 24. The averages of these points were calculated to determine the average maximum growth rates from the exponential phase of the growth periods at each salinity and temperature combination (Figure 26).

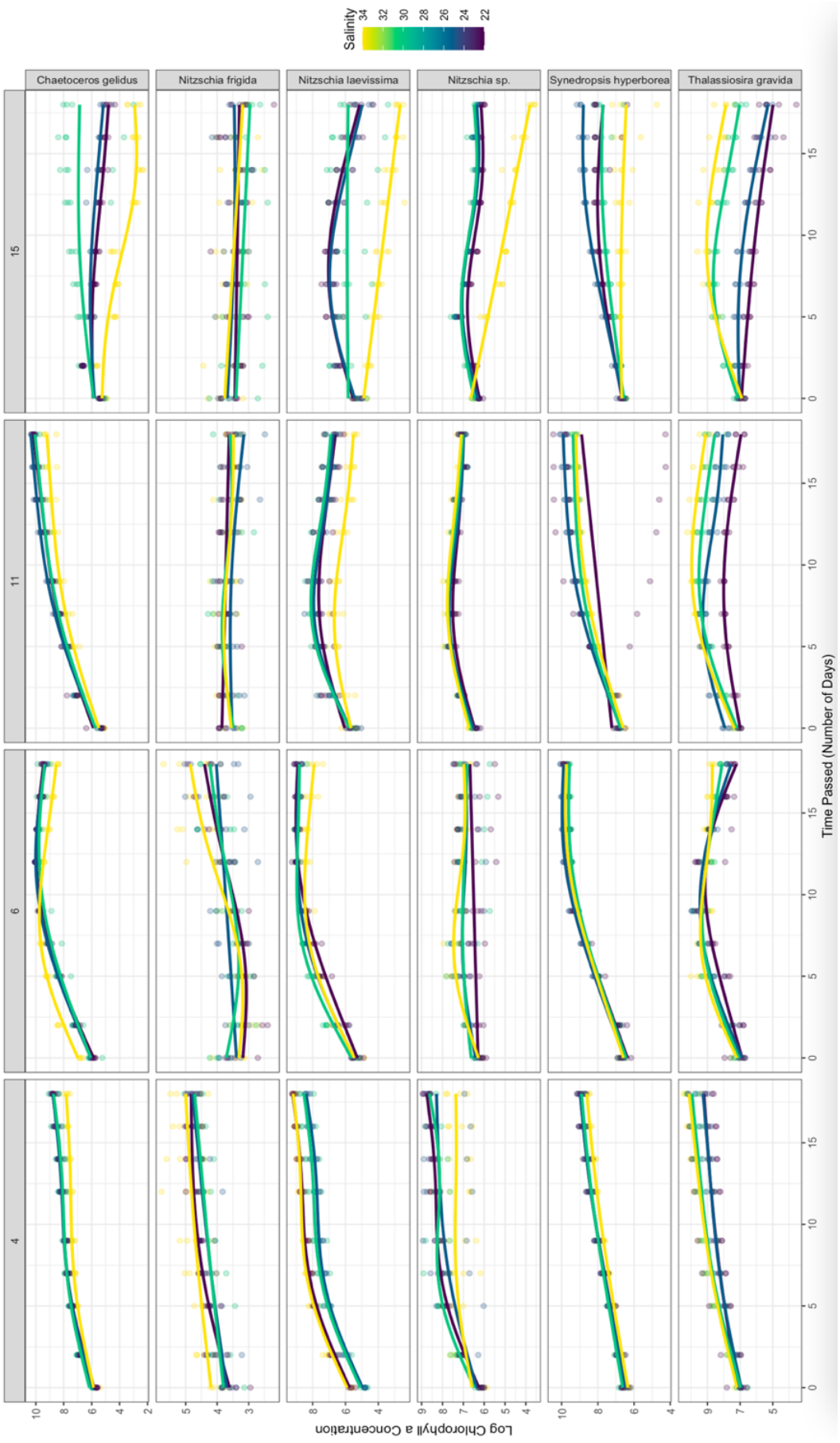

Figure 24: *Growth curves of the six diatom species summarized. The growth curves (displayed with the stat_smooth function) are visualized with the log chlorophyll a concentration (relative units) over time (days) in response to the various salinities and temperature parameters. Note differing y-axes values.*

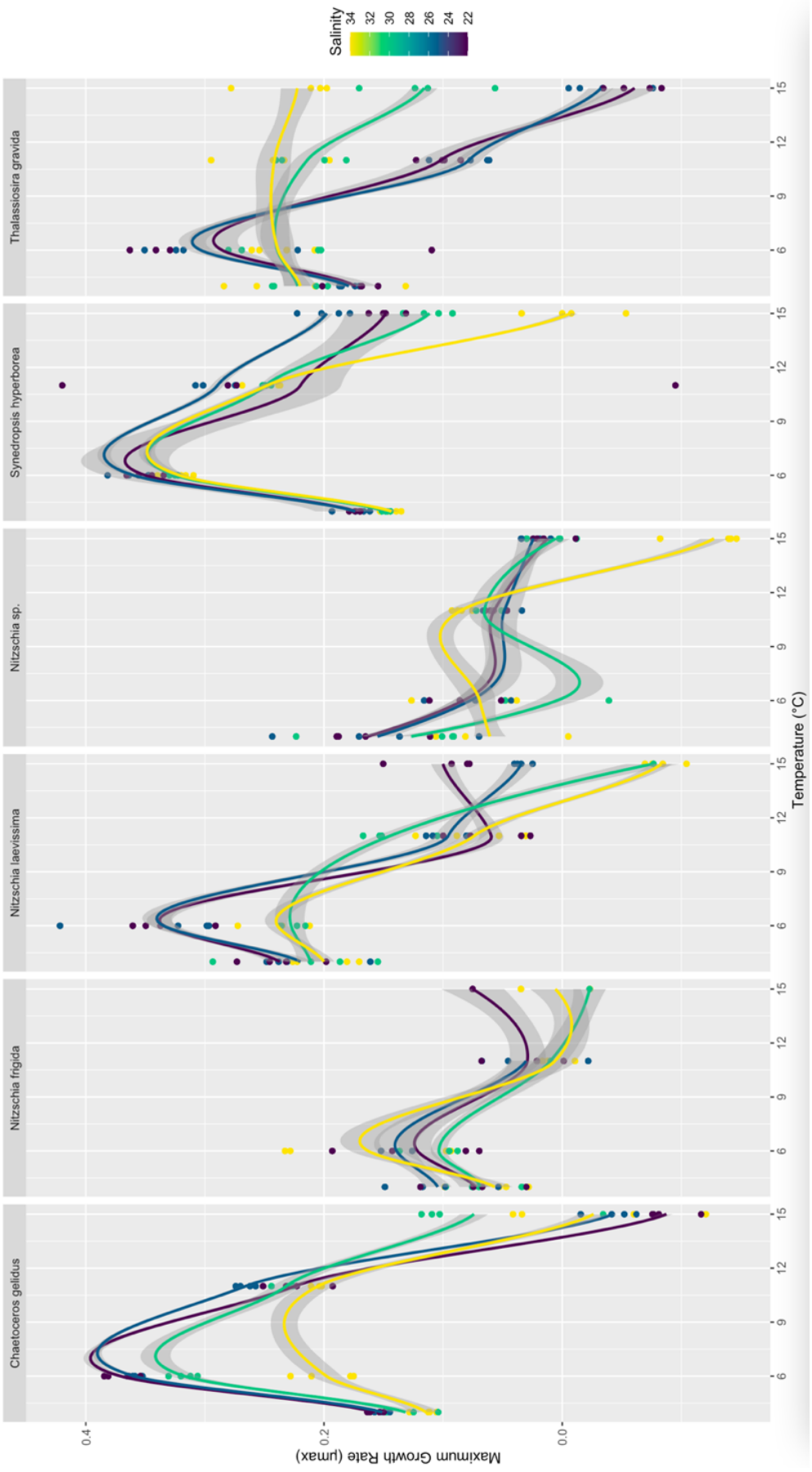

Figure 25: *Maximum growth rate (µmax) from the first growth experiment as a function of the tested temperature and salinity conditions. Each point represents the µmax of a specific well with the defined parameters, and the maximum growth rate for each well is thus plotted. A fitted curve is applied to the maximum growth rates, showing the trends across the various parameters. The associated confidence bands represent a 95% confidence interval.*

In general, it appears that temperature is the main factor influencing the growth rate of the sea-ice associated diatoms. Across all temperatures, the salinity response curves have approximately the same trajectories (Figure 25). The combination of higher salinities and higher temperatures appear to lead to lower growth rates across all species except *Thalassiosira gravida*, which appears to tolerate higher salinities at all the tested temperatures (Figure 26, Table 7). The effect of higher salinities and higher temperature can be seen with the poor growth rates of *Nitzschia* sp., *Nitzschia frigida*, *Synedropsis hyperborea*, *Nitzschia laevissima,* and *Chaetoceros gelidus* at the combination of 34 PSU and 15°C (Figures 25 and 26, Table 7). This combination of the highest tested salinity and temperature, appears to be the only parameter combination that *Synedropsis hyperborea* does not appear to grow at (Figures 25 and 24).

All species grew at the lowest tested temperatures (4°C and 6°C), while they had poorer growth rate at the highest tested temperatures (11°C and 15°C) (Figures 25 and 26, Table 7). The *Nitzschia* sp. strain appears to have the lowest salinity and temperature tolerance, growing well only at 4°C and the lower salinities (Figures 25 and 26, Table 7). The *Nitzschia frigida* strain had relatively poor growth at all parameter combinations (Figure 26, Table 7) and is possibly the species with the most restricted tolerance tested in this study.

While the higher temperatures appear to lead to lower growth in both the planktonic species, *Chaetoceros gelidus* and *Thalassiosira gravida*, they appear to have the wide thermal tolerances, growing at temperatures up to 11°C (*C. gelidus*) and 15°C (*T. gravida*) (Figure 26, Table 7).

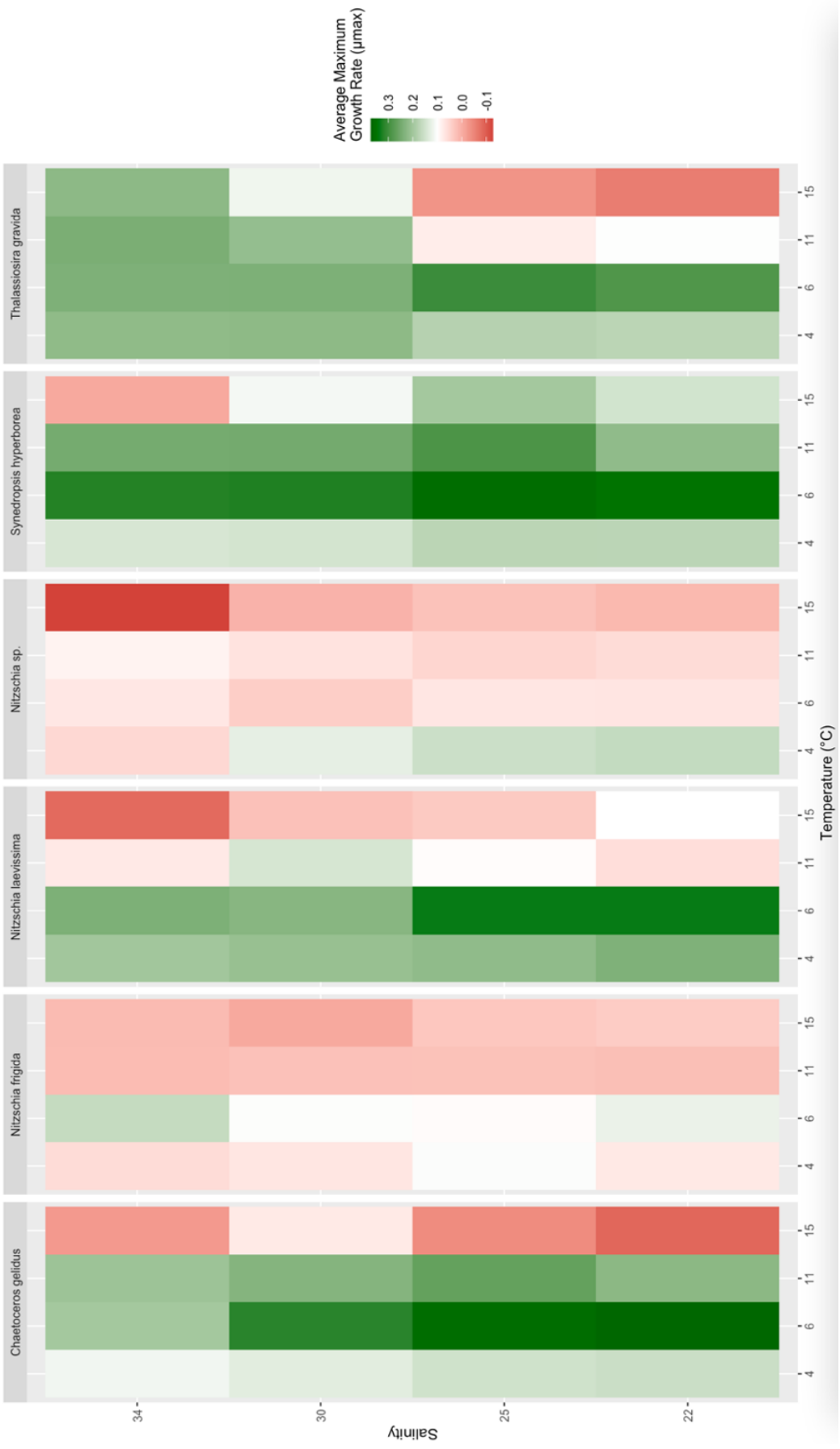

Figure 26: *Visualization of the average maximum growth rate (μmax) with each parameter combination. The midpoint is defined at 0.1 μmax, highlighting positive growth above that threshold.*

Table 7: *An overview of growth responses of individual strains based on their growth curves and growth rates in Figures 24-26.*

Species	Strain ID	Classification	Habitat	Summary
Chaetoceros gelidus	AeN707-15	Centric	Planktonic	Poor growth at 15°C across all salinities. Appears to grow and tolerate the various salinity and temperature combinations at the 4-11°C range. Highest average maximum growth rate at 6°C and 22 PSU combination. Able to grow at 11°C, but appears that temperatures above may be greater than its thermal tolerance.
Nitzschia frigida	AeN706-4	Pennate	Ice Core	Best growth at 4°C and 6°C. Poor growth at higher temperatures. Appears to respond similarly across all salinities. Highest average maximum growth rate at 6°C and 34 PSU combination. Relatively low growth rate at all tested parameter combinations.
Nitzschia laevissima	AeN707-42	Pennate	Melt pond	Best growth at 4°C and 6°C. Poor growth at higher temperatures. Appears to tolerate highest salinity (34 PSU) best at the lowest temperature, otherwise it appears to negatively affect growth. Highest average maximum growth rate at 6°C and 22/25 PSU combinations.
Nitzschia sp.	AeN706-17	Pennate	Melt pond	Appears highest salinity (34 PSU) negatively affects growth at lowest (4°C) and highest temperature (15°C). Best growth at 4°C. Highest average maximum growth rate at 4°C and 22/25 PSU combination.
Synedropsis hyperborea	AeN707-94	Pennate	Ice Core	Best growth at 6°C. Poorer growth at 4°C and 15°C. Appears to tolerate lower salinities better at higher temperatures than higher salinities. Seems to grow at most conditions. Highest average maximum growth rate at 6°C and 25 PSU combination.
Thalassiosira gravida	HE492-7	Centric	Planktonic	Best growth at 4°C and 6°C. Appears to tolerate higher salinities across all temperatures. Highest average maximum growth rate at 6°C and 25 PSU combination. Poor growth at the high temperature and low salinity combinations. Able to grow at both 11°C and 15°C, but with lower growth rates than at the coldest temperatures.

3.13 Second Growth Experiment: Light Response

The second growth experiment involved measurements over 27 days, examining the response of the six strains of diatoms subjected to the same salinities and temperatures included in the first growth experiment, as well as four different light intensities (12.5, 25, 37.5, and 50 µmol m^{-2} s^{-1}). This growth was measured in log transformed chlorophyll a concentration, which is summarized in Figure 27.

These growth curves (Figure 27) are visualizations of the specific growth rates in response to temperature and light intensity, with log chlorophyll concentration as a function of time.

The maximum growth rate (µmax) is the maximum growth rate achieved during the exponential phase of the growth period in each well across the entire growth experiment. These are plotted with a fitted curve in Figure 28, showing how the maximum growth rate changes across the parameter combinations.

Each salinity, temperature, and light intensity combination had two replicate points with maximum growth rates (µmax). The averages of these points were calculated to determine the average maximum growth rate rates from the exponential phase of the growth periods at each salinity, temperature, and light intensity combination (Figure 29).

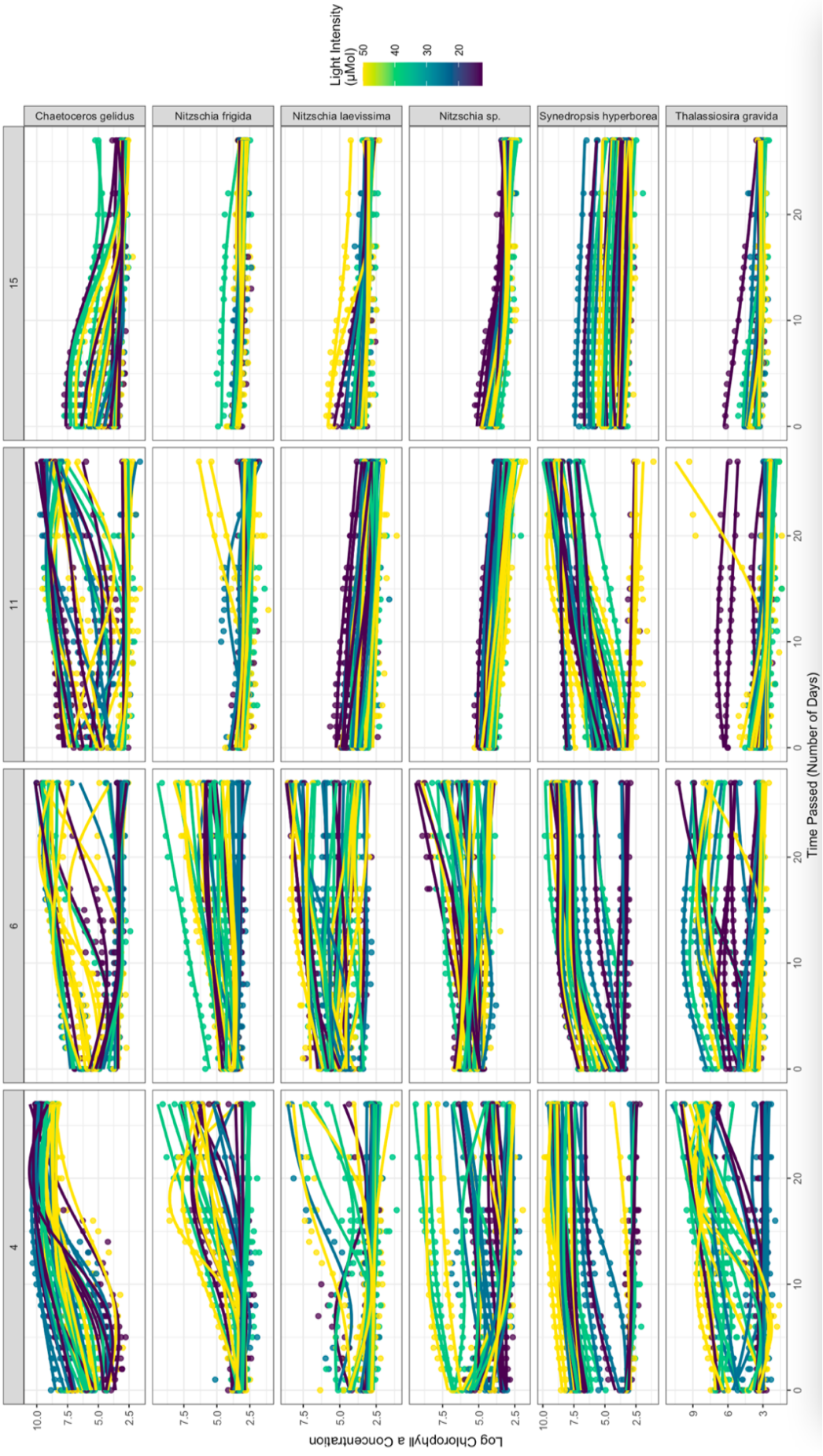

Figure 27: *Growth curves of the six diatom species summarized. The growth curves (displayed with the stat_smooth function) are visualized with the log chlorophyll a concentration (relative units) over time (days) showing the response according to the tested temperatures and light intensities. Note differing y-axes values.*

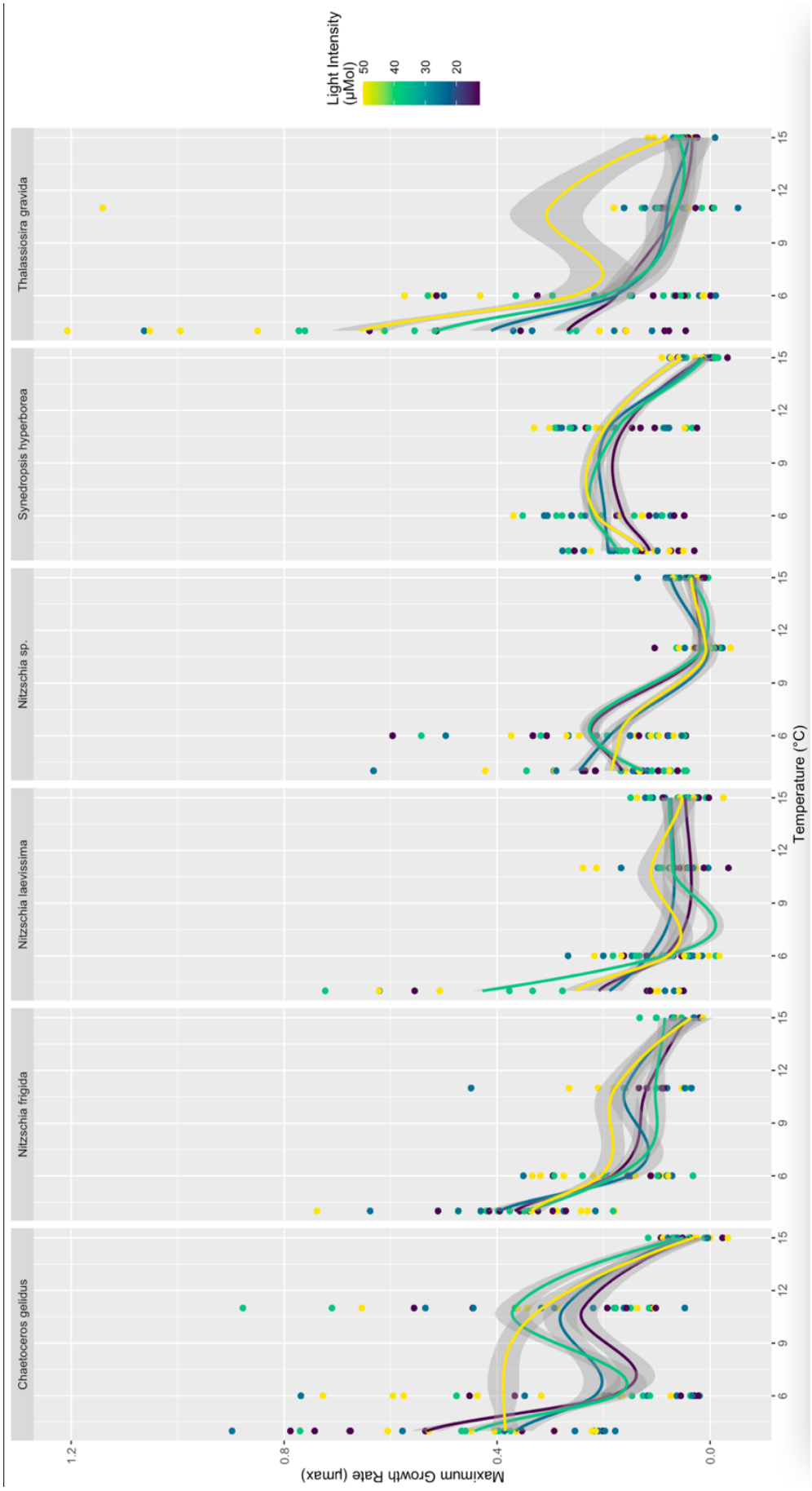

Figure 28: *Maximum growth rate (µmax) from the second growth experiment as a function of the tested temperature and light intensity conditions. Each point represents the µmax of a specific well with the defined parameters, and the maximum growth rate for each well is thus plotted. A fitted curve is applied to the maximum growth rates, showing the trends across the various parameters. The associated confidence bands represent a 95% confidence interval.*

As was seen in the results from the first experiment, the second experiment seems to suggest that temperature is the dominating influence on the growth rate of sea ice associated diatoms (Figure 29). At the highest tested temperature, 15°C, all strains grew poorly regardless of light intensity (Figure 27). At the lower temperatures, there appears to be a larger response to light. This can be seen by examining the growth curves, which show a larger variation in the growth response at 4°C and 6°C for most species (Figure 27, Table 8). This suggests a larger ability to respond to variations in light intensities at the lower end of the tested temperatures. Once the temperatures are raised, the ability to respond to these light intensity variations seems to be reduced (Figure 28 and 29, Table 8). Multiple strains displayed an ability to have higher growth rates as the light intensity increased at the lowest temperatures, suggesting that higher light intensities can be conducive to growth for certain strains (Figure 29, Table 8).

The planktonic species isolated, *Chaetoceros gelidus* and *Thalassiosira gravida*, appear to grow well at all the tested light intensities, but especially at the highest light intensity of 50 µmol m^{-2} s^{-1} (Figure 29, Table 8). The species isolated from the melt ponds, *Nitzschia* sp. and *Nitzschia laevissima*, show a slight difference in their response to light intensity. While *Nitzschia* sp. has a relatively stable and similar growth response across all the tested light intensities, *Nitzschia laevissima* displayed a somewhat increase in growth rate with an increase in light intensity (Figure 29, Table 8). The species isolated from ice cores, *Nitzschia frigida* and *Synedropsis hyperborea*, both exhibited stable growth responses across the tested light intensities. It seems as if *S. hyperborea,* however, has a lower growth rate at the lowest tested light intensity of 12 µmol m^{-2} s^{-1} (Figure 29, Table 8).

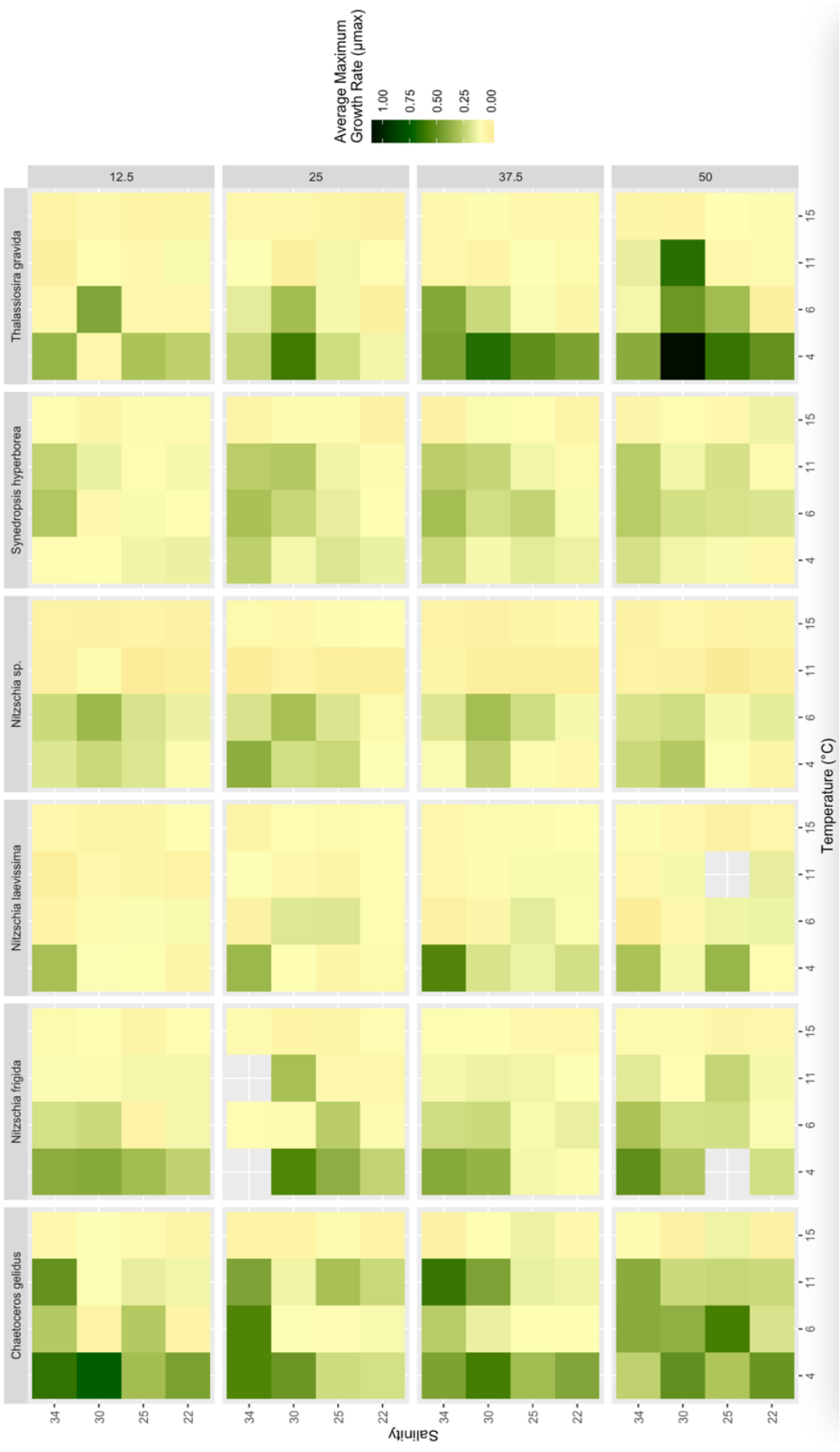

Figure 29: *Visualization of the average maximum growth rate (μmax) with each parameter combination (combining salinity, temperature, and light intensity). The midpoint is defined at 0.1 μmax, highlighting positive growth above that threshold. Note: the missing quadrants correspond to data that was removed due to contamination.*

Table 8: *An overview of growth responses of individual strains to the tested light intensities based on their growth curves and growth rates in Figures 27-29.*

Species	Strain ID	Classification	Habitat	Summary
Chaetoceros gelidus	AeN707-15	Centric	Planktonic	The highest light intensity, 50 µmol m^{-2} s^{-1}, seems to give the best growth across the various other combinations of parameters. Light intensity appears to have larger effect at 6°C and 11°C.
Nitzschia frigida	AeN706-4	Pennate	Ice Core	The highest light intensity, 50 µmol m^{-2} s^{-1}, seems to give the best growth across the various other combinations of parameters. Light intensity appears to have larger effect at 4°C and 6°C.
Nitzschia laevissima	AeN707-42	Pennate	Melt pond	Appears to have similar growth across all light intensities, possibly best growth at 37.5 µmol m^{-2} s^{-1}. Light intensity appears to have larger effect at 4°C and 6°C. Poor growth at lowest light intensity (12.5 µmol m^{-2} s^{-1}).
Nitzschia sp.	AeN706-17	Pennate	Melt pond	Appears to have similar growth across all light intensities, possibly best growth at 25 µmol m^{-2} s^{-1}. Light intensity appears to have larger effect 4°C and 6°C.
Synedropsis hyperborea	AeN707-94	Pennate	Ice Core	Appears to have similar growth across all light intensities. Light intensity does not appear to have a large impact, but possible lower growth at lowest light intensity (12.5 µmol m^{-2} s^{-1}).
Thalassiosira gravida	HE492-7	Centric	Planktonic	The highest light intensity, 50 µmol m^{-2} s^{-1}, seems to give the best growth across the various other combinations of parameters. Light intensity appears to have larger effect at 4°C and 6°C.

4. Discussion

The objective of this thesis was to get an insight into **what** diatom species are present in the sea-ice associated communities and **how** they might respond to an Arctic environment that is undergoing dramatic changes. My findings suggest that there not only remains new and undescribed species of microalgae in the Arctic, but that there is a need for further molecular data on both the unknown and known species present in the various algal communities. Additionally, I found that the tolerance levels for Arctic microalgae subjected to various environmental conditions varies depending on species and which sea-ice community they inhabit.

I have studied six strains of diatoms isolated from different sea-ice associated communities: *Chaetoceros gelidus* and *Thalassiosira gravida* from the plankton, *Nitzschia frigida* and *Synedropsis hyperborea* from the ice-cores in the interior, and *Nitzschia laevissima* and *Nitzschia* sp. from melt ponds on the sea-ice surface. It is important to keep in mind that the findings of this thesis are based on the six strains of diatoms used. This entails that there are limits to how representative the results are for the Arctic algal communities as a whole. Furthermore, there are multiple other diatom species and entire taxonomic groups that were not included, which could respond differently to the tested environmental conditions. Nonetheless, my results give a valuable indication as to the diversity of sea-ice associated diatoms, and the potential repercussions of climate change on algal communities in the Arctic.

I will discuss the two parts to this thesis, the questions they aimed to answer, and what the results indicate. This involves addressing their role in contributing to fill the knowledge gap, their place in the larger context of previous research, and the methodology used in this thesis to address the questions for each part. Then I will address the hypotheses originally made and how future studies can build upon these results to provide further insight into the research questions posed.

4.1 Part one: What diatom species are present in the sea-ice communities?

Box 1: The central message

- In exploring the diversity of sea-ice associated diatoms, new species remain to be discovered. I have described a potentially new species in the genus *Nitzschia*, a relatively small pennate diatom. The molecular work indicated a close relationship to *Nitzschia frigida*, but with a distinctly separate morphology.
- The genetic sequencing and phylogenetic tree suggest that the phylogenetic relationship of many Arctic diatoms is unclear, and that there are likely missing links that need to be added to the database of available sequences to fully understand the relationship between sea-ice associated diatoms. The 28S rRNA gene is not suitable to identify all species of Arctic diatoms.

As has been suggested previously by multiple studies (Medlin & Hasle, 1990; Poulin, 1993; Hasle et al., 1994; Antoniades et al., 2009; Zgrundo et al., 2017; Yau et al., 2020), I have confirmed that the Arctic algal communities have much undiscovered diversity. While the main focus of part one has been on the general question of what is present in the sea-ice communities studied, I have also attempted to answer two sub-questions about the examined diversity of sea-ice associated diatoms:

- What are the taxonomic identities of the sea-ice diatoms studied based on molecular and morphological approaches?

- What morphological traits do we find in the sea-ice diatoms studied from the different sea-ice associated communities?

4.2 What are the taxonomic identities of the sea-ice diatoms studied based on molecular and morphological approaches?

While the taxonomic characterization of Arctic diatoms has a fairly long history, with important contributions throughout the late 19th century and early/mid 20th century (Cleve, 1873; Grunow, 1884; Gran, 1904; Grøntved, 1950), these classifications were largely based on morphology and microscopy. As the technology available has changed, the identification of species in biological research has shifted towards a more widespread use of molecular methods (Hebert et al., 2003), which also includes the work done to describe and characterize Arctic diatoms (Ki et al., 2009; Stecher et al., 2016).

The diatoms used in this study were previously identified to species level during the isolation process, except for the *Nitzschia* sp. strain, which was indicated to be an unidentified pennate diatom. I isolated and sequenced DNA from two strains: AeN706-4 *Nitzschia frigida* and AeN706-17 *Nitzschia* sp. with partial sequencing for the 28S rRNA gene. The four remaining strains (HE492-7 *Thalassiosira gravida*, AeN707-42 *Nitzschia laevissima*, AeN707-15 *Chaetoceros gelidus*, and AeN707-94 *Synedropsis hyperborea*) were previously isolated and the DNA sequences were already available to use for analysis. These strains only had partial sequences available for the 28S rRNA gene, and it was therefore decided that the diversity of the sea-ice diatoms and their evolutionary relationships would use the genetic sequencing from solely this gene as a foundation.

Through the partial 28S rRNA genetic sequencing, I confirmed that all strains were correctly identified to genus-level (Table 6) and that the unidentified pennate most likely belonged to the *Nitzschia* genus. Matching this strain in particular against the reference sequences in the NCBI database indicated that this is probably a species either without matches in the database or undescribed. This was, however, not a unique issue with this strain, and the lack of proper reference sequences available is common for the *Nitzschia* genus in particular (Mucko et al., 2021). This can be because *Nitzschia* species are difficult to identify, as they are most readily distinguished by structures on their valves which need to be examined by electron microscopy. Many *Nitzschia* species are therefore mischaracterized (Trobajo et al., 2013; Mann & Trobajo, 2014; Carballeira et al., 2017) and the genus is a large and heterogenous clade which has previously included genera now considered separate (Hasle, 1994).

The *Nitzschia* sp., *Nitzschia laevissima*, *Nitzschia frigida*, and *Synedropsis hyperborea* strains exhibited the same issue: a lack of reference sequences in the NCBI database. This can be seen by a variety of species in the sequencing matches (Table 6 and Table S12 Appendix C: Supplementary Results). Bailet et al. (2019) had similar results in sequencing benthic diatoms from Northern Europe, concluding that the lack of reference sequences available for many diatom species leads to species not being identified or mischaracterized. While my molecular work aided in confirming the genus of these strains, the species identification was hindered by a lack of reference sequences.

Phylogenetic trees constructed on diatoms are often intricate and inconclusive. Mann et al. (2021) attempted to show the evolutionary relationships of the Bacillariaceae family of diatoms, which includes the *Nitzschia* genus. The multiple trees point to an unresolved understanding of the evolutionary relationship between the examined genera, and they concluded that *Nitzschia* is a non-monophyletic group. Lundholm et al. (2002) and Kociolek & Vouilloud (2020) also consider the *Nitzschia* genus to be non-monophyletic, and it therefore seems that this genus in particular requires more analyses to fully understand its phylogeny. This supports the results of my phylogenetic analysis, which shows that the *Nitzschia* strains have a mismatch between their highest sequence matches and their placement in the phylogenetic tree (Figure 17). The placement of *Nitzschia* sp. and *Nitzschia frigida* together as one clade with high bootstrap support, suggests that they are closely related.

As this thesis only used partial sequencing of one specific gene, the 28S rRNA gene, it is possible that the results could be more conclusive if other genes were sequenced and analyzed. While the 28S rRNA gene is commonly used to separate higher taxa (Sorhannus, 2004) it is possible other genes with more variable regions would have been more appropriate to use to separate species. Guo et al. (2015), Lim et al. (2018), Godhe et al. (2006), and Beszteri et al. (2005) for instance, all used the variable ITS (internal transcribed spacer) sequences between the 18S and 28S genes to produce robust phylogenetic trees and to separate species of diatoms.

The mitochondrial COX1 gene has also been suggested as a potential variable marker for genetic sequencing of diatoms (Evans et al., 2007), although Trobajo et al. (2010) found that this gene as a universal marker is limited by the primers available. Yamada et al. (2017) however did molecular and phylogenetical analyses on *Skeletonema* species using the COX1 gene and experienced that this was a more useful marker than the LSU rRNA genes. Alternatively, concatenated analyses through multigene sequencing have been used in exploring diatom phylogeny in previous studies (Souffreau et al., 2011; Lefebvre et al., 2017) and is a possible enhancement to single gene sequencing.

While the partial 28S rRNA sequencing has given an insight into the diversity of both known and unknown sea-ice diatoms, my results show that this gene is not sufficient to give a comprehensive understanding of diatom diversity and that many species of Arctic diatoms cannot be identified using this gene. Either doing a multigene analysis with a longer part of the 28S gene and other genes (such as the 18S rRNA gene) or choosing genes with more variable and unique regions, could help untangle the complexity of diatom taxonomy.

4.3 What morphological traits do we find in the sea-ice diatoms studied from the different sea-ice associated communities?

Except for the *Nitzschia* sp. strain, all the diatoms studied here have been previously described morphologically. My morphological analyses, using both light and electron microscopy, therefore attempts to give a brief overview of the characteristics found in the varying sea-ice associated diatom strains studied.

Surface communities

Melt ponds are a dominating feature on Arctic sea-ice during the melting season and are extreme habitats that can experience dramatic fluctuations in various environmental conditions. This, in turn, influences which diatoms are able to survive and grow in the surface community. Both Fernández-Méndez et al. (2014) and Sørensen et al. (2017) found that *Nitzschia* is a dominating genus found in diatom aggregates in melt ponds. These findings are consistent with this thesis, as both *Nitzschia laevissima* and *Nitzschia* sp. strains examined were isolated from melt ponds and are pennate diatoms belonging to this genus. While *N. laevissima* is a solitary species, *Nitzschia* sp. was observed to have the presence of both solitary individuals as well as forming ribbon shaped colonies.

Although *Nitzschia laevissima* has been reported from sea-ice earlier (Booth & Horner, 1997; Melnikov et al., 2002; Riedel et al., 2003) it does not appear that it is commonly encountered in melt ponds, often appearing in the interior sea-ice communities. Kilias et al. (2014) found that there are similar community structures in both melt ponds and interior sea-ice and explained that this could possibly be due to biomass seeping through the sea-ice from the surface into the interior. *N. laevissima* could therefore be a species encountered in both melt ponds and the sea-ice interior, depending on when the sea-ice is sampled. It is also possible that most previous studies have only characterized the melt pond communities to the genera level, as was done by Fernández-Méndez et al. (2014). The strain I examined corresponds to the phenotypic descriptions of *Nitzschia laevissima* as described by Medlin & Hasle (1990) confirmed by both light and electron microscopy (Figure 18).

As the *Nitzschia* sp. strain used in this study is to my knowledge previously undescribed, it is uncertain how common this species could be in Arctic melt pond communities. This, coupled with a lack of research on melt pond diatom communities, makes it difficult to describe its morphology in relation to other melt pond diatoms. In contrast with *N. laevissima*, the *Nitzschia* sp. strain is smaller, lacks a hyaline region, and has a clearer oval shape (Figures 18 and 22). Interestingly, the phylogenetic analysis shows that the *Nitzschia* sp. strain seems to be closely related to the *Nitzschia frigida* strain, which was isolated from the interior ice community (Figure 17). Morphologically, however, these strains are quite different as well (Figures 19 and 22). It is therefore a possibility that *Nitzschia* sp. is a new morphotype of *N. frigida* influenced by the differing environmental conditions between melt ponds and the interior of the sea-ice. Morphotypes of certain diatom species have been previously described, and certain diatoms can also potentially display a level of phenotypic plasticity in response to their environment (Witkowski et al., 2004). At the moment, however, classifying *Nitzschia* sp. as a morphotype of *Nitzschia frigida* is speculative and requires a more in-depth morphological and molecular comparison than what I provide in this thesis.

Interior/bottom communities

Among the pennate diatoms in the interior sea-ice communities, the *Nitzschia* genus again has a dominating presence (Melnikov et al., 2002). A commonly encountered species in the interior sea-ice community is *Nitzschia frigida* (Haecky et al., 1998; Krembs & Engel, 2001). It is a colony forming species (Figure 19) and it is postulated that this colony formation allows it to anchor itself to the ice, especially in the bottom section of the sea-ice (Olsen et al., 2017). This is consistent with my findings, as *Nitzschia frigida* was isolated from the interior sea-ice community and formed very typical colonies in culture. The *N. frigida* strain used corresponds to the phenotypic descriptions of *Nitzschia frigida* as described by Medlin & Hasle (1990) confirmed by both light and electron microscopy (Figure 19).

The other strain isolated from the interior sea-ice community examined, *Synedropsis hyperborea*, does not appear to be commonly found in the interior communities. If so, it seems to be concentrated in the bottom sections of the sea-ice (Melnikov et al., 2002), but is often considered an epiphyte on *Melosira arctica* colonies growing underneath sea-ice (Hasle et al., 1994; von Quillfeldt, 1997). It is not possible to determine if this strain was interior dwelling or associated with a *M. arctica* colony. The *S. hyperborea* strain used corresponds to the phenotypic descriptions of *Synedropsis hyperborea* as described by Hasle et al. (1994) (Figure 23).

While both *N. frigida* and *S. hyperborea* are pennate diatoms, they are morphologically quite different. Although both species form colonies, there are large differences in the valve ornamentations, the terminal ends of the valves, and the presence of a raphe.

Planktonic communities

Intermittently, there are phytoplankton blooms occurring below the sea-ice. Two of the genera that to a large degree dominate these blooms are *Chaetoceros* and *Thalassiosira* (von Quillfeldt, 2000; Degerlund & Eilertsen, 2010; Arrigo et al., 2012). This is consistent with this study, as both *Chaetoceros gelidus* and *Thalassiosira gravida* are centric diatom strains isolated from the plankton community. *C. gelidus* has been found to be a vital part of the phytoplankton community in the Arctic (Crawford et al., 2018) but is in fact a cosmopolitan species found in both temperate and polar waters (Schiffrine et al., 2020). This species was until fairly recently, considered an ecotype of *Chaetoceros socialis*, but was characterized as a separate species by Chamnansinp et al. in 2013. The close relationship between *C. gelidus* and *C. socialis* can also be seen by my phylogenetic analysis (Figure 17), where these strains form a solid clade. The *C. gelidus* strain used corresponds to the phenotypic descriptions as described by Chamnansinp et al. (2013) confirmed by both light and electron microscopy. (Figure 20).

The other planktonic species examined, *Thalassiosira gravida*, is one of the most abundant phytoplankton species in the Arctic, found both under the ice and in ice-free waters (Poulin et al., 2011). As von Quillfeldt (2000) concluded, *Thalassiosira gravida* is difficult to differentiate from *Thalassiosira antarctica* var. *borealis,* and it is therefore possible that there are mischaracterizations of *T. gravida* in the literature. There is also evidence to support that *Thalassiosira gravida* and *Thalassiosira rotula* are the same species (Sar et al., 2011; Whittaker et al., 2012) further complicating the identification of *T. gravida*. This is also suggested by my phylogenetic analysis (Figure 17), which shows a close relationship between *T. gravida* and *T. rotula* with strong bootstrap support. The *T. gravida* strain used corresponds to the phenotypic descriptions as described by Sar et al. (2011) confirmed by both light and electron microscopy (Figure 21).

While both *C. gelidus* and *T. gravida* are centric diatoms that form chains, they have quite distinct morphologies. The cell shapes, the interior and exterior valve structures, as well as the chain forms and sizes, make these two species easy to differentiate.

4.4 An incomprehensive morphological analysis

It is clear that this thesis does not do an in-depth adaptive morphological analysis of the diatom strains studied or the sea-ice communities they represent. While analyzing the strains using both a light and electron microscope has allowed me to identify species in accordance with earlier literature, examine cell shapes, colony formation, and details of frustules, it has not been a replacement for more detailed morphological analyses into their adaptive traits. My results do however show that light and electron microscopy of Arctic diatoms is an important tool in order to identify and compare species, both within and across genera. It has been difficult to do a morphological comparison of the studied strains against previous studies, as it appears that there is a lack of studies focusing on phenotypic descriptions of Arctic diatoms in the varying sea-ice communities. Additionally, the morphological studies that did focus on Arctic diatoms, emphasized other parameters.

Uusikivi et al. (2010) for instance, studied the ability of sea-ice algae in the Baltic Sea to produce mycosporine-like amino acids (MAAs) as a photoprotective response to harmful UV radiation. They found that the production of MAAs was higher in the surface layers of the sea-ice, which indicates that these algae are adapted to the higher light intensities present in these layers. Ligowski et al. (2012) studied planktonic vs brine channel dwelling forms of *Chaetoceros dichaeta* in Antarctic waters, and found that there are distinct differences in size, shape, and orientation of individuals between the two different environments. This morphological analysis showed that certain sea-ice diatoms can have a plastic morphology when exposed to different habitats.

Valegård et al. (2018) explored the ability of Arctic diatoms to fix CO_2 and found that they possess modified Rubisco enzymes that allow them to have a more efficient CO_2 fixation. Aslam et al. (2018) studied the ability of *Fragilariopsis cylindrus* from the Southern Ocean to produce extracellular polymeric substances (EPS). These substances aid in cell adhesion, cryoprotection, and buffer the effects of fluctuating salinity levels (Steele et al., 2014).

Aslam et al. found that *F. cylindrus* had a flexible production of EPS according to the environmental conditions it was subjected to, indicating an ability to adapt to various sea-ice conditions. Sackett et al. (2013) investigated the production of macromolecules of Antarctic sea-ice diatoms and found that the synthesis of these molecules varied according to species and sea-ice community. The production of these molecules also changed depending on the formation and melting of the sea-ice, indicating that many species exhibit plasticity according to the sea-ice conditions. They concluded that Antarctic diatoms have a synthesis of macromolecules that is adapted to the variable conditions present in the sea-ice environment. All the parameters mentioned in these studies, and more, are important to take into consideration when trying to analyze the morphological adaptations of sea-ice diatoms.

While the light and electron microscopy I have done support the findings of Fragoso et al. (2018), which showed that Arctic diatoms have approximately similar cell shapes across genera, a more thorough study of the morphology of the studied diatoms is necessary in order to draw broader conclusions on their adaptations to the sea-ice communities as a whole. In addition to the traits examined by the previously mentioned studies, this can be done by studying whether they produce resting spores, ice-binding proteins, other photoprotective molecules, or how silicified their cells are. A morphological trait analysis taking such traits into account, accompanied by an inclusion of more species of diatoms from each sea-ice community, would give an extensive understanding of how their morphology and phenotypic expression is adapted to their sea-ice habitat.

4.5 A return to part one: What diatom species are present in the sea-ice communities?

To conclude, although the molecular, phylogenetic, and morphological analyses done in this thesis show that sea-ice diatoms are a diverse and heterogenous group, much research is needed to get a detailed understanding on the composition of algal sea-ice communities. By doing expansive molecular analyses on sea-ice algae, for instance through metabarcoding or multigene sequencing, new species could be discovered, or over-arching phylogenetic trees could be constructed. Together, this could give new insights into the diversity in sea-ice algal communities, and the evolutionary relationships between the species present. Through exhaustive morphological analyses looking at a wide variety of factors, it might be possible to get an indication as to how sea-ice algae are adapted to their environment, and importantly, how they may respond to a changing Arctic.

4.6 Part two: How will they respond to change?

Box 2: The central message

- It appears that temperature is the driving factor behind the growth rate of the tested sea-ice diatoms. All strains had highest growth at lowest temperatures, suggesting that their growth optimum is between 4°C and 6°C.
- The two growth experiments suggest that the planktonic species, *Chaetoceros gelidus* and *Thalassiosira gravida*, have the highest tolerance to the tested parameter combinations.
- The two growth experiments suggest that the melt pond species, *Nitzschia* sp. and *Nitzschia laevissima*, have the lowest tolerance to the tested parameter combinations.
- These findings support previous studies suggesting that future ice-free conditions in the Arctic may be most conducive to planktonic species of algae.

My experiments have shown that the response of Arctic sea-ice diatoms to environmental conditions varies according to the sea-ice habitat they inhabit. While the main focus of part two has been on the general question of how sea-ice diatoms will respond to change, I have also attempted to answer two sub-questions about the potential growth responses of the studied diatoms:

- What are the effects of various environmental conditions on the growth rates of the studied sea-ice diatoms?

- Which potential morphological and physiological traits observed in the various sea-ice diatoms could influence their ability to adapt to a changing Arctic?

4.7 What are the effects of various environmental conditions on the growth rates of the studied sea-ice diatoms?

The novelty of this thesis lies in the two multistressor high-throughput experiments, testing multiple parameters simultaneously on the growth of sea-ice diatoms. The results of these experiments indicate that temperature is the driving force behind the growth of sea-ice diatoms, with a temperature optimum observed for all species between 4°C and 6°C. At the lowest tested temperatures, the effects of salinity and light intensity played a larger role than at the highest temperatures, where most species experienced close to no growth regardless of salinity or light intensity.

DISCUSSION

It is already known that the growth of microalgae is controlled by, among other factors, temperature. Thomas et al. (2012) created an eco-evolutionary model based on multiple earlier studies and over 5000 growth measurements of global phytoplankton, concluding that temperature has a strong selection pressure on microalgae and that they are adapted to the temperatures found in their local environments. While the comprehensive study by Thomas et al. provides a global model of temperature response among phytoplankton, they are lacking findings from above 75°N, and their model therefore lacks input from the Arctic. While my experiments support the findings by Thomas et al., suggesting that temperature is a dominating factor influencing the growth of algae, my results provide insight into a region considered understudied.

Fiala & Oriol (1990) conducted a similar growth experiment as the ones I have done, testing the combined effects of various temperatures and light intensities on the growth of diatoms from Antarctic waters and sea-ice. Although not Arctic species, they found similar temperature optima across all tested light intensities as the strains I have studied, varying from 3°C to 6°C. They also experienced that temperatures above 6°C tend to have negative effects on most of the diatom strains, which supports my findings that temperatures above 11°C are most likely higher than the thermal range most cold-adapted diatoms can tolerate.

Fiala & Oriol included light intensities well above those we tested (from 46-220 µmol m^{-2} s^{-1}) and found that the lowest light irradiance dramatically slowed growth. The highest light intensity tested in my second growth experiment was 50 µmol m^{-2} s^{-1}, approximately the same as the lowest intensity included in the study by Fiala & Oriol. It is therefore difficult to compare the results of light intensities between these studies. Gilstad & Sakshaug (1990), however, looked at the effect of both low and high light irradiance on the growth of ten species of diatoms isolated from the Barents Sea. With constant temperature conditions for all species, they found that diatoms had higher growth rates with increasing light irradiance up to 50 or 70 µmol m^{-2} s^{-1}, after which many species potentially experienced photoinhibition. These are similar values as was found by Hegseth (1992) and the result of my experiments suggests similar results, with an apparently slight increase of growth rates for most species as the irradiance levels increased. It is likely, however, that the tested light intensities (12.5, 25, 37.5, and 50 µmol m^{-2} s^{-1}) are within the irradiance levels that all the tested strains can tolerate, as many strains exhibited approximately similar maximum growth rates across all light intensities (Figure 29).

The findings of the first growth experiment, however, suggests that *Synedropsis hyperborea* has a temperature optimum between 6°C and 11°C (Figure 26). A previous study found that other species within the same phylogenetic *Fragilaria–Synedropsis* clade had optimum temperatures between 12°C and 14°C (Karsten et al., 2006). With that in mind, my experiments indicate that *S. hyperborea* is a more eurythermal species than the other pennate diatoms included, the *Nitzschia* strains. This is supported by Suzuki & Takahashi (1995) which found that *Nitzschia frigida* for instance, has a small range of tolerated temperatures.

DISCUSSION

While many Arctic diatoms have been shown to grow well in temperatures above that found in their environment (Schlie & Karsten, 2017), my experiments imply that temperatures in the range of 11°C to 15°C are not conducive to diatom growth in the sea-ice communities in the Arctic. Both planktonic species appear to tolerate the higher temperatures, with *Chaetoceros gelidus* able to grow in 11°C and *Thalassiosira gravida* able to grow in both 11°C and 15°C. These findings support previous studies that suggest *T. gravida* has an ability to tolerate a wide variety of temperature and light conditions (Lacour et al., 2018), but demonstrates that *T. gravida* might not tolerate a combination of higher temperatures and lower salinities (Figure 26). Since climate change is associated with a freshening of the Arctic water masses, the lower salinities may void any beneficial changes in temperatures or light intensities for *T. gravida*.

Grant & Horner (1976) tested growth of Arctic diatoms in response to changes in salinity concentration and found that many of the tested species of diatoms grew at a broad range of salinities, well below and above the salinity values tested in my experiments. Additionally, it has been found that many cold-water diatoms exhibit a temperature-dependent tolerance of changes in salinity, with the ability to adjust to higher salinities at lower temperatures, as shown by Aletsee & Jahnke (1992). These findings are in-line with the results of my experiments, which show that at the lowest temperatures, all strains demonstrated a tolerance of the tested salinity range of 22-34 PSU.

In a study done by Zhang et al. (1999), a sea-ice community was exposed to salinity levels from 4 to 98 PSU. They found that at constant temperatures, the salinity level had a large impact on the growth rate of certain species, with for instance a *Chaetoceros spp.* growing best at a relatively low salinity (12.2 PSU) and *Nitzschia* species growing faster at higher salinities. While the *Nitzschia* species tested in this thesis correspond to the results of Zhang et al. (1999), with higher growth at higher salinities, the *Chaetoceros gelidus* strain exhibits a different result, with faster growth at higher rather than lower salinities. It is likely that I did not test a wide enough range of salinity values to appropriately get an indication as to how salinity might affect growth rate, as salinity values can range from 0 to 150 PSU in different sea-ice associated communities across seasons (Zhang et al., 1999).

While temperature, light intensity, and salinity are important factors contributing to the growth rate of Arctic species, I did not test the influence of nutrients. Although the growth experiments were conducted in a nutrient rich medium, it is possible that the strains could have lower or higher growth rates in solutions with different nutrient concentrations. For instance, Hagman et al. (2019) conducted a growth experiment including a gradient of light intensities and dissolved organic carbon (DOC) on a freshwater raphidophyte, *Gonyostomum semen*. The addition of DOC to the growth medium had a clear effect on the growth of *G. semen* across the examined light intensities. It is therefore likely to assume that the inclusion of added nutrients into the solutions could influence the growth rates of the diatoms tested in this thesis, as was also found by Gudmundsdottir et al. (2013).

While the results of my experiments have given an idea as to how different abiotic factors influence the growth rates of the tested diatoms, there are certain improvements that can be made on the methodology. For instance, the inoculation for the second growth experiment should have been done when the diatoms were in the exponential phase of their growth in the first experiment. Previous research has indicated that this phase is when the cells are healthiest (Pan et al., 1996) and would therefore likely serve as a more appropriate inoculate than cells taken in the stationary phase of their growth curve, as was done for the second growth experiment. It is possible that the results of the second growth experiment were influenced by cells in a deteriorated state, even though they were placed in fresh medium.

Additionally, the nutrient levels during the experiments were never measured. It is therefore possible, if unlikely, that some strains were nutrient limited during the growth experiments. Additionally, as we had relatively high cellular concentration in the 96-well plates, it is likely that there was cellular shading occurring, which could have negatively affected the growth rates of individual wells. The effects of nutrient limitation and cellular shading could be mitigated by diluting the wells regularly during the experiments.

4.8 Which potential morphological and physiological traits observed in the various sea-ice diatoms could influence their ability to adapt to a changing Arctic?

The results of these experiments suggest that as the Arctic sea-ice thins and the region begins to experience ice-free periods, conditions will be advantageous to the growth of phytoplankton rather than sympagic algae. In many ways, this can already be seen by the more frequent phytoplankton blooms occurring in the Arctic (Assmy et al., 2017; Horvat et al., 2017) as a result of thinner ice coverage. The results of this study show that the two planktonic species tested, *Chaetoceros gelidus* and *Thalassiosira gravida*, have the highest growth rates out of all the strains tested and were able to grow in the warmer and more light intensive conditions tested (Figure 29). This is supported by the results of Kvernvik et al. (2020) where cultures of the pelagic *Thalassiosira hyalina* and the sympagic *Nitzschia frigida* were subjected to various stress conditions of light intensity and pCO2. They found that *T. hyalina* could change their photosystems, synthesize photoprotective compounds, and increase their cell size in response to the stressful light conditions. This entailed that *T. hyalina* showed a larger resilience to light stress than the sympagic *N. frigida*, which exhibited a weaker photoacclimated response. This was followed up by another study done by Kvernvik et al. (2021), which found that phytoplankton can assimilate carbon more efficiently than sympagic algae in both low and high light irradiance environments. Phytoplankton appear therefore to possess physiological adaptations that provide them with relatively wide ranges of tolerance when it comes to multiple environmental conditions. With a changing Arctic, the results of my experiments and previous studies, implies the possibility of a community shift occurring, with a more phytoplankton dominated algal biomass in the future.

The idea of a community shift has also been supported by Stock et al. (2019), which conducted growth experiments on temperate, polar, and tropical strains of the benthic diatom *Cylindrotheca closterium*. The polar strains had much narrower thermal tolerance ranges than the temperate and tropical strains. This corresponds to my results, with the sympagic algae exhibiting lower temperature tolerances than the more cosmopolitan pelagic species. However, it appears that the picture is more nuanced.

Aranguren-Gassis et al. (2019) conducted experiments testing the ability of *Chaetoceros simplex* to grow in various temperature conditions. They found that the temperature range tolerated was connected with the nitrogen concentration: in replete N conditions, *C. simplex* could survive temperatures well above its threshold, while in N-limited conditions, the thermal adaptation of *C. simplex* was inhibited. Phytoplankton in the Arctic Ocean are often N-limited (von Friesen & Riemann, 2020) and it is therefore possible that this places a limit on the ability of phytoplankton to take advantage of ice-free conditions in the Arctic, regardless of their thermal tolerances.

Interestingly, it appears that the species isolated from melt ponds, *Nitzschia* sp. and *Nitzschia laevissima*, have the lowest tolerances out of the strains tested in this thesis. Melt ponds are characterized by fluctuating conditions, and it would therefore be natural to assume that species adapted to these conditions have wide tolerances. It is possible *Nitzschia* sp. and *Nitzschia laevissima* are not true melt pond species or that they are melt pond species adapted to specific conditions. Padfield et al. (2016) found that algal species with short generation times can experience rapid evolution, so it is possible that *Nitzschia laevissima* and *Nitzschia* sp. could adapt to the tested environmental conditions given sufficient time and provided they have the physiological foundation for evolution to occur.

4.9 A return to part two: How will they respond to change?

To conclude, the two multistressor high-throughput growth experiments conducted in this thesis show that Arctic sea-ice diatoms have optimal growth conditions in lower temperatures, and that higher temperatures lead to lower growth rates. The two species isolated from the plankton community, *Chaetoceros gelidus* and *Thalassosira gravida*, appear to tolerate the widest parameter conditions, potentially reflecting how a future ice-free Arctic may be dominated by species with wide tolerances. However, it is important to remember that this thesis has conducted two growth experiments on only six diatom strains. These experiments have been carried out in a simulated setting and do not comprehensively cover all the in-situ parameters that can potentially influence the growth rate of algal species. Additionally, testing growth conditions on single strains does not mean that entire species or algal communities will respond similarly. Wolf et al. (2018) demonstrated that there are often intraspecific responses to environmental conditions, and that different strains of the same species can exhibit a wide variety of tolerance ranges. This in turn places a limit on the conclusions that can be made to determine how specific species and algal communities may respond to change based on analyses of single strains.

4.9 A return to the hypotheses

At the beginning of this thesis, I came with two hypotheses for what I imagined the results of this thesis would show. Below, I will briefly readdress each hypothesis made and whether the results support my predictions.

Hypothesis one: The ice diatoms isolated from exposed melt ponds will be able to tolerate higher fluctuations in environmental conditions than ice diatoms isolated from sheltered habitats inside and under the sea ice.

The results of the growth experiments do not support hypothesis one. They show that *Nitzschia laevissima* and *Nitzschia* sp. isolated from melt ponds had the lowest tolerances for the tested conditions, while the planktonic species had the highest.

Hypothesis two: There will be a clear relationship between the morphological and phylogenetic analyses done on the selected ice diatom species with the results of the growth experiments: Species closely related phylogenetically will have similar growth responses to the tested environmental parameters.

The second hypothesis was supported by the findings of the growth experiments and the phylogenetic analysis. If we examine the pennate diatoms and centric diatoms as two clades, we see that they exhibited similar growth responses according to their phylogeny. However, we did not test any pennate diatoms from the plankton community nor any centric diatoms from the sympagic communities. It is therefore possible that including this would influence whether there is a clear relationship between the phylogeny and growth response. The ecological role of a species can potentially play a more important role than their phylogeny.

This thesis attempted to contribute to filling the knowledge gaps that exist both on what is present in algal Arctic communities and how these communities may respond to change. While I have shown that Arctic algal communities are a diverse group, with much diversity left to be discovered, the lack of proper reference sequences available in the databases hinder our understanding of the molecular and phylogenetic relationships of Arctic algae. The growth experiments conducted in this thesis have shown that different communities may respond differently to the projected changes in the Arctic. While laboratory settings can never completely replicate the conditions present in-situ, building on and continuing to conduct multistressor growth experiments with a wide variety of parameters are necessary to get an accurate understanding of how communities will respond to changing conditions. Future studies will need to focus on gathering more genetic information on algal species in the Arctic, as well as continuing growth experiments that assess multiple parameters simultaneously.

I have barely touched upon the diversity and growth responses present in Arctic algal communities, but I have shown that the overarching question of *how* a community may respond to change is intricately linked to *what* species are present in that community.

4.11 Conclusion

With climate change threatening many aspects of the Arctic ecosystem, we have yet to thoroughly understand the implications on the biological communities found in both the water column and sea-ice. I have described a potential new species within the *Nitzschia* genus and shown that the sea-ice diatom communities are a heterogenous group, with much diversity left to explore. My analyses show that there are limitations to taxonomically identifying species through molecular tools, with the commonly used 28S rRNA gene unable to identify all species of Arctic diatoms. It is therefore important to continue using a multimethod approach, combining taxonomic identification through both genetic sequencing and morphological analyses, as was done in this thesis. These methods complement each other, and future studies that use only one method to examine the biodiversity of diatoms in sea-ice communities risk mischaracterizing the diversity present. I have also shown that the diatom species present in a sea-ice community will respond differently to the projected changes due to climate change. It appears that sympagic sea-ice algae are adapted to their specific habitats, while phytoplankton are broadly adapted and able to flexibly adjust to various conditions beyond their current habitat conditions. The biochemical mechanisms behind these adaptive traits in phytoplankton are not fully understood, but one can theorize that they are somehow more efficient at nutrient uptake, carbon assimilation, and production of photoprotective chemicals. It is likely that climate change will lead to an algal community shift in the Arctic, with phytoplankton playing a more prominent role in the future. This will have repercussions on the entire food web, which will need to adapt to shifting bloom conditions and new algal communities. The question therefore seems not to be *if* but *how* recognizable these algal communities will be in an unrecognizable Arctic.

References

Aagaard, K., et al. (1981). "On the halocline of the Arctic Ocean." Deep Sea Research Part I: Oceanographic Research Papers **28**(6): 529-545.

Aletsee, L. and Jahnke, J. (1992). "Growth and productivity of the psychrophilic marine diatoms *Thalassiosira antarctica* (Comber) and *Nitzschia frigida* (Grunow) in batch cultures at temperatures below the freezing point of sea water." Polar Biology **11**(8): 643-647.

Antoniades, D., et al. (2009). "Seven new species of freshwater diatoms (Bacillariophyceae) from the Canadian Arctic Archipelago." Nova Hedwigia **88**(1-2): 57-80.

Aranguren-Gassis, M., et al. (2019). "Nitrogen limitation inhibits marine diatom adaptation to high temperatures." Ecology Letters **22**(11): 1860-1869.

Arrigo, K. R. (2014). "Sea ice ecosystems." Annual Review of Marine Science **6**(1): 439-467.

Arrigo, K. R. (2017). "Sea ice as a habitat for primary producers." In: Thomas, DN (ed.). Sea ice **3**: 352-369. Oxford, UK: Wiley-Blackwell.

Arrigo, K. R. and van Dijken, G. L. (2011). "Secular trends in Arctic Ocean net primary production." Journal of Geophysical Research: Oceans **116**(C9): C09011.

Arrigo, K. R., et al. (2008). "Impact of a shrinking Arctic ice cover on marine primary production." Geophysical Research Letters **35**(19): L19603.

Arrigo, K. R., et al. (2012). "Massive phytoplankton blooms under Arctic sea ice." Science **336**(6087): 1408-1408.

Asch, R. G., et al. (2019). "Climate change impacts on mismatches between phytoplankton blooms and fish spawning phenology." Global Change Biology **25**(8): 2544-2559.

Aslam, S. N., et al. (2018). "Identifying metabolic pathways for production of extracellular polymeric substances by the diatom Fragilariopsis cylindrus inhabiting sea ice." The ISME Journal: Multidisciplinary Journal of Microbial Ecology **12**(5): 1237-1251.

Assmy, P., et al. (2017). "Leads in Arctic pack ice enable early phytoplankton blooms below snow-covered sea ice." Scientific Reports **7**(1): 1-9.

Bailet, B., et al. (2019). "Molecular versus morphological data for benthic diatoms biomonitoring in Northern Europe freshwater and consequences for ecological status." Metabarcoding and Metagenomics **3**: 21-35.

Bates, S. S. and Cota, G. (1986). "Fluorescence induction and photosynthetic responses of Arctic ice algae to sample treatment and salinity 1." Journal of Phycology **22**(4): 421-429.

Belzile, C., et al. (2000). "Ultraviolet attenuation by dissolved and particulate constituents of first-year ice during late spring in an Arctic polynya." Limnology and Oceanography **45**(6): 1265-1273.

REFERENCES

Beszteri, B., et al. (2005). "Ribosomal DNA sequence variation among sympatric strains of the *Cyclotella meneghiniana* complex (Bacillariophyceae) reveals cryptic diversity." Protist **156**(3): 317-333.

Bluhm, B. A., et al. (2017). "Sea ice as a habitat for macrograzers." In: Thomas, DN (ed.). Sea Ice **3**: 394-414. Oxford, UK: Wiley-Blackwell.

Boetius, A., et al. (2013). "Export of algal biomass from the melting Arctic sea ice." Science **339**(6126): 1430-1432.

Booth, B. C. and Horner, R. A. (1997). "Microalgae on the Arctic Ocean Section, 1994: species abundance and biomass." Deep Sea Research Part II: Topical Studies in Oceanography **44**(8): 1607-1622.

Bowler, C., et al. (2008). "The *Phaeodactylum* genome reveals the evolutionary history of diatom genomes." Nature **456**(7219): 239-244.

Box, J. E., et al. (2019). "Key indicators of Arctic climate change: 1971–2017." Environmental Research Letters **14**(4): 045010.

Campbell, K., et al. (2016). "Community dynamics of bottom-ice algae in Dease Strait of the Canadian Arctic." Progress in Oceanography **149**: 27-39.

Carballeira, R., et al. (2017). "A combined morphological and molecular approach to *Nitzschia varelae* sp. nov., with discussion of symmetry in Bacillariaceae." European Journal of Phycology **52**(3): 342-359.

Chamnansinp, A., et al. (2013). "Global diversity of two widespread, colony-forming diatoms of the marine plankton, *Chaetoceros socialis* (syn. *C. radians*) and *Chaetoceros gelidus* sp. nov." Journal of Phycology **49**(6): 1128-1141.

Cleve, P. T. (1873). “On diatoms from the Arctic Sea”. Bihang till Kongliga Svenska Vetenskaps-Akademiens Handlingar **1**(13): 1-28.

Coello-Camba, A., et al. (2014). "Interactive effect of temperature and CO2 increase in Arctic phytoplankton." Frontiers in Marine Science **1**(49): 1-10.

Comiso, J. C. (2012). "Large decadal decline of the Arctic multiyear ice cover." Journal of Climate **25**(4): 1176-1193.

Cota, G. (1985). "Photoadaptation of high Arctic ice algae." Nature **315**(6016): 219-222.

Cota, G., et al. (1991). "Ecology of bottom ice algae: I. Environmental controls and variability." Journal of Marine Systems **2**(3-4): 257-277.

Cottier, F., et al. (1999). "Linkages between salinity and brine channel distribution in young sea ice." Journal of Geophysical Research **104**(C7): 15859-15871.

Crawford, D. W., et al. (2018). "Spatial patterns in abundance, taxonomic composition and carbon biomass of nano-and microphytoplankton in Subarctic and Arctic Seas." Progress in Oceanography **162**: 132-159.

REFERENCES

Degerlund, M. and Eilertsen, H. C. (2010). "Main species characteristics of phytoplankton spring blooms in NE Atlantic and Arctic waters (68–80 N)." Estuaries and Coasts **33**(2): 242-269.

Doel, R. E., et al. (2014). "Science, environment, and the New Arctic." Journal of Historical Geography **44**: 2-14.

Eldevik, T. and Nilsen, J. E. Ø. (2013). "The Arctic–Atlantic thermohaline circulation." Journal of Climate **26**(21): 8698-8705.

Elliott, A., et al. (2015). "Spring production of mycosporine-like amino acids and other UV-absorbing compounds in sea ice-associated algae communities in the Canadian Arctic." Marine Ecology Progress Series **541**: 91-104.

Eppley, R. W., et al. (1967). "Sinking rates of marine phytoplankton measured with a fluorometer." Journal of Experimental Marine Biology and Ecology **1**(2): 191-208.

Evans, K. M., et al. (2007). "An assessment of potential diatom “barcode” genes (cox1, rbcL, 18S and ITS rDNA) and their effectiveness in determining relationships in *Sellaphora* (Bacillariophyta)." Protist **158**(3): 349-364.

Fer, I. (2009). "Weak vertical diffusion allows maintenance of cold halocline in the central Arctic." Atmospheric and Oceanic Science Letters **2**(3): 148-152.

Fernández-Méndez, M., et al. (2014). "Composition, buoyancy regulation and fate of ice algal aggregates in the Central Arctic Ocean." PLoS One **9**(9): e107452.

Fetterer, F. and Untersteiner, N. (1998). "Observations of melt ponds on Arctic sea ice." Journal of Geophysical Research: Oceans **103**(C11): 24821-24835.

Fiala, M. and Oriol, L. (1990). "Light-temperature interactions on the growth of Antarctic diatoms." Polar Biology **10**(8): 629-636.

Fragoso, G. M., et al. (2018). "Diatom biogeography from the Labrador Sea revealed through a trait-based approach." Frontiers in Marine Science **5**(297): 1-15.

Galindo, V., et al. (2017). "Pigment composition and photoprotection of Arctic sea ice algae during spring." Marine Ecology Progress Series **585**: 49-69.

Gilstad, M. and E. Sakshaug (1990). "Growth rates of ten diatom species from the Barents Sea at different irradiances and day lengths." Marine Ecology Progress Series. **64**(1): 169-173.

Godhe, A., et al. (2006). "Comparison of three common molecular tools for distinguishing among geographically separated clones of the diatom *Skeletonema marinoi* Sarno et Zingone (Bacillariophyceae) 1." Journal of Phycology **42**(2): 280-291.

Gosselin, M., et al. (1997). "New measurements of phytoplankton and ice algal production in the Arctic Ocean." Deep Sea Research Part II: Topical Studies in Oceanography **44**(8): 1623-1644.

Gradinger, R. (2002). "Sea ice microorganisms." In: Bitton, G (ed.). Encyclopedia of Environmental Microbiology. 2833-2844. New York, USA: John Wiley.

Gran, H. H. (1904). "Die Diatomeen der arktischen Meere. I. Teil. Die Diatomeen des Planktons" Fauna arct. **3**: 511-554.

Grant, W. and Horner, R. A. (1976). "Growth responses to salinity variation in four Arctic ice diatoms 1,2." Journal of Phycology **12**(2): 180-185.

Grunow, A. (1884). "Die Diatomeen von Franz Josefs-Land." Denkschriften der kaiserlichen Akademie der Wissenschaften. Mathematischnaturwissenschaftliche Classe **48**: 53-112.

Grøntved, J. (1950). "Phytoplankton studies." Det kgl. Danske Vitenskabernes Selskab Biologiske Meddelelser **18**(12): 3-19.

Gudmundsdottir, R., et al. (2013). "Diatoms as indicators: the influences of experimental nitrogen enrichment on diatom assemblages in sub-Arctic streams." Ecological Indicators **32**: 74-81.

Guo, L., et al. (2015). "Comparison of potential diatom 'barcode'genes (the 18S rRNA gene and ITS, COI, rbcL) and their effectiveness in discriminating and determining species taxonomy in the Bacillariophyta." International Journal of Systematic and Evolutionary Microbiology **65**(4): 1369-1380.

Gutt, J. (1995). "The occurrence of sub-ice algal aggregations off northeast Greenland." Polar Biology **15**(4): 247-252.

Haecky, P., et al. (1998). "Influence of sea ice on the composition of the spring phytoplankton bloom in the northern Baltic Sea." Polar Biology **20**(1): 1-8.

Hagman, C. H. C., et al. (2019). "Growth responses of the nuisance algae *Gonyostomum semen* (Raphidophyceae) to DOC and associated alterations of light quality and quantity." Aquatic Microbial Ecology **82**(3): 241-251.

Hancke, K., et al. (2018). "Extreme low light requirement for algae growth underneath sea ice: A case study from Station Nord, NE Greenland." Journal of Geophysical Research: Oceans **123**(2): 985-1000.

Harrison, W. and Cota, G. (1991). "Primary production in polar waters: relation to nutrient availability." Polar Research **10**(1): 87-104.

Hasle, G. R. and Fryxell, G. A. (1970). "Diatoms: cleaning and mounting for light and electron microscopy." Transactions of the American Microscopical Society **89**(4): 469-474.

Hasle, G. R., et al. (1994). "*Synedropsis* gen. nov., a genus of araphid diatoms associated with sea ice." Phycologia **33**(4): 248-270.

Hasle, G. R. (1994). "*Pseudo-nitzschia* as a genus distinct from *Nitzschia* (Bacillariophyceae) 1." Journal of Phycology **30**(6): 1036-1039.

Hassol, S. (2004). "Impacts of a warming Arctic: Arctic Climate Impact Assessment". Arctic Climate Impact Assessment., Arctic Monitoring and Assessment Programme., Program for the Conservation of Arctic Flora and Fauna., & International Arctic Science Committee: 112-113. Cambridge, U.K: Cambridge University Press.

Hawley, K. L., et al. (2017). "Freezer on, lights off! Environmental effects on activity rhythms of fish in the Arctic." Biology Letters **13**(12): 20170575.

Hebert, P. D., et al. (2003). "Biological identifications through DNA barcodes." Proceedings of the Royal Society of London. Series B: Biological Sciences **270**(1512): 313-321.

Hegseth, E. N. (1992). "Sub-ice algal assemblages of the Barents Sea: species composition, chemical composition, and growth rates." Polar Biology **12**(5): 485-496.

Horner, R. A., et al. (1988). "Proposed terminology and reporting units for sea ice algal assemblages." Polar Biology **8**(4): 249-253.

Horner, R. A., et al. (1992). "Ecology of sea ice biota." Polar Biology **12**(3): 417-427.

Horvat, C., et al. (2017). "The frequency and extent of sub-ice phytoplankton blooms in the Arctic Ocean." Science Advances **3**(3): e1601191.

Hoshiai, T. and Fukuchi, M. (1981). "Sea ice colored by ice algae in a lagoon, Lake Saroma, Hokkaido, Japan." Nankyoku Shiryo **71**: 113-120

Hsiao, S. I. (1980). "Quantitative composition, distribution, community structure and standing stock of sea ice microalgae in the Canadian Arctic." Arctic **33**(4): 768-793.

Hsiao, S. I. (1988). "Spatial and seasonal variations in primary production of sea ice microalgae and phytoplankton in Frobisher Bay, Arctic Canada." Marine Ecology Progress Series **44**(3): 275-285.

Jakobsson, M. (2002). "Hypsometry and volume of the Arctic Ocean and its constituent seas." Geochemistry, Geophysics, Geosystems **3**(5): 1-18.

Jansen, E., et al. (2020). "Past perspectives on the present era of abrupt Arctic climate change." Nature Climate Change **10**(8): 714-721.

Ji, R., et al. (2013). "Sea ice phenology and timing of primary production pulses in the Arctic Ocean." Global Change Biology **19**(3): 734-741.

Juhl, A. R. and Krembs, C. (2010). "Effects of snow removal and algal photoacclimation on growth and export of ice algae." Polar Biology **33**(8): 1057-1065.

Kale, A. and Karthick, B. (2015). "The diatoms." Resonance **20**(10): 919-930.

Karsten, U., et al. (2006). "Temperature and light requirements for growth of two diatom species (Bacillariophyceae) isolated from an Arctic macroalga." Polar Biology **29**(6): 476-486.

Katayama, T. and Taguchi, S. (2013). "Photoprotective responses of an ice algal community in Saroma-Ko Lagoon, Hokkaido, Japan." Polar Biology **36**(10): 1431-1439.

Ki, J.-S., et al. (2009). "Comprehensive comparisons of three pennate diatoms, *Diatoma tenuae*, *Fragilaria vaucheriae*, and *Navicula pelliculosa*, isolated from summer Arctic reservoirs (Svalbard 79 N), by fine-scale morphology and nuclear 18S ribosomal DNA." Polar Biology **32**(2): 147-159.

Kilias, E. S., et al. (2014). "Insight into protist diversity in Arctic sea ice and melt-pond aggregate obtained by pyrosequencing." Polar Research **33**(1): 23466.

Kociolek, J. P. and Vouilloud, A. A. (2020). "*Hantzschia subandina* Frenguelli (Bacillariophyceae): Morphology, status and typification, as well as the description of a new species of *Nitzschia*." Boletín de la Sociedad Argentina de Botánica. **55**(4): 521-534.

Krell, A., et al. (2007). "Regulation of proline metabolism under salt stress in the psychrophilic diatom *Fragilariopsis cylindrus* (Bacillariophyceae) 1." Journal of Phycology **43**(4): 753-762.

Krembs, C. and Engel, A. (2001). "Abundance and variability of microorganisms and transparent exopolymer particles across the ice–water interface of melting first-year sea ice in the Laptev Sea (Arctic)." Marine Biology **138**(1): 173-185.

Krembs, C., et al. (2001). "A mesocosm study of physical-biological interactions in artificial sea ice: effects of brine channel surface evolution and brine movement on algal biomass." Polar Biology **24**(5): 356-364.

Kvernvik, A. C., et al. (2020). "Higher sensitivity towards light stress and ocean acidification in an Arctic sea-ice-associated diatom compared to a pelagic diatom." New Phytologist **226**(6): 1708-1724.

Kvernvik, A. C., et al. (2021). "Arctic sea ice algae differ markedly from phytoplankton in their ecophysiological characteristics." Marine Ecology Progress Series **666**: 31-55.

Kwok, R. and Rothrock, D. (2009). "Decline in Arctic sea ice thickness from submarine and ICESat records: 1958–2008." Geophysical Research Letters **36**(15): 1-5.

Lacour, T., et al. (2018). "The role of sustained photoprotective non-photochemical quenching in low temperature and high light acclimation in the bloom-forming arctic diatom *Thalassiosira gravida*." Frontiers in Marine Science **5**(354): 1-16.

Lee, S. H., et al. (2012). "Phytoplankton productivity in newly opened waters of the Western Arctic Ocean." Deep Sea Research Part II: Topical Studies in Oceanography **81**: 18-27.

Lee, S. H., et al. (2011). "Holes in progressively thinning Arctic sea ice lead to new ice algae habitat." Oceanography **24**(3): 302-308.

Lefebvre, K. E., et al. (2017). "A comparison of molecular markers and morphology for *Neidium* taxa (Bacillariophyta) from eastern North America." Journal of Phycology **53**(3): 680-702.

Leu, E., et al. (2010). "Increased irradiance reduces food quality of sea ice algae." Marine Ecology Progress Series **411**: 49-60.

Li, W. K., et al. (2009). "Smallest algae thrive as the Arctic Ocean freshens." Science **326**(5952): 539-539.

Ligowski, R., et al. (2012). "Morphological adaptation of a planktonic diatom to growth in Antarctic sea ice." Marine Biology **159**(4): 817-827.

Lim, H. C., et al. (2018). "Phylogeny and species delineation in the marine diatom *Pseudo-nitzschia* (Bacillariophyta) using cox1, LSU, and ITS 2 rRNA genes: A perspective in character evolution." Journal of Phycology **54**(2): 234-248.

Lizotte, M. P. (2001). "The contributions of sea ice algae to Antarctic marine primary production." Integrative and Comparative Biology **41**(1): 57-73.

Lund-Hansen, L. C., et al. (2020). "Effects of increased irradiance on biomass, photobiology, nutritional quality, and pigment composition of Arctic sea ice algae." Marine Ecology Progress Series **648**: 95-110.

Lundholm, N., et al. (2002). "Phylogeny of the Bacillariaceae with emphasis on the genus *Pseudo-nitzschia* (Bacillariophyceae) based on partial LSU rDNA." European Journal of Phycology **37**(1): 115-134.

Mann, D. G. and Droop, S. (1996). "Biodiversity, biogeography and conservation of diatoms." Hydrobiologia (The Hague) **336**(1-3): 19-32.

Mann, D. G. and Trobajo, R. (2014). "Symmetry and sex in Bacillariaceae (Bacillariophyta), with descriptions of three new Nitzschia species." European Journal of Phycology **49**(3): 276-297.

Mann, D. G., et al. (2021). "Ripe for reassessment: a synthesis of available molecular data for the speciose diatom family Bacillariaceae." Molecular Phylogenetics and Evolution **158**(106985): 1-19.

Maslanik, J., et al. (2007). "A younger, thinner Arctic ice cover: Increased potential for rapid, extensive sea-ice loss." Geophysical Research Letters **34**(24): L24501

McMahon, K. W., et al. (2006). "Benthic community response to ice algae and phytoplankton in Ny Ålesund, Svalbard." Marine Ecology Progress Series **310**: 1-14.

Medlin, L. K. and Hasle, G. R. (1990). "Some *Nitzschia* and related diatom species from fast ice samples in the Arctic and Antarctic." Polar Biology **10**(6): 451-479.

Melling, H. and Lewis, E. (1982). "Shelf drainage flows in the Beaufort Sea and their effect on the Arctic Ocean pycnocline." Deep Sea Research Part I: Oceanographic Research Papers **29**(8): 967-985.

Melnikov, I. A., et al. (2002). "Sea ice biological communities and nutrient dynamics in the Canada Basin of the Arctic Ocean." Deep Sea Research Part I: Oceanographic Research Papers **49**(9): 1623-1649.

Metzner, E. P., et al. (2020). "Arctic Ocean surface energy flux and the cold halocline in future climate projections." Journal of Geophysical Research: Oceans **125**(2): e2019JC015554.

Miller, G. H., et al. (2010). "Arctic amplification: can the past constrain the future?" Quaternary Science Reviews **29**(15-16): 1779-1790.

Mock, T. and Hoch, N. (2005). "Long-term temperature acclimation of photosynthesis in steady-state cultures of the polar diatom *Fragilariopsis cylindrus*." Photosynthesis Research **85**(3): 307-317.

Mock, T. and Thomas, D. N. (2005). "Recent advances in sea-ice microbiology." Environmental Microbiology **7**(5): 605-619.

Mucko, M., et al. (2021). "A polyphasic approach to the study of the genus *Nitzschia* (Bacillariophyta): three new planktonic species from the Adriatic Sea." Journal of Phycology **57**(1): 143-159.

Mundy, C., et al. (2011). "Characteristics of two distinct high-light acclimated algal communities during advanced stages of sea ice melt." Polar Biology **34**(12): 1869-1886.

Nicolaus, M., et al. (2012). "Changes in Arctic sea ice result in increasing light transmittance and absorption." Geophysical Research Letters **39**(24): L24501.

Olsen, L. M., et al. (2017). "The seeding of ice algal blooms in Arctic pack ice: the multiyear ice seed repository hypothesis." Journal of Geophysical Research: Biogeosciences **122**(7): 1529-1548.

Onarheim, I. H., et al. (2018). "Seasonal and regional manifestation of Arctic sea ice loss." Journal of Climate **31**(12): 4917-4932.

Padfield, D., et al. (2016). "Rapid evolution of metabolic traits explains thermal adaptation in phytoplankton." Ecology Letters **19**(2): 133-142.

Pan, Y., et al. (1996). "Effects of silicate limitation on production of domoic acid, a neurotoxin, by the diatom *Pseudo-nitzschia* multiseries. I. Batch culture studies." Marine Ecology Progress Series **131**: 225-233.

Perovich, D. K., et al. (2011). "Arctic sea-ice melt in 2008 and the role of solar heating." Annals of Glaciology **52**(57): 355-359.

Perovich, D. K., et al. (1998). "Variability in Arctic sea ice optical properties." Journal of Geophysical Research: Oceans **103**(C1): 1193-1208.

Petty, A. A., et al. (2018). "The Arctic sea ice cover of 2016: a year of record-low highs and higher-than-expected lows." The Cryosphere **12**(2): 433-452.

Post, E., et al. (2009). "Ecological dynamics across the Arctic associated with recent climate change." Science **325**(5946): 1355-1358.

Poulin, M. (1993). "*Craspedopleura* (Bacillariophyta), a new diatom genus of arctic sea ice assemblages." Phycologia **32**(3): 223-233.

Poulin, M., et al. (2011). "The pan-Arctic biodiversity of marine pelagic and sea-ice unicellular eukaryotes: a first-attempt assessment." Marine Biodiversity **41**(1): 13-28.

Poulin, M., et al. (2014). "Sub-ice colonial *Melosira arctica* in Arctic first-year ice." Diatom Research **29**(2): 213-221.

Řezanka, T., et al. (2004). "Natural microbial UV radiation filters—Mycosporine-like amino acids." Folia Microbiologica **49**(4): 339-352.

Riedel, A., et al. (2003). "Taxonomy and abundance of microalgae and protists at a first-year sea ice station near Resolute Bay, Nunavut, spring to early summer." Canadian Data Report of Hydrography and Ocean Sciences **159**: 1-53.

Rothschild, L. J. and Mancinelli, R. L. (2001). "Life in extreme environments." Nature **409**(6823): 1092-1101.

Różańska, M., et al. (2008). "Protist entrapment in newly formed sea ice in the Coastal Arctic Ocean." Journal of Marine Systems **74**(3-4): 887-901.

Rudels, B., et al. (1991). "Stratification and water mass formation in the Arctic Ocean: some implications for the nutrient distribution." Polar Research **10**(1): 19-32.

Ryan, K., et al. (2004). "Acclimation of Antarctic bottom-ice algal communities to lowered salinities during melting." Polar Biology **27**(11): 679-686.

Rysgaard, S., et al. (2001). "Biomass, production and horizontal patchiness of sea ice algae in a high-Arctic fjord (Young Sound, NE Greenland)." Marine Ecology Progress Series **223**: 15-26.

Sackett, O., et al. (2013). "Phenotypic plasticity of Southern Ocean diatoms: key to success in the sea ice habitat?" PLoS One **8**(11): e81185.

Sar, E. A., et al. (2011). "*Thalassiosira rotula*, a heterotypic synonym of *Thalassiosira gravida*: morphological evidence." Diatom Research **26**(1): 109-119.

Schiffrine, N., et al. (2020). "Growth and elemental stoichiometry of the ecologically-relevant Arctic diatom *Chaetoceros gelidus*: a mix of polar and temperate." Frontiers in Marine Science **6**: 790.

Schlie, C. and Karsten, U. (2017). "Microphytobenthic diatoms isolated from sediments of the Adventfjorden (Svalbard): growth as function of temperature." Polar Biology **40**(5): 1043-1051.

Scholin, C. A., et al. (1994). "Identification of group and strain specific genetic markers for globally distributed *Alexandrium* (Dinophyceae). II. Sequence analysis of a fragment of the LSU rRNA gene 1." Journal of Phycology **30**(6): 999-1011.

Shu, Q., et al. (2018). "Projected freshening of the Arctic Ocean in the 21st century." Journal of Geophysical Research: Oceans **123**(12): 9232-9244.

Shu, Q., et al. (2019). "Assessment of the Atlantic water layer in the Arctic Ocean in CMIP5 climate models." Climate Dynamics **53**(9): 5279-5291.

Smith, L. M., et al. (2003). "Sensitivity of the Northern Hemisphere climate system to extreme changes in Holocene Arctic sea ice." Quaternary Science Reviews **22**(5-7): 645-658.

Smith, R. E., et al. (1993). "Growth and lipid composition of high Arctic ice algae during the spring bloom at Resolute, Northwest Territories, Canada." Marine Ecology Progress Series **97**(1): 19-29.

Smith, R., E. et al. (1997). "The influence of major inorganic nutrients on the growth and physiology of high arctic ice algae." Journal of Marine Systems **11**(1-2): 63-70.

Søreide, J. E., et al. (2006). "Seasonal food web structures and sympagic–pelagic coupling in the European Arctic revealed by stable isotopes and a two-source food web model." Progress in Oceanography **71**(1): 59-87.

Søreide, J. E., et al. (2010). "Timing of blooms, algal food quality and *Calanus glacialis* reproduction and growth in a changing Arctic." Global Change Biology **16**(11): 3154-3163.

Sørensen, H. L., et al. (2017). "Nutrient availability limits biological production in Arctic sea ice melt ponds." Polar Biology **40**(8): 1593-1606.

Sorhannus, U. (2004). "Diatom phylogenetics inferred based on direct optimization of nuclear-encoded SSU rRNA sequences." Cladistics **20**(5): 487-497.

Souffreau, C., et al. (2011). "A time-calibrated multi-gene phylogeny of the diatom genus *Pinnularia*." Molecular Phylogenetics and Evolution **61**(3): 866-879.

Spindler, M. (1994). "Notes on the biology of sea ice in the Arctic and Antarctic." Polar Biology **14**(5): 319-324.

Stecher, A., et al. (2016). "rRNA and rDNA based assessment of sea ice protist biodiversity from the central Arctic Ocean." European Journal of Phycology **51**(1): 31-46.

Steele, D. J., et al. (2014). "Protection of cells from salinity stress by extracellular polymeric substances in diatom biofilms." Biofouling **30**(8): 987-998.

Stock, W., et al. (2019). "Thermal niche differentiation in the benthic diatom *Cylindrotheca closterium* (Bacillariophyceae) complex." Frontiers in Microbiology **10**(1395): 1-12.

Stoecker, D. K., et al. (2000). "Primary production in the upper sea ice." Aquatic Microbial Ecology **21**(3): 275-287.

Strass, V. H. and Nöthig, E.-M. (1996). "Seasonal shifts in ice edge phytoplankton blooms in the Barents Sea related to the water column stability." Polar Biology **16**(6): 409-422.

Stroeve, J. C., et al. (2012). "Trends in Arctic sea ice extent from CMIP5, CMIP3 and observations." Geophysical Research Letters **39**(16): L16502.

Sullivan, C. W. and Palmisano, A. C. (1981). "Sea-ice microbial communities in McMurdo Sound." Antarctic Journal of the United States **16**(5): 126-127.

Suzuki, Y., et al. (1997). "Photosynthetic and respiratory characteristics of an Arctic ice algal community living in low light and low temperature conditions." Journal of Marine Systems **11**(1-2): 111-121.

Suzuki, Y. and Takahashi, M. (1995). "Growth responses of several diatom species isolated from various environments to temperature." Journal of Phycology **31**(6): 880-888.

Syvertsen, E. E. (1991). "Ice algae in the Barents Sea: types of assemblages, origin, fate and role in the ice-edge phytoplankton bloom." Polar Research **10**(1): 277-288.

Szymanski, A. and Gradinger, R. (2016). "The diversity, abundance and fate of ice algae and phytoplankton in the Bering Sea." Polar Biology **39**(2): 309-325.

Thomas, D. N. and Dieckmann, G. S. (2002). "Antarctic sea ice- a habitat for extremophiles." Science **295**(5555): 641-644.

Thomas, M. K., et al. (2012). "A global pattern of thermal adaptation in marine phytoplankton." Science **338**(6110): 1085-1088.

Torstensson, A., et al. (2021). "Sea-ice microbial communities in the Central Arctic Ocean: Limited responses to short-term pCO2 perturbations." Limnology and Oceanography **66**: S383-S400.

Trobajo, R., et al. (2010). "The use of partial cox 1, rbc L and LSU rDNA sequences for phylogenetics and species identification within the *Nitzschia palea* species complex (Bacillariophyceae)." European Journal of Phycology **45**(4): 413-425.

Trobajo, R., et al. (2013). "Morphology and identity of some ecologically important small *Nitzschia* species." Diatom Research **28**(1): 37-59.

Uusikivi, J., et al. (2010). "Contribution of mycosporine-like amino acids and colored dissolved and particulate matter to sea ice optical properties and ultraviolet attenuation." Limnology and Oceanography **55**(2): 703-713.

Valegård, K., et al. (2018). "Structural and functional analyses of Rubisco from arctic diatom species reveal unusual posttranslational modifications." Journal of Biological Chemistry **293**(34): 13033-13043.

von Friesen, L. W. and Riemann, L. (2020). "Nitrogen fixation in a changing Arctic Ocean: An overlooked source of nitrogen?" Frontiers in microbiology **11**: 3149.

von Quillfeldt, C. H. (1997). "Distribution of diatoms in the Northeast Water polynya, Greenland." Journal of Marine Systems **10**(1-4): 211-240.

von Quillfeldt, C. H. (2000). "Common diatom species in Arctic spring blooms: their distribution and abundance." Botanica Marina **43** (6): 499-516.

Wakatsuchi, M. and Kawamura, T. (1987). "Formation processes of brine drainage channels in sea ice." Journal of Geophysical Research: Oceans **92**(C7): 7195-7197.

Walsh, J. E., et al. (2011). "Ongoing climate change in the Arctic." Ambio- A Journal of Environment and Society **40**(1): 6-16.

Weller, G. (2019). "The weather and climate of the Arctic." The Arctic **1**: 143-160.

Werner, I., et al. (2007). "Sea-ice algae in Arctic pack ice during late winter." Polar Biology **30**(11): 1493-1504.

Whittaker, K. A., et al. (2012). "Molecular subdivision of the marine diatom *Thalassiosira rotula* in relation to geographic distribution, genome size, and physiology." BMC Evolutionary Biology **12**(1): 1-14.

Witkowski, A., et al. (2004). "Four new species of *Nitzschia* sect. *Tryblionella* (Bacillariophyceae) resembling *N. parvula*." Phycologia **43**(5): 579-595.

Wolf, K. K., et al. (2018). "Resilience by diversity: Large intraspecific differences in climate change responses of an Arctic diatom." Limnology and Oceanography **63**(1): 397-411.

Yamada, M., et al. (2017). "Utility of mitochondrial-encoded cytochrome c oxidase I gene for phylogenetic analysis and species identification of the planktonic diatom genus *Skeletonema*." Phycological Research **65**(3): 217-225.

Yau, S., et al. (2020). "*Mantoniella beaufortii* and *Mantoniella baffinensis* sp. nov. (Mamiellales, Mamiellophyceae), two new green algal species from the high Arctic 1." Journal of Phycology **56**(1): 37-51.

Young, J. N. and Schmidt, K. (2020). "It's what's inside that matters: physiological adaptations of high-latitude marine microalgae to environmental change." New Phytologist **227**(5): 1307-1318.

Zgrundo, A., et al. (2017). "Diatom communities in the high Arctic aquatic habitats of northern Spitsbergen (Svalbard)." Polar Biology **40**(4): 873-890.

Zhang, Q., et al. (1999). "Experimental study on the effect of salinity on growth rates of Arctic-sea-ice algae from the Greenland Sea." Boreal Environment Research **4**: 1-8.

Zhang, T., et al. (2019). "Comparison of phytoplankton communities between melt ponds and open water in the central Arctic Ocean." Journal of Ocean University of China **18**(3): 573-579.

Zurzolo, C. and Bowler, C. (2001). "Exploring bioinorganic pattern formation in diatoms. A story of polarized trafficking." Plant Physiology **127**(4): 1339-1345.

Appendix A: Supplementary Methods

Calculating the Inoculate Volume

The algal strains used in the second growth experiment were inoculated from the corresponding 96-well plates used in the first growth experiment. For the second growth experiment, the aim was to have 300 µl of medium and algal inoculate in each well, with the amount of medium and inoculate based on the conditions in the plates used for the first growth experiment. This would allow the second growth experiment to have an inoculate already acclimated to the tested salinity and temperature conditions.

Before calculating the inoculate volume, the 96-well plates used in the first growth experiment were transported on ice and the concentration of algal cells was measured using the plate reader. This measurement served as the basis for calculating the inoculate volume we would use for the second growth experiment. The aim was to have the same starting concentration of approximately 100 fluorescence value across all wells.

To calculate the inoculate volume, I used the formula $C_1V_1=C_2V_2$

C_1= Concentration of algal cells in the wells from the first growth experiment measured same day as determining the inoculate volume.
V_1= The inoculate volume of algal cells from the first growth experiment.
C_2= The desired concentration of algal cells in the second growth experiment (Here we used the fluorescence value of 100)
V_2= The desired volume of medium and algal inoculate for the second growth experiment (Here we used 300 µl)

V_1 was therefore calculated for each well, as this was the volume of algal inoculate we would transfer from each well of the first growth experiment into each well of the second growth experiment.

Before transferring the inoculate, the health of the cells in each well was examined using a light microscope. If the health of the diatom cells were deemed insufficient to serve as an inoculate, cells from the closest parameter were used. For instance, while we were examining the cells from the 96-well plate used in the 15°C temperature room, we determined that the plate had experienced too much evaporation to use as a source of inoculate. It was therefore decided that the 96-well plate from the 11°C and 6°C would serve as inoculate for the plate used in the 15°C in the second growth experiment.

Programming Light Panels

To program the desired light intensities onto the light panels (12, 25, 35 and 50 µmol m^{-2} s^{-1}), I used the Arduino boards and the associated Arduino coding program. The entire script used for coding in Arduino can be seen in Figure S1.

neopixel_general_RGB_gradient

```
#include <Adafruit_NeoPixel.h>
#include <avr/power.h>

#define NUMPIXELS   96
#define PIN      6
#define BRIGHTNESS  50

Adafruit_NeoPixel pixels = Adafruit_NeoPixel(NUMPIXELS, PIN, NEO_GRB + NEO_KHZ800);

// R = G = B for simplicity but could of course be changed individually

byte R_pixel[] = {
   45,  30,  20,  10,  45,  30,  20,  10,  45,  30,  20,  10,
   45,  30,  20,  10,  45,  30,  20,  10,  45,  30,  20,  10,
   45,  30,  20,  10,  45,  30,  20,  10,  45,  30,  20,  10,
   45,  30,  20,  10,  45,  30,  20,  10,  45,  30,  20,  10,
   45,  30,  20,  10,  45,  30,  20,  10,  45,  30,  20,  10,
   45,  30,  20,  10,  45,  30,  20,  10,  45,  30,  20,  10,
   45,  30,  20,  10,  45,  30,  20,  10,  45,  30,  20,  10,
   45,  30,  20,  10,  45,  30,  20,  10,  45,  30,  20,  10};

byte G_pixel[] = {
   45,  30,  20,  10,  45,  30,  20,  10,  45,  30,  20,  10,
   45,  30,  20,  10,  45,  30,  20,  10,  45,  30,  20,  10,
   45,  30,  20,  10,  45,  30,  20,  10,  45,  30,  20,  10,
   45,  30,  20,  10,  45,  30,  20,  10,  45,  30,  20,  10,
   45,  30,  20,  10,  45,  30,  20,  10,  45,  30,  20,  10,
   45,  30,  20,  10,  45,  30,  20,  10,  45,  30,  20,  10,
   45,  30,  20,  10,  45,  30,  20,  10,  45,  30,  20,  10,
   45,  30,  20,  10,  45,  30,  20,  10,  45,  30,  20,  10};

byte B_pixel[] = {
   45,  30,  20,  10,  45,  30,  20,  10,  45,  30,  20,  10,
   45,  30,  20,  10,  45,  30,  20,  10,  45,  30,  20,  10,
   45,  30,  20,  10,  45,  30,  20,  10,  45,  30,  20,  10,
   45,  30,  20,  10,  45,  30,  20,  10,  45,  30,  20,  10,
   45,  30,  20,  10,  45,  30,  20,  10,  45,  30,  20,  10,
   45,  30,  20,  10,  45,  30,  20,  10,  45,  30,  20,  10,
   45,  30,  20,  10,  45,  30,  20,  10,  45,  30,  20,  10,
   45,  30,  20,  10,  45,  30,  20,  10,  45,  30,  20,  10};


void setup() {

  pixels.setBrightness(BRIGHTNESS);
  pixels.begin();
  pixels.show();

  for(int i=0; i<NUMPIXELS; i++){
    pixels.setPixelColor(i, pixels.Color(R_pixel[i], G_pixel[i], B_pixel[i]));
  }

  pixels.show();
}

void loop() {
  delay(10000);
}
```

Figure S1: *The Arduino script in the programming screen with the corresponding values used for the second growth experiment.*

In the script the red (R), green (G) and blue (B) LED lights can be programmed individually, which means that for the second growth experiment the values for all the lights were the same, as can be seen in Figure S1. Since I wanted the light panels to emit white light, all RGB channels in each neopixel were used and programmed with the same value.

The light panels used have an inverse arrangement when placed on the 96-well plates, meaning that the first column of the light panel covers the last column of the plate. This was important to take into consideration when programming the light panels, as the first row of the light panel needed to have the highest light intensity, and so forth.

The values in the script do not correspond to µmol. It was therefore necessary to attempt various values to get an indication as to how the values used in Arduino translate into photons (measured in µmol). While attempting different values in the Arduino script, the light panel was measured using a photometer (LI-1000 Light Sensor Logger, LI-COR Biosciences, United States) with an attached photosynthetic active radiation (PAR) sensor (Spherical Micro Quantum Sensor US-SQS/L, Heinz Walz, Germany) and this allowed us to translate the values in the code to µmol. As can be seen in Figure S1, 45 ≈ 50 µmol m^{-2} s^{-1}, 30 ≈ 35 µmol m^{-2} s^{-1}, 20 ≈ 25 µmol m^{-2} s^{-1}, and 10 ≈ 12 µmol m^{-2} s^{-1}.

Measuring the Light Intensity

Once the light panels were programmed with the desired µmol emission, each individual light was measured on each light panel. An empty white 96-well plate with the plastic membrane removed was placed on the light panels, and the photometer was used to measure the light in each individual well. This was done for all eight light panels (see Figure S2).

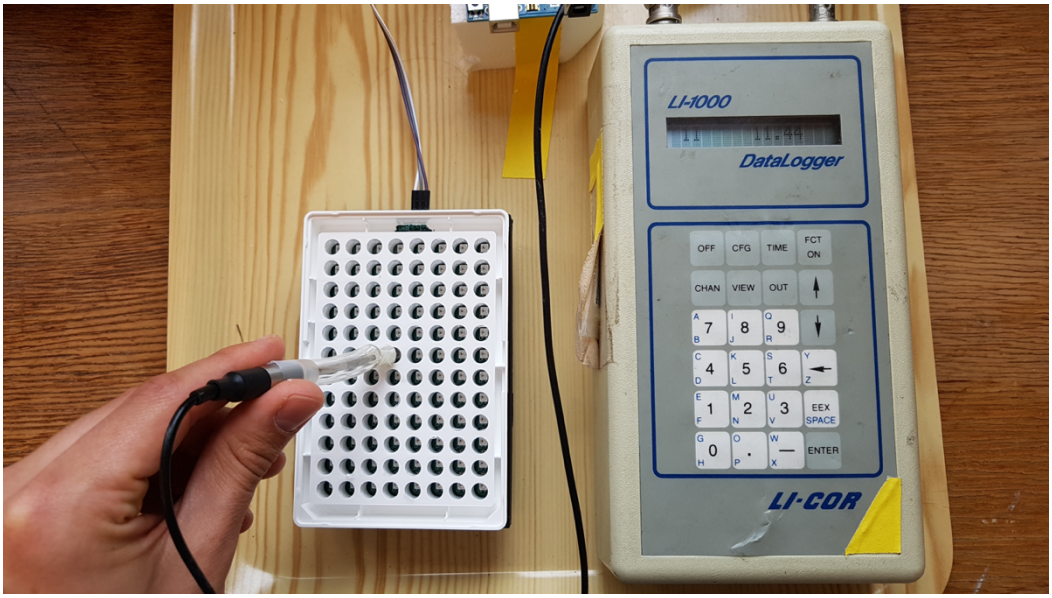

Figure S2: *Measuring the light intensity (in* µmol m^{-2} s^{-1}*) for each individual LED light across all eight light panels, using the Li-Cor photometer with attached PAR-sensor.*

The purpose of this was to determine whether there was any overflow of light between the wells and to confirm that each light emitted approximately the desired µmol. The results of the light panel measurements can be seen in Appendix C: Supplementary Results.

Connecting Arduino Boards, Light Panels, and Power Supply

On the light panels used in the second growth experiment there are three inputs: GND, data and VCC. The GND and data inputs are connected to one of the corresponding GND and data inputs on the power board, while the VCC input on the light panel is connected to one of the +5V input on the power board (Figure S4, A).

Additionally, the power board for the light panel is connected to the Arduino board using the same type of insulated electrical wiring. The second GND input on the light panel power board is connected to the associated GND input on the Arduino board. The second data input on the power board is connected to the digital (PWM~) nr 6 input on the Arduino board, while the second +5V on the power board is connected to the Vin input on the Arduino board (Figure S4, B).

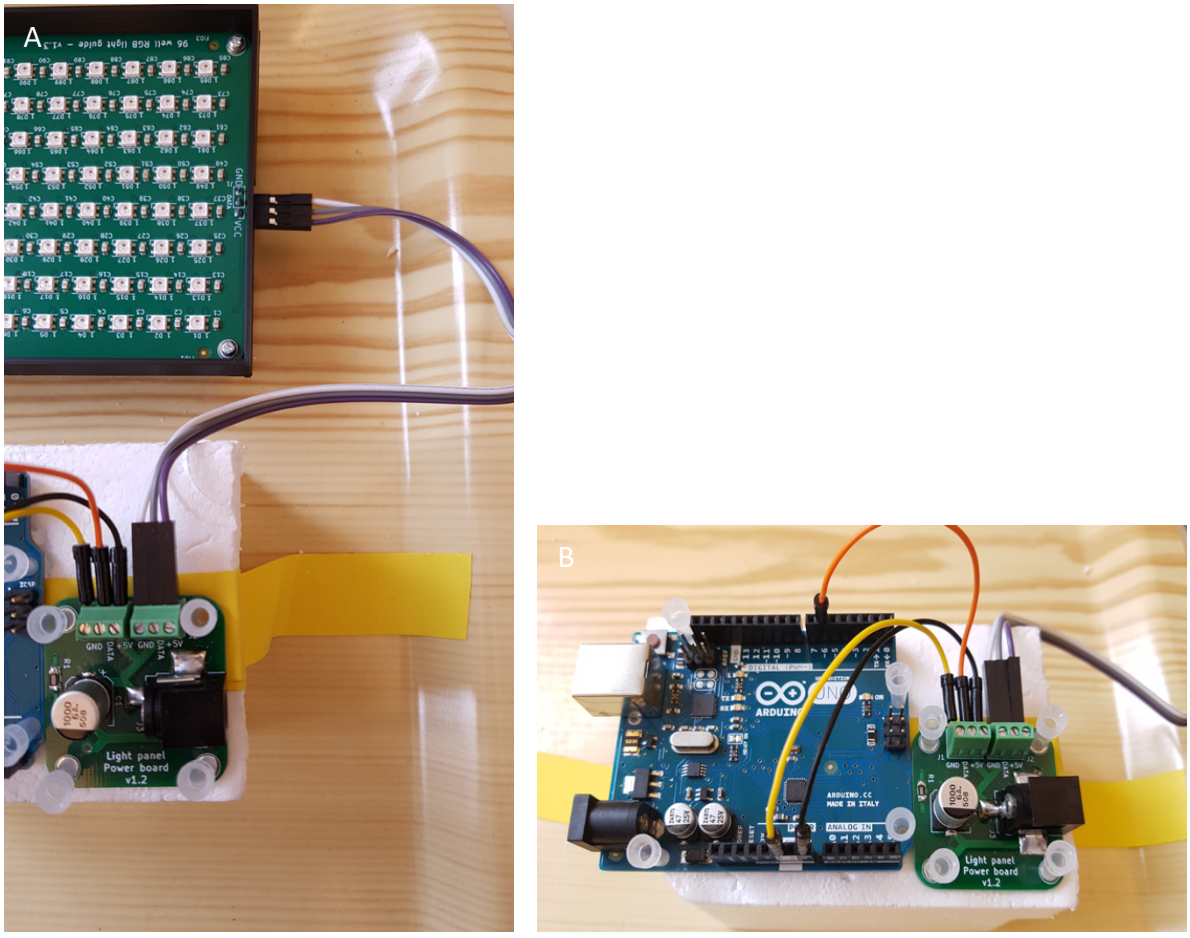

Figure S3: *(A) The position of the electrical wires connecting the light panels and power boards. The white wire is connected to the GND inputs, the gray wire is connected to the data inputs, and the purple wire is connected to the VCC/+5V inputs. (B) The position of the electrical wires connecting the light panel power boards and the Arduino programming boards. The yellow wire is connected to the GND inputs, the orange wire is connected to the nr 6 PWM~/data inputs, and the black wire is connected to the Vin/+5V inputs.*

Measuring pH

When algal cells grow, they respire and produce CO_2. This leads to a chemical reaction causing the production of carbonic acid, which lowers the pH in the medium. By comparing the pH in the wells with clean medium, we get an indication as to whether the algal cells have grown.

Once the second growth experiment was concluded, the pH in certain wells with medium and algal strain were measured using a pH meter (MeterLab PHM201 Portable pH Meter, Radiometer Copenhagen, Denmark). The pH sensor was cleaned before each measurement in the wells by placing it into medium with a corresponding PSU (Figure S4).

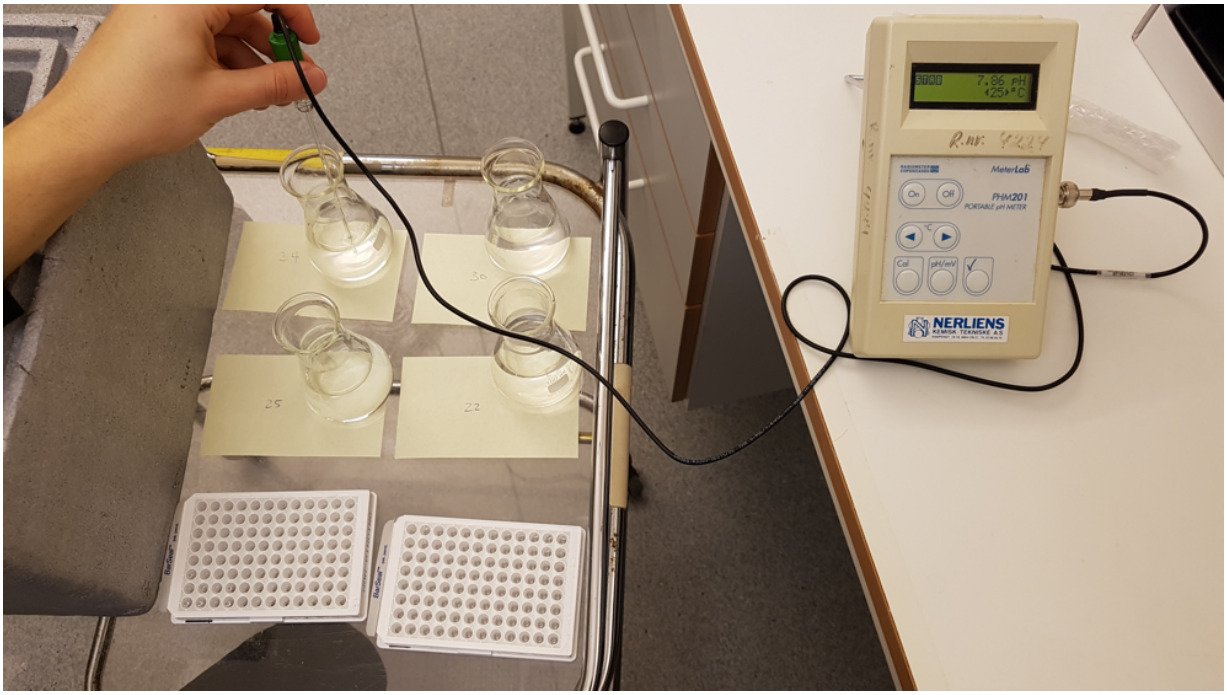

Figure S4: *Measuring the pH of each well at the conclusion of the second growth experiment, using the portable pH meter. Between each measurement, the sensor was rinsed in medium with a corresponding PSU.*

Measurements were taken from all wells with *Nitzschia frigida* and *Synedropsis hyperborea* on plates 1, 2, 7 and 8 as a representative sample. The pH measurements results can be seen in Appendix C: Supplementary Results.

Appendix B: Scripts

Growth Curves (First Growth Experiment)

````
---
        title: "Growth screening"
        output:
          bookdown::html_document2:
            code_folding: hide
            theme: cosmo
            toc: true
            toc_depth: 3
            toc_float: true
        editor_options:
          chunk_output_type: console
        ---

        ```{r setup, include=FALSE}
        knitr::opts_chunk$set(echo = TRUE)
        ```

        ```{r message=FALSE, warning = FALSE}
        require(readr)  # for read_csv()
        require(dplyr)  # for mutate()
        require(tidyr)  # for unnest()
        require(purrr)  # for map(), reduce()
        library(lubridate)
        library(ggplot2)
        library(broom)
        library(modelr)

        '%!in%' <- function(x,y)!('%in%'(x,y))


        viridis_hcl <- colorspace::sequential_hcl(11,
          h = c(300, 75), c = c(35, 95), l = c(15, 90), power = c(0.8, 1.2))

        ```



        ```{r }
        data_path <- "platedata"   # path to the data
        files <- dir(data_path, pattern = "*.csv") # get file names
        ```

        ```{r message=FALSE, warning = FALSE}
````
````

```
data <- tibble(filename = files) %>% # create a data frame
  mutate(file_contents = map(filename,          # read files into
           ~ read_csv2(file.path(data_path, .)) %>%
             rename(Row = X1) %>%
             select(Row:`12`) %>%
             pivot_longer(cols = `1`:`12`, names_to = "Col", values_to =
"Chl")%>%
             unite("ID", Row:Col, remove = FALSE)))  %>%
  unnest(cols = c(filename, file_contents)) %>%
  separate(filename, c("Date","Cultname","CultID"), sep = "_") %>%
  separate(CultID, c("Temperature","leftover"), sep = -4) %>%
  separate(Temperature, c("Temperature","leftover2"), sep = -1) %>%
  mutate(Temperature = as.numeric(Temperature)) %>%
  select(-leftover, -leftover2) %>%
  mutate(Date = ymd(Date))
```

add experimental data

```{r message=FALSE, warning = FALSE}
expdata = read_csv2("Plate Variable values (CSV File).csv") %>%
  mutate(Row = as.character(Row),
         Col = as.character(Column)) %>%
  mutate(Light = 1) ### Remember to take this away for the Second growth
experiment

data %>%
  left_join(expdata) %>%
  mutate(Date = ymd(Date)) %>%
  mutate(Timepassed = int_length(interval(ymd("2020-11-04"), Date))) %>%
  mutate(Timepassed = Timepassed/ (60*60*24)) %>%
  unite("IDunique", c("Temperature","ID"), remove = FALSE)%>%
filter(IDunique %!in% c("11_F_8")) -> df_acclimation #Removing
contaminated well
```

```{r fig.width = 12, fig.height=10}
df_acclimation %>%
 #filter(Species == "Nitzschia sp.") %>%
  unite("IDunique2", c("Temperature","Species", "Salinity"), remove =
FALSE) %>%
  ggplot(aes(x = Timepassed, y = log(Chl), group = IDunique, color =
Temperature,  )) +
  geom_point(alpha = 0.3) +
  #geom_line(alpha = 0.2) +
  xlab("Time Passed (Number of Days)") +
```

```
  ylab ("Log Chlorophyll a Concentration")+
  facet_grid(Species ~Salinity, scales = "free_y",) +
  scale_color_gradientn(colors = viridis_hcl, name="Temperature (°C)") +
theme_bw(base_size=9.8)+ #Remember to change size of text when looking at
specific species
  stat_smooth(aes(group = IDunique2), method = "gam", formula = y ~ s(x,
k = 4), size = 1, se = FALSE)


df_acclimation %>%
#filter(Species == "Synedropsis hyperborea") %>%
  unite("IDunique2", c("Temperature","Species", "Salinity"), remove =
FALSE)  %>%
  ggplot(aes(x = Timepassed, y = log(Chl), group = IDunique, color =
Salinity )) +
  geom_point(alpha = 0.3) +
  #geom_line(alpha = 0.2) +
    xlab("Time Passed (Number of Days)") +
  ylab ("Log Chlorophyll a Concentration")+
  facet_grid(Species ~Temperature, scales = "free_y")+
  scale_color_gradientn(colors = viridis_hcl) +
  theme_bw(base_size=9.8)+ #Remember to change size of text when looking
at specific species
  stat_smooth(aes(group = IDunique2), method = "gam", formula = y ~ s(x,
k = 4), size = 1, se = FALSE)


```
```

Growth Rates (First Experiment)

```
library(growthrates)
install.packages('ggthemes')
library(colorspace)
#First Growth Experiment


#Whole data set

df_acclimation %>% filter(Timepassed> 1)-> df_acclimation_data

df_acclimation_data_fits <- all_splines(Chl ~ Timepassed | IDunique,
                            data = df_acclimation_data, spar = 0.5) #spar best
at 0.5

par(mfrow = c(8, 4))
```
```

```
par(mar = c(1, 1, 1, 1))
plot(df_acclimation_data_fits)

df_acclimation_data_results<-results (df_acclimation_data_fits) #Results

df_acclimation_data_maxgrowth<-inner_join(df_acclimation_data,
df_acclimation_data_results, by="IDunique")

df_acclimation_data_maxgrowth %>%
  filter (r2>0.5) %>%
  ggplot(aes(x = Temperature, y = mumax, color = Salinity )) +
  geom_point() +
  facet_grid(~Species, scales = "free_y") +
  xlab("Temperature (°C)") +
  ylab ("Maximum Growth Rate (µmax)")+
  scale_color_gradientn(colors = viridis_hcl) +
  geom_smooth(aes(group=as.factor(Salinity)), method = "loess")


#Mumax, bruker ikke 0,5 filter:
df_acclimation_data_maxgrowth %>%
  group_by(Species,Salinity, Temperature) %>% summarise(mean_mumax=mean(mumax))
%>%
  ggplot(aes(x = as.factor (Temperature), y = as.factor (Salinity), fill=
mean_mumax)) +
  geom_tile() +
  xlab("Temperature (°C)") +
  ylab ("Salinity")+
  facet_grid(~Species, scales = "free_y") +
  scale_fill_gradient2(low = "firebrick", mid = "white", high = "darkgreen",
midpoint= 0.1, name="Average Maximum\nGrowth Rate (µmax)")
```

Growth Curves (Second Growth Experiment)

```
---
       title: "Growth screening"
       output:
         bookdown::html_document2:
           code_folding: hide
           theme: cosmo
           toc: true
           toc_depth: 3
           toc_float: true
       editor_options:
         chunk_output_type: console
```

```
---

```{r setup, include=FALSE}
knitr::opts_chunk$set(echo = TRUE)
```

```{r message=FALSE, warning = FALSE}
require(readr)  # for read_csv()
require(dplyr)  # for mutate()
require(tidyr)  # for unnest()
require(purrr)  # for map(), reduce()
library(lubridate)
library(ggplot2)
library(broom)
library(modelr)

'%!in%' <- function(x,y)!('%in%'(x,y))


viridis_hcl <- colorspace::sequential_hcl(11,
  h = c(300, 75), c = c(35, 95), l = c(15, 90), power = c(0.8, 1.2))

```



```{r }
data_path <- "platedata"   # path to the data
files <- dir(data_path, pattern = "*.csv") # get file names
```

```{r message=FALSE, warning = FALSE}
data <- tibble(filename = files) %>% # create a data frame
  mutate(file_contents = map(filename,          # read files into
           ~ read_csv2(file.path(data_path, .)) %>%
             rename(Row = X1) %>%
             select(Row:`12`) %>%
             pivot_longer(cols = `1`:`12`, names_to = "Col", values_to =
"Chl") %>%
             unite("ID", Row:Col, remove = FALSE)))  %>%
  unnest(cols = c(filename, file_contents)) %>%
  separate(filename, c("Date","Cultname","Temperature", "Plate"), sep =
"_") %>%
  separate(Temperature, c("Temperature","leftover"), sep = -1) %>%
  separate(Plate, c("Plate","leftover2"), sep = -4) %>%
  separate(Plate, c("leftover3", "Plate"), sep = 5) %>%
  mutate(Temperature = as.numeric(Temperature)) %>%
```
```

```
  select(-starts_with("lefto")) %>%
  mutate(Date = ymd(Date)) -> data
```

add experimental data

```{r message=FALSE, warning = FALSE}
expdata = read_csv2("Plate Variable values (CSV File).csv") %>%
  mutate(Row = as.character(Row),
         Col = as.character(Column))
#  mutate(Light = 1) ### REMEMBER TO TAKE THIS AWAY

data %>%
  left_join(expdata) %>%
  mutate(Date = ymd(Date)) %>%
  mutate(Timepassed = int_length(interval(ymd("2020-12-09"), Date))) %>%
  mutate(Timepassed = Timepassed/ (60*60*24)) %>%
  unite("IDunique", c("Temperature","ID", "Plate"), remove = FALSE) %>%
  filter(IDunique %!in% c( "11_C_4_6", "11_E_6_6", "11_C_4_5",
"11_E_6_5", "4_E_6_2", "4_G_8_2", "4_E_6_1","4_G_8_1")) -> df_final
```

```{r fig.width = 12, fig.height=10}

#df_final %>% filter(IDunique=="15_H_12_8") -> df_4_E_6_1

#max(df_4_E_6_1$Chl)


df_final %>%
  #filter(Species=="Nitzschia frigida", Plate=="2") %>%
  unite("IDunique2", c("Temperature","Species", "Salinity"), remove =
FALSE)  %>%
  ggplot(aes(x = Timepassed, y = log(Chl), group = IDunique, color =
Light )) +
  geom_point(alpha = 0.8) +
  #geom_line(alpha = 0.3) +
    xlab("Time Passed (Number of Days)") +
  ylab ("Log Chlorophyll a Concentration")+
  facet_grid(Species ~Temperature, scales = "free_y") +
  scale_color_gradientn(colors = viridis_hcl, name="Light
Intensity\n(µMol)") +
  theme_bw(base_size=9.8)+ #Remember to change size of text when looking
at specific species
 stat_smooth(aes(group = IDunique), method = "gam", formula = y ~ s(x, k
= 4), size = 1, se = FALSE)
```

```
df_final %>%
#  filter(Species == "Nitzschia frigida", Plate=="1") %>%
  unite("IDunique2", c("Temperature","Species", "Salinity"), remove =
FALSE)  %>%
  ggplot(aes(x = Timepassed, y = log(Chl), group = IDunique, color =
Salinity )) +
  geom_point(alpha = 0.8) +
  geom_line(alpha = 0.3) +
  facet_grid(Species ~Temperature, scales = "free_y")+
  scale_color_gradientn(colors = viridis_hcl) # +
  #stat_smooth(aes(group = IDunique2), method = "lm")
```

Growth Rates (Second Experiment)

```
library(growthrates)
install.packages('ggthemes')
library(colorspace)

#Final experiment
#Whole data set (timepassed only used for second growth experiment, set at 3
days)

df_final %>% filter(Timepassed> 3)-> df_data

df_data_fits <- all_splines(Chl ~ Timepassed | IDunique,
                                  data = df_data, spar = 0.5) #spar 0.5

par(mfrow = c(8, 4))
par(mar = c(1, 1, 1, 1))
plot(df_data_fits)

df_data_results<-results (df_data_fits) #Results

df_data_maxgrowth<-inner_join(df_data, df_data_results, by="IDunique")

#Test
df_data_maxgrowth %>%
  filter (r2>0.5) %>%
  ggplot(aes(x = Light, y = mumax, color = Temperature )) +
  geom_point() +
  ylim(0,1.2)+
  facet_grid(Salinity~Temperature, scales = "free_y") +
  scale_color_gradientn(colors = viridis_hcl) +
```

```
  geom_smooth(aes(group=as.factor(Salinity)), method = "loess")

#Salinity vs Temp
df_data_maxgrowth %>%
  filter (r2>0.5) %>%
  ggplot(aes(x = Temperature, y = mumax, color = Salinity )) +
  geom_point() +
  xlab("Temperature (°C)") +
  ylab ("Maximum Growth Rate (µmax)")+
facet_grid(~Species, scales = "free_y") +
  scale_color_gradientn(colors = viridis_hcl) +
  geom_smooth(aes(group=as.factor(Salinity)), method = "loess")

#Temp vs Light
df_data_maxgrowth %>%
  filter (r2>0.5) %>%
  ggplot(aes(x = Temperature, y = mumax, color = Light )) +
  geom_point() +
  xlab("Temperature (°C)") +
  ylab ("Maximum Growth Rate (µmax)")+
  facet_grid(~Species, scales = "free_y") +
  scale_color_gradientn(colors = viridis_hcl, name= "Light Intensity\n(µMol)") +
  geom_smooth(aes(group=as.factor(Light)), method = "loess")

#Light vs Temp
df_data_maxgrowth %>%
  filter (r2>0.5) %>%
  ggplot(aes(x = Light, y = mumax, color = Temperature )) +
  geom_point() +
  facet_grid(~Species, scales = "free_y") +
  scale_color_gradientn(colors = viridis_hcl) +
  geom_smooth(aes(group=as.factor(Light)), method = "loess")

#Mumax bruker ikke 0,5 filter Option 1:
df_data_maxgrowth %>%
  group_by(Species,Salinity, Temperature, Light ) %>%
summarise(mean_mumax=mean(mumax)) %>%
  ggplot(aes(x = as.factor (Temperature), y = as.factor (Salinity), fill=
mean_mumax)) +
  geom_tile() +
  xlab("Temperature (°C)") +
  ylab ("Salinity")+
  facet_grid(Light~Species, scales = "free_y") +
  scale_fill_gradient2(low = "firebrick", mid = "white", high = "darkgreen",
midpoint= 0.1, name="Average Maximum\nGrowth Rate (µmax)") #+
  #geom_smooth(aes(group=as.factor(Light)), method = "loess")
```

```
#Mumax bruker ikke 0,5 filter Option 2:
df_data_maxgrowth %>%
  group_by(Species,Salinity, Temperature, Light ) %>%
summarise(mean_mumax=mean(mumax)) %>%
  ggplot(aes(x = as.factor (Temperature), y = as.factor (Salinity), fill=
mean_mumax)) +
  geom_tile() +
  xlab("Temperature (°C)") +
  ylab ("Salinity")+
  facet_grid(Light~Species, scales = "free_y") +
  scale_fill_continuous_divergingx(palette = 'RdYlGn', mid = 0.1, l3 = .9, p3 =
.1, p4 = .9, name="Average Maximum\nGrowth Rate (µmax)") #+
#geom_smooth(aes(group=as.factor(Light)), method = "loess")

#without light:
df_data_maxgrowth %>%
  group_by(Species,Salinity, Temperature) %>% summarise(mean_mumax=mean(mumax))
%>%
  ggplot(aes(x = as.factor (Temperature), y = as.factor (Salinity), fill=
mean_mumax)) +
  geom_tile() +
  facet_grid(~Species, scales = "free_y") +
  scale_color_gradientn(colors = viridis_hcl) #+
#geom_smooth(aes(group=as.factor(Light)), method = "loess")

#without salinity:
df_data_maxgrowth %>%
  group_by(Species,Light, Temperature) %>% summarise(mean_mumax=mean(mumax)) %>%
  ggplot(aes(x = as.factor (Temperature), y = as.factor (Light), fill=
mean_mumax)) +
  geom_tile() +
  facet_grid(~Species, scales = "free_y") +


                                                    scale_color_gradientn(colors
                                                    = viridis_hcl) #+
```

Appendix C: Supplementary Results

Table S4: *Light panel measurements for each panel as described in Appendix A: Supplementary Methods, measured in µmol m^{-2} s^{-1}. The last row in each panel is the average light intensity.*

Panel 1	1	2	3	4	5	6	7	8	9	10	11	12
A	7.9	21.3	33.8	48.6	11.9	20.1	31.8	44.4	10.9	17.4	29.1	42.7
B	8.1	23.1	35	51.6	12.8	21.6	31.8	45.8	11.5	19.4	31.8	45.7
C	8.8	22.1	35.5	53.4	12.5	20	34	48.7	11.7	19.9	32.1	47
D	8.9	22.3	36	53.6	13.2	20.9	34.6	43.6	11.6	20.1	33.1	46.7
E	8.8	22.3	35.3	50.5	13	20.7	33.8	48.8	12.1	20.2	33.1	52.3
F	8.9	22.1	37.2	52.4	13	22.5	33.8	48.7	11.7	20.9	33.5	48.4
G	8.8	21.6	35	50.6	12.4	21	33.1	49.5	11.7	20.4	31.4	46.4
H	8.7	21.4	32.7	46.2	11.3	21	30.9	46.5	11.1	19.3	31.7	46.8
	8.6	22	35	50.9	12.5	20.9	32.9	47	11.5	19.7	31.9	47

Panel 2	1	2	3	4	5	6	7	8	9	10	11	12
A	7.9	20.7	32.9	49	12.2	21.8	35.1	48.8	11.2	23	34.9	49.9
B	8.5	21.6	35.4	51.7	13.3	22.4	36.6	48.3	12.6	22.1	32.5	53
C	8.7	21.8	34	51	13.8	22	34	47.4	12.7	21.9	33.1	50.6
D	8.7	22.8	35.7	51	13.5	22	36.2	48.9	13.2	22	34	46.9
E	8.5	21.7	35	53.3	13.5	23	35.5	47.3	13.3	22.4	32.8	48.4
F	8.8	21.3	35.6	51.6	13.8	21.6	34.2	48.5	12.7	21.4	35	50.4
G	8.6	21.6	34.7	51.8	13.3	22.2	35.5	49.1	12.7	22.4	37	50.8
H	8.1	19.8	33.8	49.5	12	20.8	33.8	46.2	12.2	20.7	36.1	52.7
	8.4	21.4	34.6	51.1	13.1	21.9	35.1	48	12.5	21.9	34.4	50.3

Panel 3	1	2	3	4	5	6	7	8	9	10	11	12
A	8.9	22.3	34.7	48.3	12.3	22.8	34.1	44	13.1	23.1	34.5	45.8
B	9.3	23	36.2	48.2	13.2	22.7	33.4	47.9	14.1	23.7	35.7	48.6
C	9.5	22.7	36.2	47.4	13.4	22.8	35.2	48.7	14.4	23.2	35.9	49.9
D	9.4	22.7	36.1	50.5	13.1	22.8	32.9	47.2	14.3	24	35.5	49.6
E	9.3	22.3	34.4	48.5	12.8	22.5	32.9	48.8	14.2	23.3	36.2	49.6
F	9.9	21.3	35.3	48.2	12.9	22	33.2	46.8	13.4	22.4	37.7	47.9
G	9.7	20.2	36.1	49.8	13.6	22.7	35.6	49.5	13.7	22.6	36.6	47
H	9	21.3	32.7	47.7	12.3	22.1	33.7	50.5	13.6	22	34.9	47.8
	9.3	21.9	35.2	48.5	12.9	22.5	33.8	47.9	13.8	23	35.8	48.2

Panel 4	1	2	3	4	5	6	7	8	9	10	11	12
A	10	24	35.3	51.1	14.4	21	32.3	46.5	13.1	21.2	33	49.1
B	10.4	24.6	35.4	51.3	14.9	21.1	35.8	47.7	15	22.4	35.1	48.5
C	10.4	24.5	39.7	49.2	15.5	21.6	34.5	47.7	14.5	22.8	34.8	48.7
D	10.2	24	39.7	53.5	15.9	22.4	34.6	47.1	14.9	22.8	34.3	50.8
E	10.3	24.6	38	54	15.8	22.3	34.5	49.7	14.9	22.2	35.1	50.6
F	10.6	25.1	37.1	53	15.5	23.3	33.8	48.5	14.6	22.1	34.8	49.3
G	10	23.6	37.6	54.4	15.5	23.1	36.3	51.2	15	22.1	34.5	51.9
H	9.2	22.1	36.2	51.4	14.5	21.5	34.3	50	14.4	21.7	33.9	48.9
	10.1	24	37.3	52.2	15.2	22	34.5	48.5	14.5	22.1	34.4	49.7

Panel 5	1	2	3	4	5	6	7	8	9	10	11	12
A	8.9	23.4	34.1	50.1	13.4	21.5	32.5	43.6	11.9	19.6	32.6	48.8
B	9.3	23.1	35.8	50.9	14.4	22.6	35.2	48.9	13.1	22.1	35.1	53.2
C	9.7	22.8	38.8	51.9	14.5	22.5	34.6	49.7	13.3	21.2	34.9	48.5
D	9.5	23.4	38.1	54.7	14.6	23.1	34.8	48.6	13.2	21.2	34.4	51.2
E	10.1	23.9	36.9	51.5	14.7	22.8	33	47.1	13.2	22.2	33.8	47.9
F	10.1	24.1	36.2	52.9	14.4	23.5	33.6	48.8	13.3	23.4	34.5	49.6
G	9.6	23.2	36.6	50.2	14.2	22.8	33.8	48.6	13.1	21.6	33.9	50
H	9	21.8	35.5	49.3	13.1	21.7	31.9	47.8	12.6	21.2	33.3	47.6
	9.5	23.2	36.5	51.4	14.1	22.5	33.6	47.8	12.9	21.5	34	49.6

Panel 6	1	2	3	4	5	6	7	8	9	10	11	12
A	8.1	21.6	33.3	47.1	11.6	20.4	32	46.2	11.8	19.6	33.8	44.8
B	8.6	22	35.6	50.2	13	21.4	33.1	44.9	12.4	20.7	33.3	47.7
C	8.5	21.6	33.7	49.3	13.3	21.4	33.7	46.3	12.7	20.7	33.4	50.6
D	8.6	21.8	35.4	48.3	13.3	20.6	32.9	45	12.7	20.3	34.9	45.6
E	8.8	22.1	37	50.2	13.3	20.6	32.2	49.4	13.2	21	34.9	47.8
F	8.6	22.5	36.8	52.9	13.1	21	32.7	46.9	12.8	20.6	33.1	46.4
G	8.7	20.5	34.6	50	13	20.8	32.1	46.7	12.4	21.7	32.8	45.7
H	7.8	21.6	32.6	49.7	12.2	19.7	29.5	44.7	11.7	21.6	32.4	50
	8.4	21.7	34.8	49.7	12.8	20.7	32.2	46.2	12.4	20.7	33.5	47.3

Panel 7	1	2	3	4	5	6	7	8	9	10	11	12
A	8.3	20.2	32.7	45.6	12.2	19	33.3	45	11.4	19.6	32.4	46.5
B	8.9	22	33.6	47.3	13.5	20.9	33.9	47.3	12.7	20.9	32.4	49
C	9.1	22.1	34.6	49.2	13.4	21.2	33.1	48.8	13	19.6	33.5	48.2
D	9.1	21.5	36.4	51.9	13.5	21.4	33.6	49	12.6	20.6	34.1	49.1
E	8.9	21.7	38.4	51.4	13.3	21.2	32.9	48.2	13.5	21.4	33.8	46.9
F	9.2	22.7	36.3	50.4	13.4	21.3	32.6	47.5	13.3	21.5	35.5	47.2
G	8.8	21.9	35.6	51	13.3	21.1	32.5	47.9	12.9	21.7	34.4	48.9
H	8.1	21.2	33.4	49.2	12.4	19.9	31.8	51.1	12.3	19.9	33.9	47.5
	8.8	21.6	35.1	49.5	13.1	20.7	32.9	48.1	12.7	20.6	33.7	47.9

Panel 8	1	2	3	4	5	6	7	8	9	10	11	12
A	8.8	20.9	33.3	47	12.3	19.6	30.5	44.5	11	19.7	32.9	49.2
B	8.5	21.6	36.9	48.6	12.5	21.3	32	46.5	12.6	20.2	33.9	50.3
C	8.8	22.2	36.4	51.4	13.5	21.3	32.3	47.3	12.9	20.9	33.7	48.8
D	8.9	21.5	35.1	50	13.3	21.9	32.8	45.5	12.9	20.7	35.5	47.5
E	8.9	21.2	34.7	50.3	13.4	21.1	32	46.3	13.3	20.4	34.4	49
F	8.8	21.6	35.2	49.7	13.5	21.9	33.7	47.9	13.1	20.3	34.3	50
G	8.6	20.5	37.3	49.6	13.2	22.7	34.9	49	13.3	22.6	34.2	50
H	7.8	20.4	33.2	49.6	12.3	19.6	32.3	49.6	12.2	21.7	34.2	46.7
	8.6	21.2	35.2	49.5	13	21.1	32.5	47	12.6	20.8	34.1	48.9

Table S5: *Light panel measurements for a sample panel, measured in µmol m^{-2} s^{-1}. The light panels were programmed with one light emitting approximately 42,7 µmol m^{-2} s^{-1}. The surrounding wells were measured to examine the amount of crosstalk that was registered from the one emitting LED light. Shows minimal amounts of crosstalk between wells.*

	1	2	3	4	5	6	7	8	9	10	11	12
A							0.9					
B							0.9					
C					1	1.1	1.2	1.1	0.9			
D					1	1.8	3.1	1.8	0.9			
E	0.8	0.9	0.8	0.9	1	3.3	**42.7**	2.9	1.1	0.9	0.8	0.7
F					0.9	1.8	3.6	1.9	0.9			
G					0.8	0.9	0.9	0.8	0.8			

Table S6: *Average of temperatures during the growth experiments placed in the temperature rooms, to ensure that the rooms were approximately at the desire temperature conditions. The averages are from 2690 data points recorded by the temperature loggers.*

Temperature Logger 1 (4C room)	Temperature Logger 2 (6C room)	Temperature Logger 3 (11C room)	Temperature Logger 4 (15C room)
3,75	7,03	11,08	14,89

A

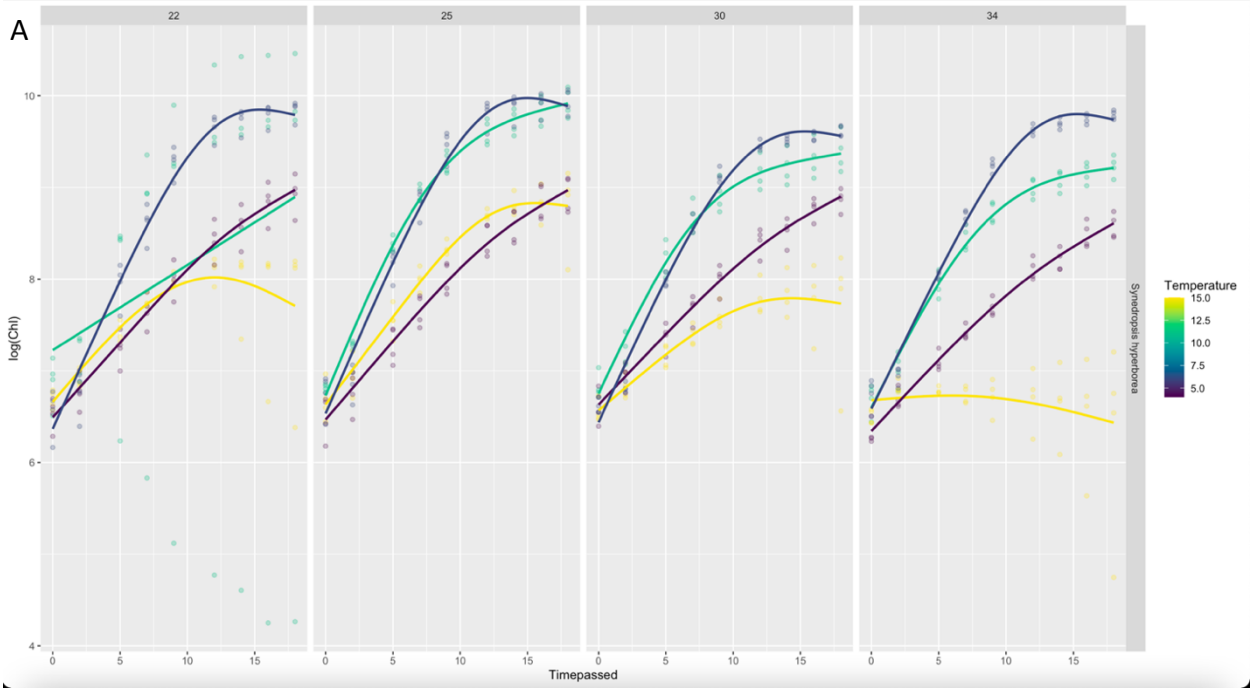
22
25
30
34
log(Chl)
Timepassed
Synedropsis hyperborea
Temperature
15.0
12.5
10.0
7.5
5.0

B

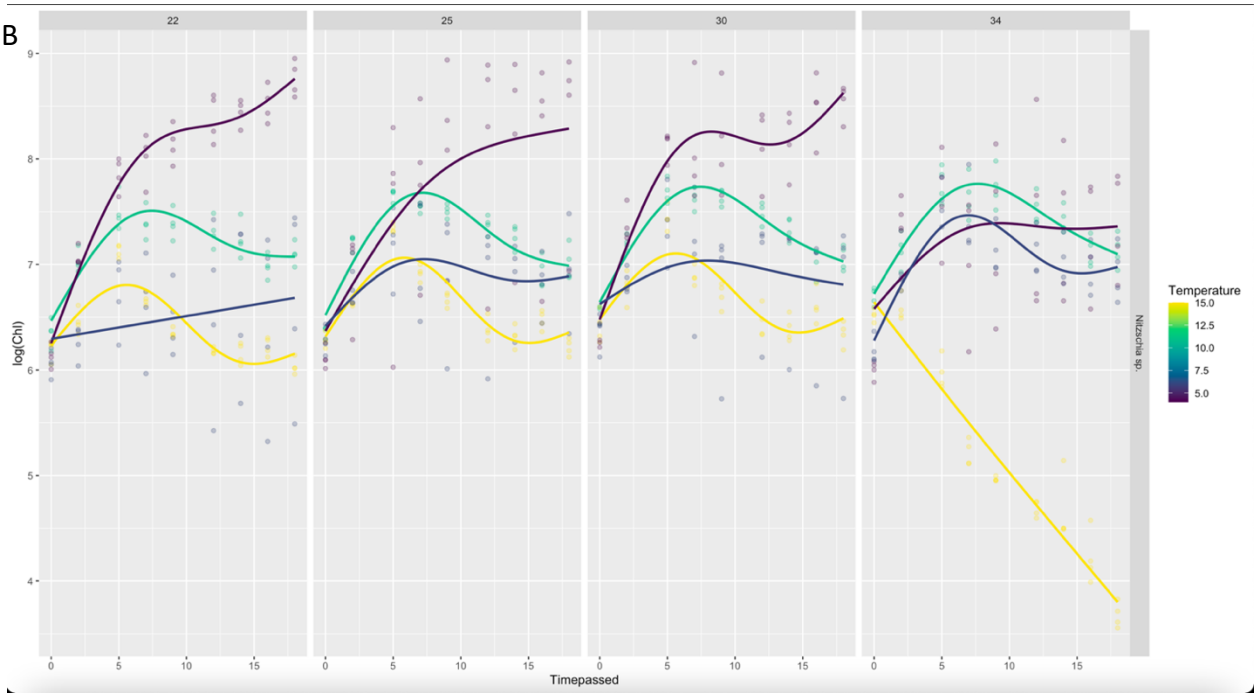
22
25
30
34
log(Chl)
Timepassed
Nitzschia sp.
Temperature
15.0
12.5
10.0
7.5
5.0

C

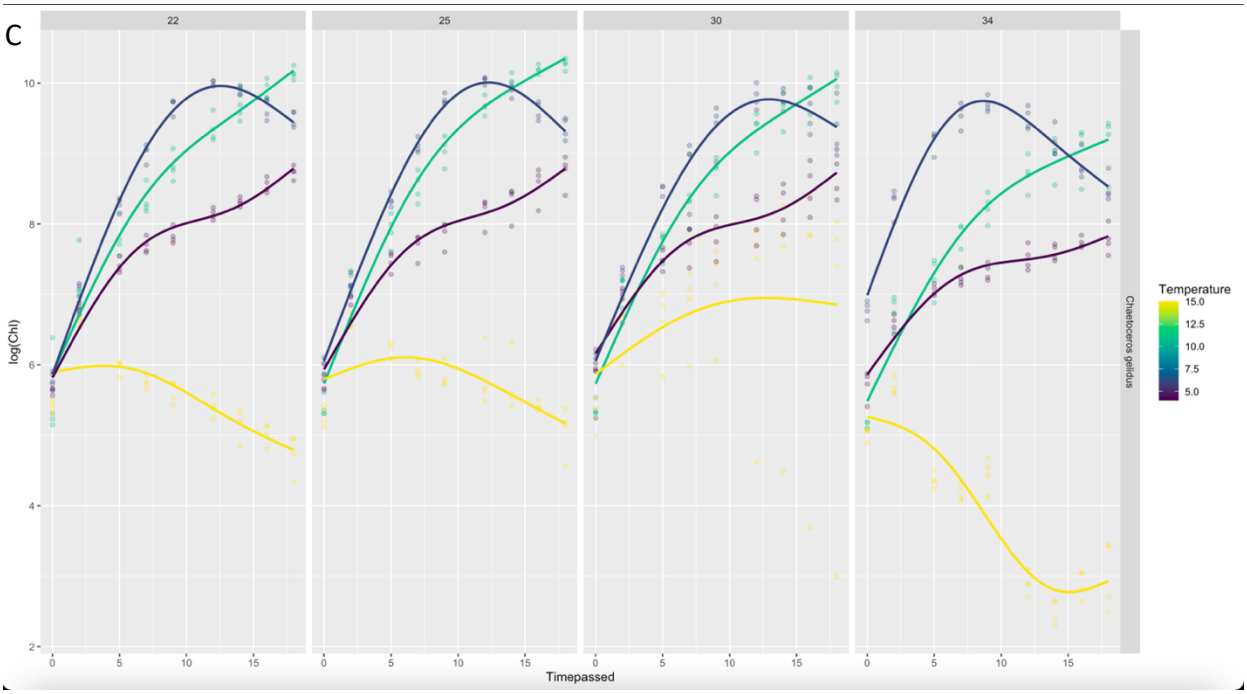
22
25
30
34
log(Chl)
Timepassed
Temperature
15.0
12.5
10.0
7.5
5.0
Chaetoceros gelidus

D

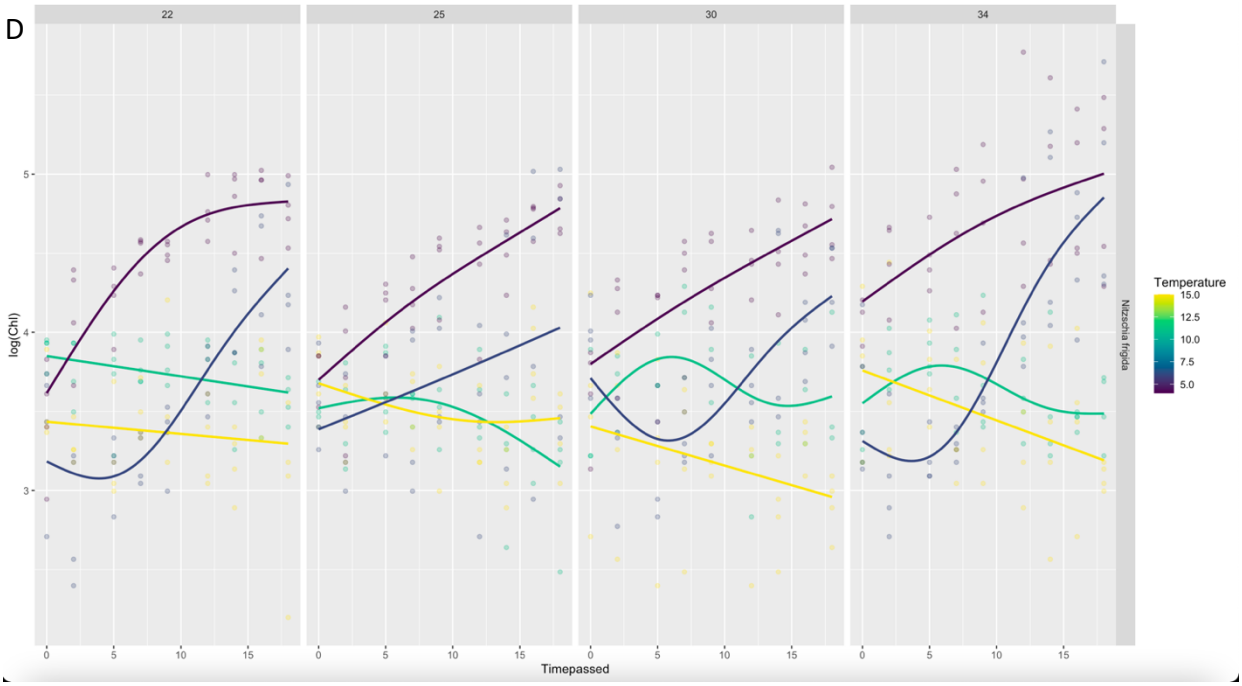
22
25
30
34
log(Chl)
Timepassed
Temperature
15.0
12.5
10.0
7.5
5.0
Nitzschia frigida

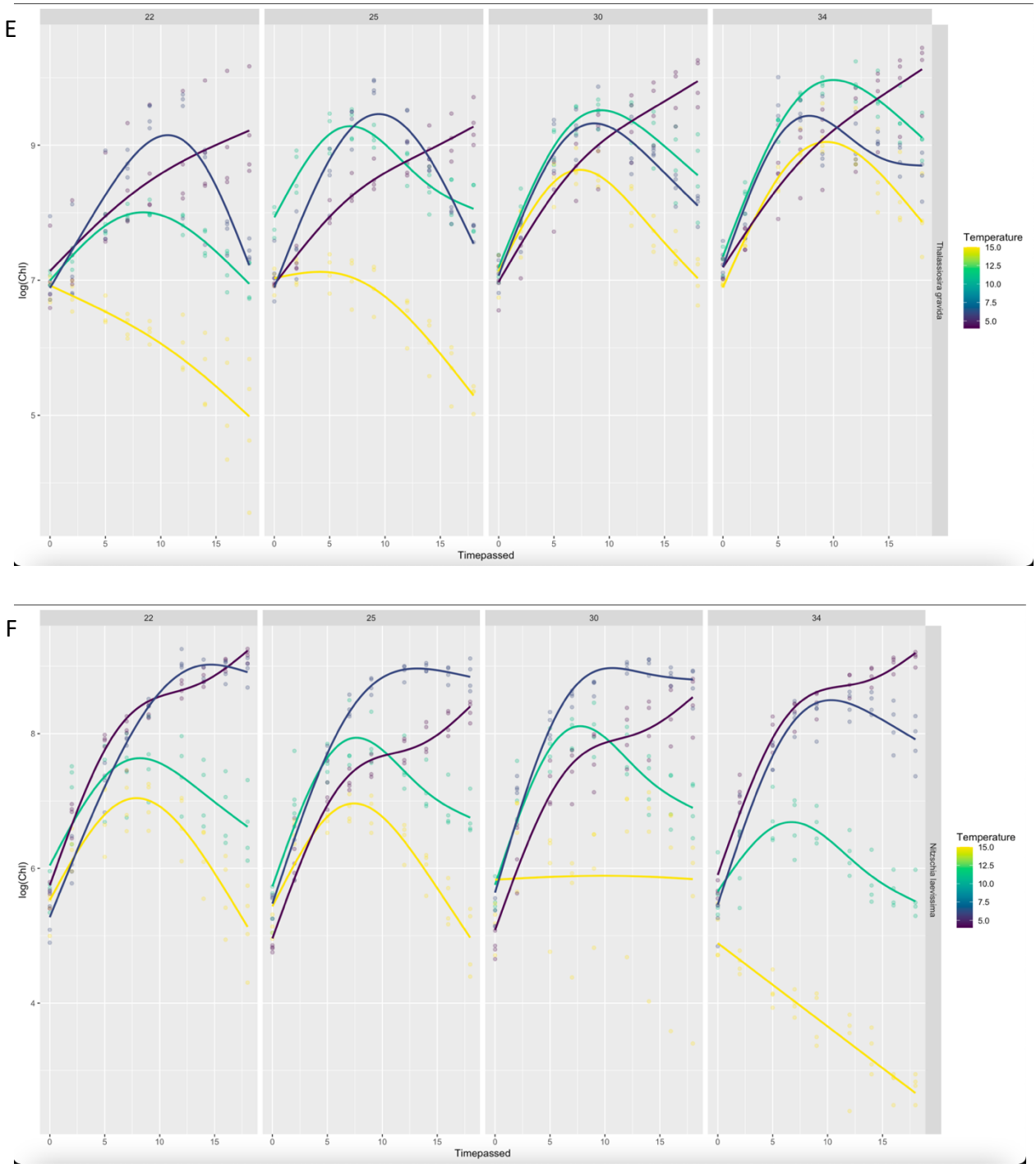

Figure S7: *Growth curves of each diatom strain from the first growth experiment; (A): Synedropsis hyperborea; (B) Nitzschia* sp.*; (C) Chaetoceros gelidus; (D) Nitzschia frigida; (E) Thalassiosira gravida; (F) Nitzschia laevissima.*

APPENDIX C: SUPPLEMENTARY RESULTS

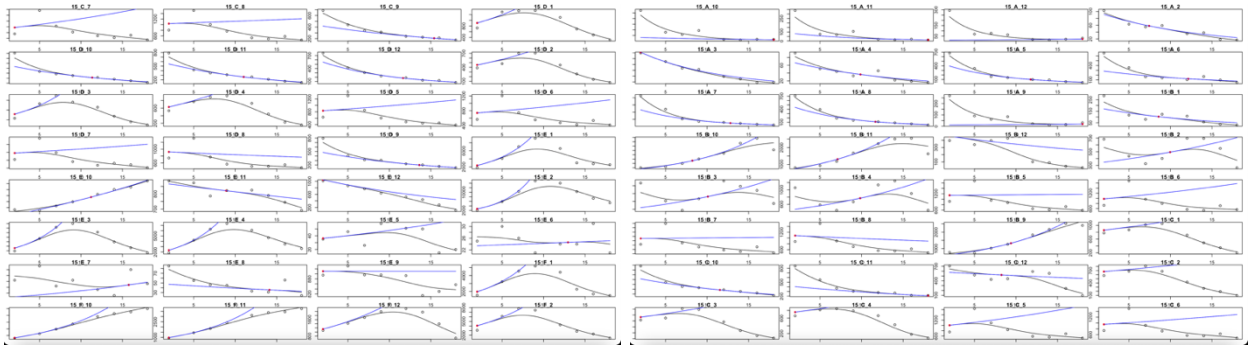

Figure S8: *Growth rates in individual wells from the first growth experiment.*

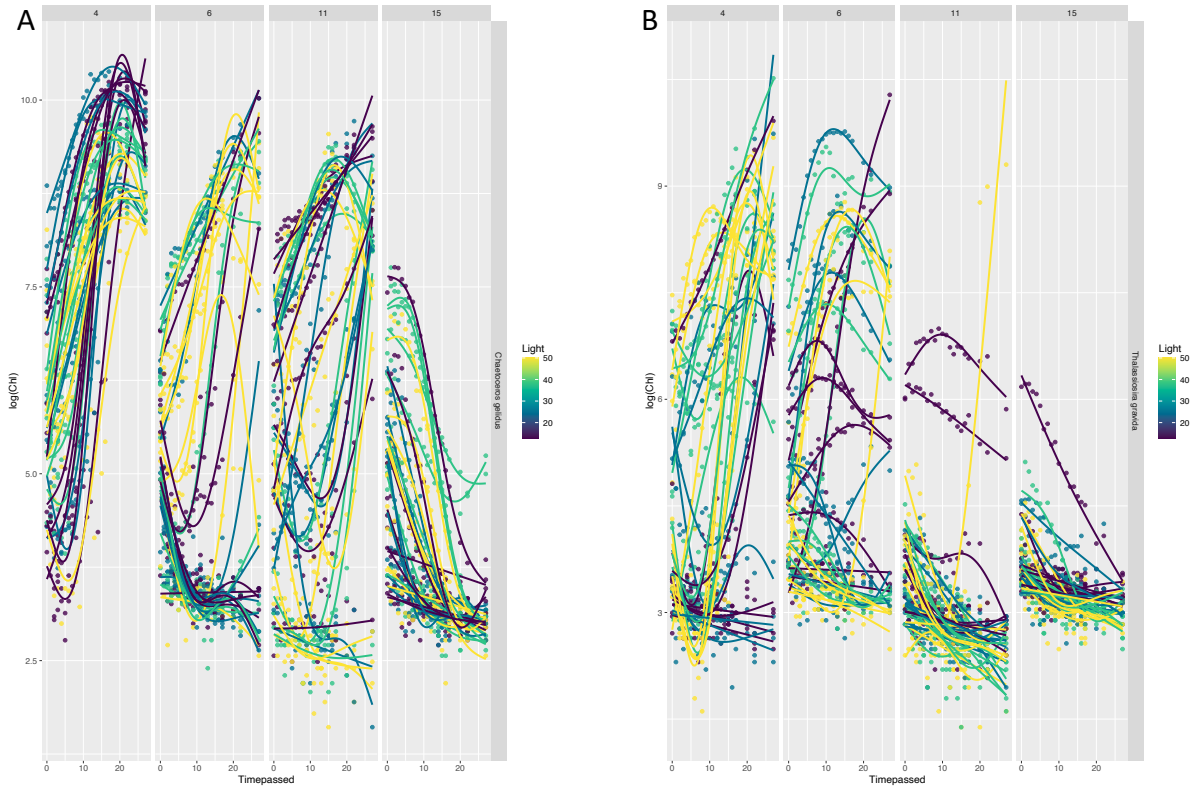

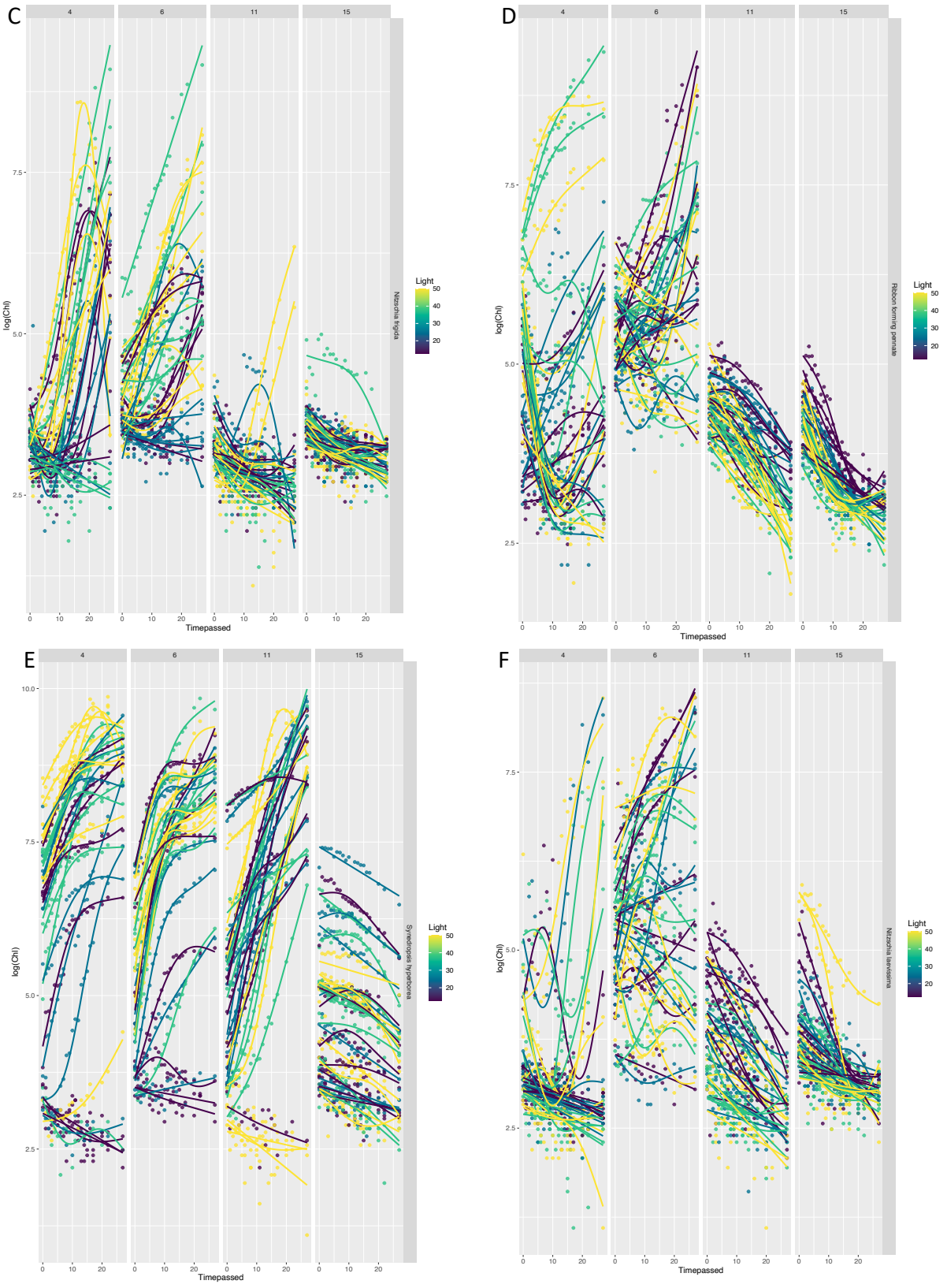

Figure S9: *Growth curves from the second growth experiment by species; (A) Chaetoceros gelidus; (B) Thalassiosira gravida; (C) Nitzschia frigida; (D) Nitzschia sp., here referred to as Ribbon Forming Pennate; (E) Synedropsis hyperborea; (F) Nitzschia laevissima*

APPENDIX C: SUPPLEMENTARY RESULTS

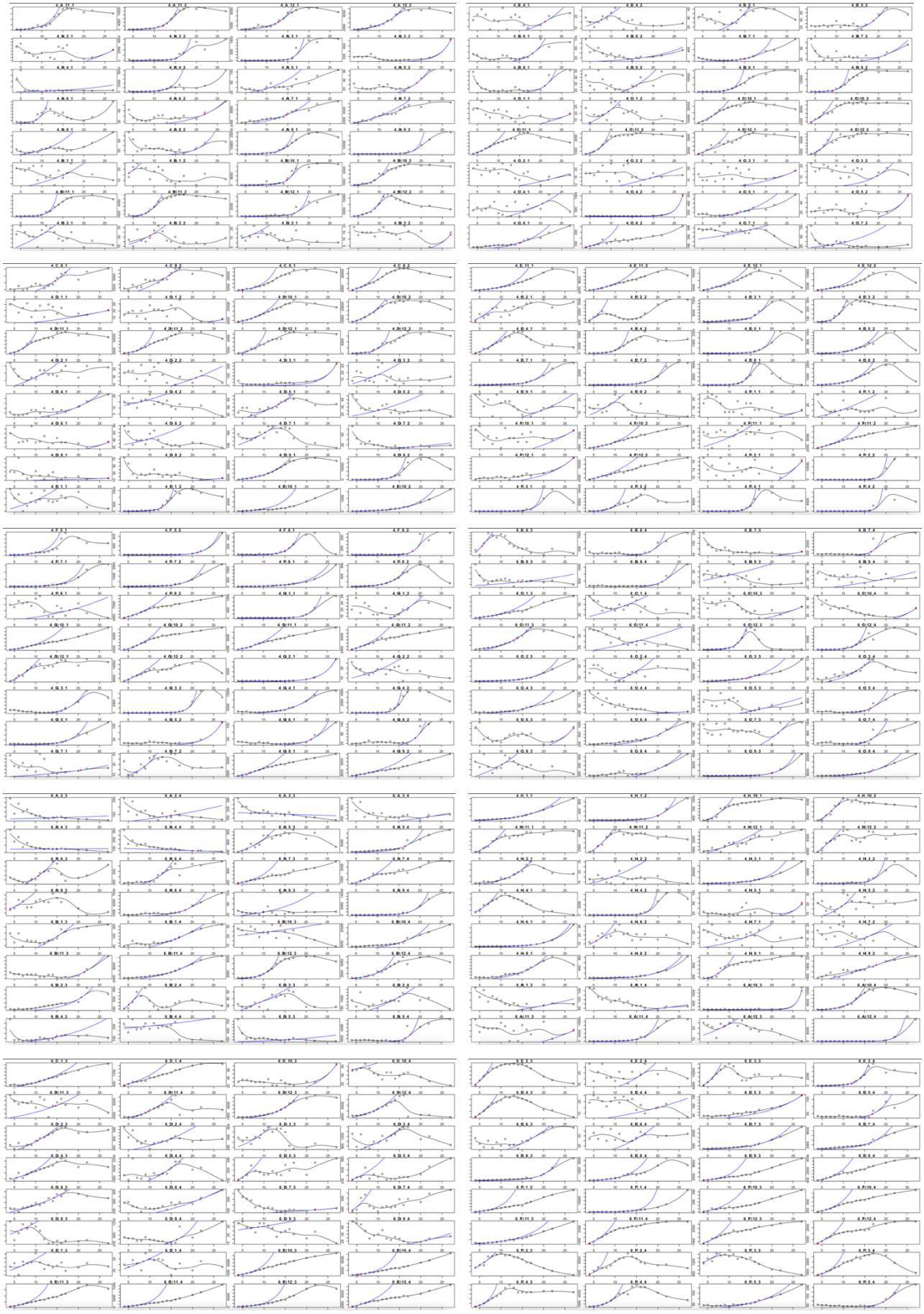

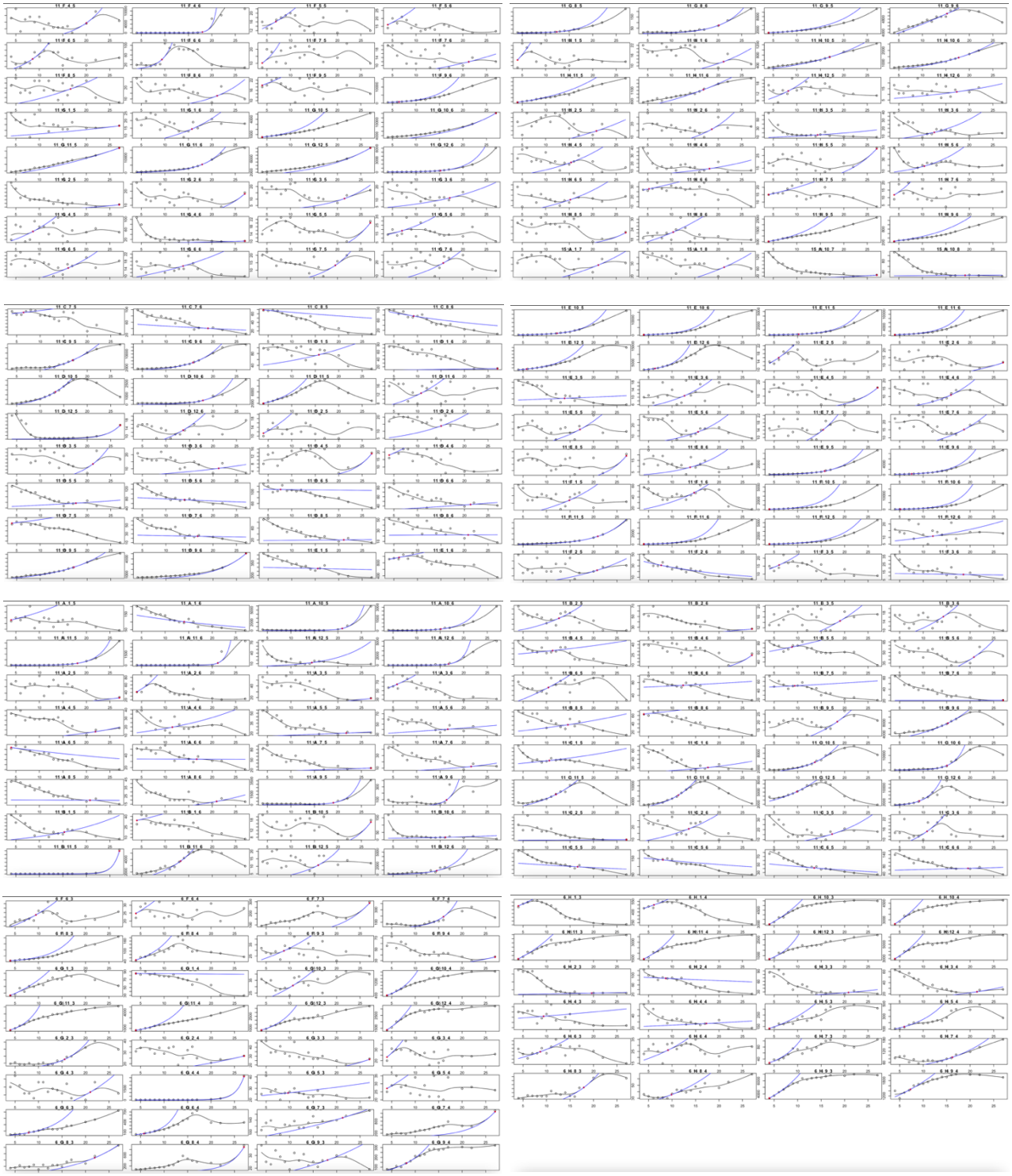

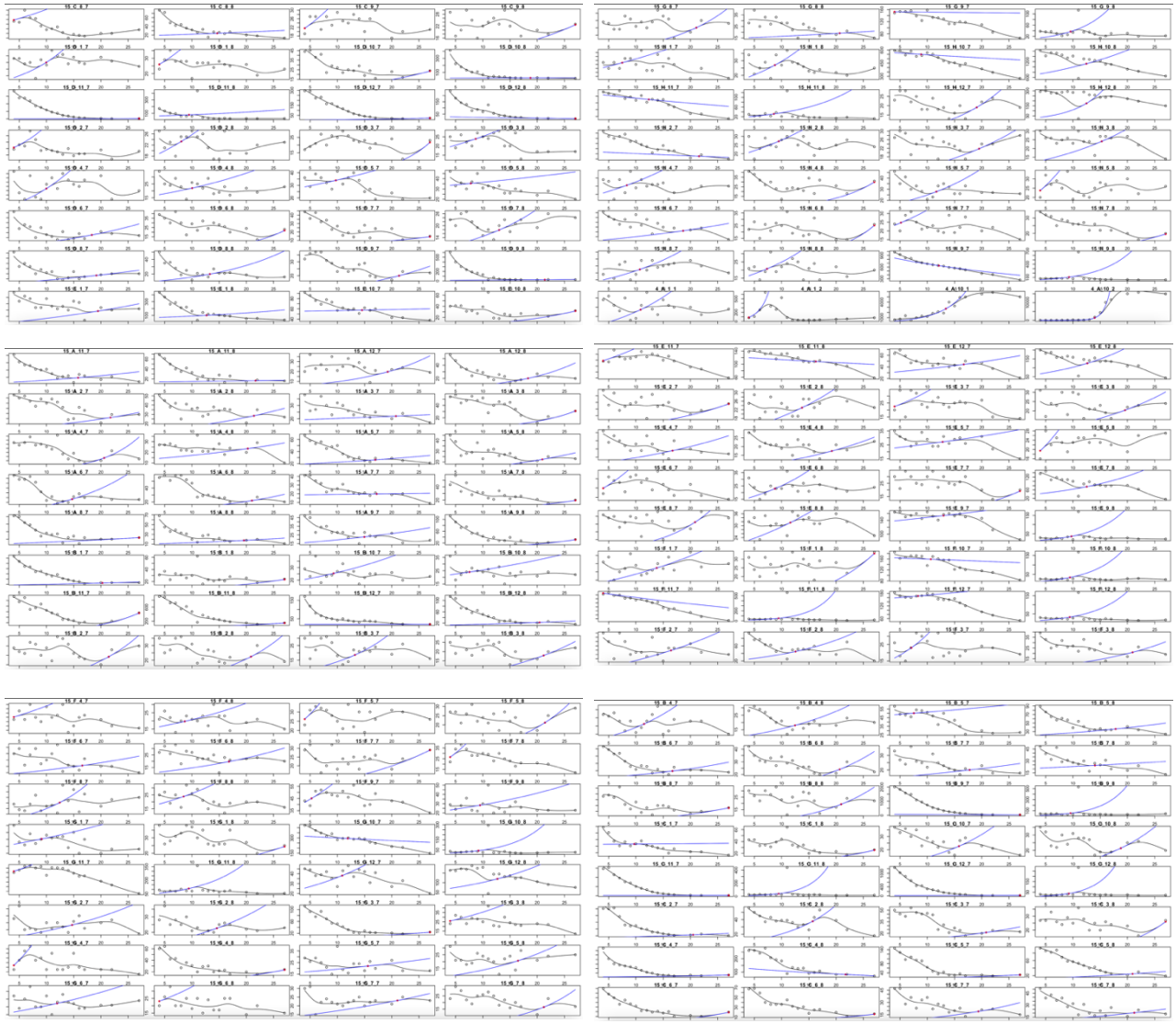

Figure S10: *Growth rates in individual wells from the second growth experiment.*

	AB4306...	AeN706...	AeN706...	AF4176...	KX8392...	AeN707...	KX8392...	KT3900...	MN725...	JQ9954...	KU2128...	AM710...	AeN707...	JQ9954...	JQ9954...	JQ9954...	JQ9954...	AeN707...	HE5735...	JQ9954...	JQ9954...	JQ9954...	KF2197...	JQ9954...	DQ512...	JQ9954...	DQ512...	EF4233...	HE492-...	JQ9954...	JQ9954...	JQ9954...	KT6929...	JQ9954...	FR8234...	LC2583...	JQ9954...	JQ9954...
AB430658.1 Bolidomon...		0.747	0.747	0.746	0.778	0.769	0.785	0.743	0.793	0.787	0.786	0.707	0.742	0.742	0.742	0.745	0.750	0.816	0.816	0.816	0.816	0.816	0.816	0.869	0.757	0.752	0.678	0.678	0.685	0.685	0.685	0.677	0.647	0.674	0.800	0.812	0.845	0.845
AeN706-04 Nitzschia fri...	0.747		0.000	0.048	0.079	0.071	0.050	0.071	0.074	0.193	0.192	0.290	0.496	0.496	0.496	0.499	0.503	0.738	0.738	0.738	0.738	0.738	0.738	0.791	0.679	0.674	0.600	0.600	0.606	0.607	0.607	0.599	0.568	0.596	0.722	0.734	0.767	0.767
AeN706-17 Nitzschia sp.	0.747	0.000		0.048	0.079	0.071	0.050	0.071	0.074	0.193	0.192	0.290	0.496	0.496	0.496	0.499	0.503	0.738	0.738	0.738	0.738	0.738	0.738	0.791	0.679	0.674	0.600	0.600	0.606	0.607	0.607	0.599	0.568	0.596	0.722	0.734	0.767	0.767
AF417667 Nitzschia lec...	0.746	0.048	0.048		0.070	0.062	0.086	0.071	0.094	0.192	0.192	0.290	0.495	0.495	0.495	0.498	0.503	0.737	0.737	0.737	0.737	0.737	0.737	0.790	0.678	0.673	0.599	0.599	0.606	0.606	0.606	0.598	0.568	0.596	0.721	0.733	0.766	0.766
KX839237 Nitzschia sp.	0.778	0.079	0.079	0.070		0.052	0.117	0.102	0.126	0.224	0.223	0.321	0.526	0.526	0.526	0.529	0.534	0.768	0.768	0.768	0.768	0.768	0.768	0.821	0.709	0.704	0.631	0.631	0.637	0.637	0.637	0.630	0.599	0.627	0.753	0.764	0.798	0.798
AeN707-42 Nitzschia la...	0.769	0.071	0.071	0.062	0.052		0.109	0.093	0.117	0.215	0.214	0.312	0.518	0.518	0.518	0.521	0.525	0.760	0.760	0.760	0.760	0.760	0.760	0.813	0.701	0.696	0.622	0.622	0.629	0.629	0.629	0.621	0.590	0.618	0.744	0.756	0.789	0.789
KX839245 Nitzschia fru...	0.785	0.050	0.050	0.086	0.117	0.109		0.109	0.112	0.231	0.230	0.328	0.534	0.534	0.534	0.537	0.541	0.776	0.776	0.776	0.776	0.776	0.776	0.829	0.717	0.712	0.638	0.638	0.645	0.645	0.645	0.637	0.606	0.634	0.760	0.772	0.805	0.805
KT390088 Nitzschia cf. ...	0.743	0.071	0.071	0.071	0.102	0.093	0.109		0.118	0.189	0.188	0.286	0.492	0.492	0.492	0.494	0.499	0.733	0.733	0.733	0.733	0.733	0.733	0.786	0.674	0.669	0.596	0.596	0.602	0.602	0.602	0.595	0.564	0.592	0.718	0.729	0.763	0.763
MN725814 Nitzschia lin...	0.793	0.074	0.074	0.094	0.126	0.117	0.112	0.118		0.239	0.239	0.337	0.542	0.542	0.542	0.545	0.550	0.784	0.784	0.784	0.784	0.784	0.784	0.837	0.725	0.720	0.646	0.646	0.653	0.653	0.653	0.646	0.615	0.643	0.768	0.780	0.814	0.814
JQ995420.1 Pseudo-nitz...	0.787	0.193	0.193	0.192	0.224	0.215	0.231	0.189	0.239		0.015	0.331	0.536	0.536	0.536	0.539	0.544	0.778	0.778	0.778	0.778	0.778	0.778	0.831	0.719	0.714	0.640	0.640	0.647	0.647	0.647	0.639	0.609	0.637	0.762	0.774	0.807	0.807
KU212806.1 Pseudo-nit...	0.786	0.192	0.192	0.192	0.223	0.214	0.230	0.188	0.239	0.015		0.330	0.535	0.535	0.535	0.538	0.543	0.777	0.777	0.777	0.777	0.777	0.777	0.830	0.718	0.713	0.639	0.639	0.646	0.646	0.646	0.639	0.608	0.636	0.762	0.773	0.807	0.807
AM710588.1 Achnanthi...	0.707	0.290	0.290	0.290	0.321	0.312	0.328	0.286	0.337	0.331	0.330		0.455	0.455	0.455	0.458	0.463	0.697	0.697	0.697	0.697	0.697	0.697	0.750	0.638	0.633	0.559	0.559	0.566	0.566	0.566	0.559	0.528	0.556	0.682	0.693	0.727	0.727
AeN707-94 Synedropsi...	0.742	0.496	0.496	0.495	0.526	0.518	0.534	0.492	0.542	0.536	0.535	0.455		0.000	0.000	0.003	0.021	0.733	0.733	0.733	0.733	0.733	0.733	0.786	0.674	0.669	0.595	0.595	0.602	0.602	0.602	0.594	0.564	0.592	0.717	0.729	0.763	0.763
JQ995434 Fragilariacea...	0.742	0.496	0.496	0.495	0.526	0.518	0.534	0.492	0.542	0.536	0.535	0.455	0.000		0.000	0.003	0.021	0.733	0.733	0.733	0.733	0.733	0.733	0.786	0.674	0.669	0.595	0.595	0.602	0.602	0.602	0.594	0.564	0.592	0.717	0.729	0.763	0.763
JQ995463 Fragilariacea...	0.742	0.496	0.496	0.495	0.526	0.518	0.534	0.492	0.542	0.536	0.535	0.455	0.000	0.000		0.003	0.021	0.733	0.733	0.733	0.733	0.733	0.733	0.786	0.674	0.669	0.595	0.595	0.602	0.602	0.602	0.594	0.564	0.592	0.717	0.729	0.763	0.763
JQ995400 Fragilariacea...	0.745	0.499	0.499	0.498	0.529	0.521	0.537	0.494	0.545	0.539	0.538	0.458	0.003	0.003	0.003		0.024	0.736	0.736	0.736	0.736	0.736	0.736	0.789	0.677	0.672	0.598	0.598	0.604	0.604	0.604	0.597	0.566	0.594	0.720	0.732	0.765	0.765
JQ995460 Fragilariacea...	0.750	0.503	0.503	0.503	0.534	0.525	0.541	0.499	0.550	0.544	0.543	0.463	0.021	0.021	0.021	0.024		0.740	0.740	0.740	0.740	0.740	0.740	0.794	0.681	0.676	0.603	0.603	0.609	0.609	0.609	0.602	0.571	0.599	0.725	0.736	0.770	0.770
AeN707-15 Chaetocero...	0.816	0.738	0.738	0.737	0.768	0.760	0.776	0.733	0.784	0.778	0.777	0.697	0.733	0.733	0.733	0.736	0.740		0.000	0.000	0.000	0.000	0.000	0.279	0.576	0.571	0.497	0.497	0.504	0.504	0.504	0.497	0.466	0.494	0.619	0.631	0.541	0.541
HE573580.1 Chaetocer...	0.816	0.738	0.738	0.737	0.768	0.760	0.776	0.733	0.784	0.778	0.777	0.697	0.733	0.733	0.733	0.736	0.740	0.000		0.000	0.000	0.000	0.000	0.279	0.576	0.571	0.497	0.497	0.504	0.504	0.504	0.497	0.466	0.494	0.619	0.631	0.541	0.541
JQ995409.1 Chaetocero...	0.816	0.738	0.738	0.737	0.768	0.760	0.776	0.733	0.784	0.778	0.777	0.697	0.733	0.733	0.733	0.736	0.740	0.000	0.000		0.000	0.000	0.000	0.279	0.576	0.571	0.497	0.497	0.504	0.504	0.504	0.497	0.466	0.494	0.619	0.631	0.541	0.541
JQ995435 Chaetoceros ...	0.816	0.738	0.738	0.737	0.768	0.760	0.776	0.733	0.784	0.778	0.777	0.697	0.733	0.733	0.733	0.736	0.740	0.000	0.000	0.000		0.000	0.000	0.279	0.576	0.571	0.497	0.497	0.504	0.504	0.504	0.497	0.466	0.494	0.619	0.631	0.541	0.541
JQ995446 Chaetoceros ...	0.816	0.738	0.738	0.737	0.768	0.760	0.776	0.733	0.784	0.778	0.777	0.697	0.733	0.733	0.733	0.736	0.740	0.000	0.000	0.000	0.000		0.000	0.279	0.576	0.571	0.497	0.497	0.504	0.504	0.504	0.497	0.466	0.494	0.619	0.631	0.541	0.541
KF219704 Chaetoceros ...	0.816	0.738	0.738	0.737	0.768	0.760	0.776	0.733	0.784	0.778	0.777	0.697	0.733	0.733	0.733	0.736	0.740	0.000	0.000	0.000	0.000	0.000		0.279	0.576	0.571	0.497	0.497	0.504	0.504	0.504	0.497	0.466	0.494	0.619	0.631	0.541	0.541
JQ995458.1 Chaetocero...	0.869	0.791	0.791	0.790	0.821	0.813	0.829	0.786	0.837	0.831	0.830	0.750	0.786	0.786	0.786	0.789	0.794	0.279	0.279	0.279	0.279	0.279	0.279		0.629	0.624	0.551	0.551	0.557	0.557	0.557	0.550	0.519	0.547	0.673	0.684	0.594	0.594
DQ512395.1 Porosira gl...	0.757	0.679	0.679	0.678	0.709	0.701	0.717	0.674	0.725	0.719	0.718	0.638	0.674	0.674	0.674	0.677	0.681	0.576	0.576	0.576	0.576	0.576	0.576	0.629		0.005	0.302	0.302	0.308	0.308	0.308	0.301	0.270	0.298	0.424	0.435	0.606	0.606
JQ995468.1 Porosira sp.	0.752	0.674	0.674	0.673	0.704	0.696	0.712	0.669	0.720	0.714	0.713	0.633	0.669	0.669	0.669	0.672	0.676	0.571	0.571	0.571	0.571	0.571	0.571	0.624	0.005		0.297	0.297	0.303	0.303	0.303	0.296	0.265	0.293	0.419	0.430	0.601	0.601
DQ512433 Thalassiosir...	0.678	0.600	0.600	0.599	0.631	0.622	0.638	0.596	0.646	0.640	0.639	0.559	0.595	0.595	0.595	0.598	0.603	0.497	0.497	0.497	0.497	0.497	0.497	0.551	0.302	0.297		0.000	0.007	0.007	0.007	0.032	0.065	0.069	0.195	0.206	0.527	0.527
EF423391 Thalassiosira...	0.678	0.600	0.600	0.599	0.631	0.622	0.638	0.596	0.646	0.640	0.639	0.559	0.595	0.595	0.595	0.598	0.603	0.497	0.497	0.497	0.497	0.497	0.497	0.551	0.302	0.297	0.000		0.007	0.007	0.007	0.032	0.065	0.069	0.195	0.206	0.527	0.527
HE492-07 Thalassiosira...	0.685	0.606	0.606	0.606	0.637	0.629	0.645	0.602	0.653	0.647	0.646	0.566	0.602	0.602	0.602	0.604	0.609	0.504	0.504	0.504	0.504	0.504	0.504	0.557	0.308	0.303	0.007	0.007		0.000	0.000	0.039	0.072	0.075	0.201	0.213	0.533	0.533
JQ995402 Thalassiosira...	0.685	0.607	0.607	0.606	0.637	0.629	0.645	0.602	0.653	0.647	0.646	0.566	0.602	0.602	0.602	0.604	0.609	0.504	0.504	0.504	0.504	0.504	0.504	0.557	0.308	0.303	0.007	0.007	0.000		0.000	0.039	0.072	0.075	0.201	0.213	0.533	0.533
JQ995414 Thalassosira ...	0.685	0.607	0.607	0.606	0.637	0.629	0.645	0.602	0.653	0.647	0.646	0.566	0.602	0.602	0.602	0.604	0.609	0.504	0.504	0.504	0.504	0.504	0.504	0.557	0.308	0.303	0.007	0.007	0.000	0.000		0.039	0.072	0.075	0.201	0.213	0.533	0.533
JQ995408.1 Shionodisc...	0.677	0.599	0.599	0.598	0.630	0.621	0.637	0.595	0.646	0.639	0.639	0.559	0.594	0.594	0.594	0.597	0.602	0.497	0.497	0.497	0.497	0.497	0.497	0.550	0.301	0.296	0.032	0.032	0.039	0.039	0.039		0.064	0.068	0.194	0.205	0.526	0.526
KT692948.1 Bacterosir...	0.647	0.568	0.568	0.568	0.599	0.590	0.606	0.564	0.615	0.609	0.608	0.528	0.564	0.564	0.564	0.566	0.571	0.466	0.466	0.466	0.466	0.466	0.466	0.519	0.270	0.265	0.065	0.065	0.072	0.072	0.072	0.064		0.061	0.187	0.199	0.495	0.495
JQ995428.1 Thalassiosi...	0.674	0.596	0.596	0.596	0.627	0.618	0.634	0.592	0.643	0.637	0.636	0.556	0.592	0.592	0.592	0.594	0.599	0.494	0.494	0.494	0.494	0.494	0.494	0.547	0.298	0.293	0.069	0.069	0.075	0.075	0.075	0.068	0.061		0.176	0.187	0.523	0.523
FR823449.1 Skeletone...	0.800	0.722	0.722	0.721	0.753	0.744	0.760	0.718	0.768	0.762	0.762	0.682	0.717	0.717	0.717	0.720	0.725	0.619	0.619	0.619	0.619	0.619	0.619	0.673	0.424	0.419	0.195	0.195	0.201	0.201	0.201	0.194	0.187	0.176		0.028	0.649	0.649
LC258389.1 Skeletone...	0.812	0.734	0.734	0.733	0.764	0.756	0.772	0.729	0.780	0.774	0.773	0.693	0.729	0.729	0.729	0.732	0.736	0.631	0.631	0.631	0.631	0.631	0.631	0.684	0.435	0.430	0.206	0.206	0.213	0.213	0.213	0.205	0.199	0.187	0.028		0.661	0.661
JQ995412.1 Eucampia g...	0.845	0.767	0.767	0.766	0.798	0.789	0.805	0.763	0.814	0.807	0.807	0.727	0.763	0.763	0.763	0.765	0.770	0.541	0.541	0.541	0.541	0.541	0.541	0.594	0.606	0.601	0.527	0.527	0.533	0.533	0.533	0.526	0.495	0.523	0.649	0.661		0.000
JQ995430.1 Eucampia g...	0.845	0.767	0.767	0.766	0.798	0.789	0.805	0.763	0.814	0.807	0.807	0.727	0.763	0.763	0.763	0.765	0.770	0.541	0.541	0.541	0.541	0.541	0.541	0.594	0.606	0.601	0.527	0.527	0.533	0.533	0.533	0.526	0.495	0.523	0.649	0.661	0.000	

***Figure S11**: Distance matrix based off phylogenetic analysis, which shows the estimated genetic distance between the sequences included in the phylogenetic tree.*

Table S12: *The six strains of diatoms used in this study with their three highest BLAST results matches of the 28S rRNA gene. The description of their highest matches, the pairwise ID % and the accession numbers of the matches are included.*

Species	Strain ID	BLAST LSU NCBI	Pairwise ID %	Query Cover %	Accession Number
Thalassiosira gravida	HE492-7	Thalassiosira gravida voucher Iceland1 28S ribosomal RNA gene, partial sequence	100	89.01	JX069343
		Thalassiosira rotula voucher GSO101 28S ribosomal RNA gene, partial sequence	99.5	88.85	JX069335
		Thalassiosira rotula 28S rRNA gene, strain thal.rot	99.3	95.3	AJ633505
Nitzschia laevissima	AeN707-42	Nitzschia frustulum isolate kd92 large subunit ribosomal RNA gene, partial sequence	93.7	97.9	KX839245
		Nitzschia cf. pusilla clone ZX28-3-9 18S ribosomal RNA gene, partial sequence; internal transcribed spacer 1, 5.8S ribosomal RNA gene, and internal transcribed spacer 2, complete sequence; and 28S ribosomal RNA gene, partial sequence	93.5	99.3	KT390088
		Nitzschia cf. frequens isolate ccmp1500 28S ribosomal RNA gene, partial sequence	93.5	95.8	MH017363
Nitzschia sp.	AeN706-17	Nitzschia lecointei strain 5-21 large subunit ribosomal RNA gene, partial sequence	96.6	99.3	AF417667
		Pseudo-nitzschia delicatissima clone KJ22-0.2-69 18S ribosomal RNA gene, partial sequence; internal transcribed spacer 1, 5.8S ribosomal RNA gene, and internal transcribed spacer 2, complete sequence; and 28S ribosomal RNA gene, partial sequence	95.8	99.3	KT389889
		Nitzschia sp. 1 SuS-2017 isolate pgmky44 large subunit ribosomal RNA gene, partial sequence	95.7	98.9	KX839237
Chaetoceros gelidus	AeN707-15	Chaetoceros gelidus clone D8 28S ribosomal RNA gene, partial sequence	100	94.28	KF219703
		Chaetoceros socialis strain RCC1994 28S ribosomal RNA gene, partial sequence	100	97.5	JQ995411
		Chaetoceros socialis strain RCC1992 28S ribosomal RNA gene, partial sequence	100	98.7	JQ995409

Nitzschia frigida	AeN706-4	Nitzschia lecointei strain 5-21 large subunit ribosomal RNA gene, partial sequence	96.8	100	AF417667
		Nitzschia frustulum isolate kd92 large subunit ribosomal RNA gene, partial sequence	96.2	99.1	KX839245
		Pseudo-nitzschia delicatissima clone KJ22-0.2-69 18S ribosomal RNA gene, partial sequence; internal transcribed spacer 1, 5.8S ribosomal RNA gene, and internal transcribed spacer 2, complete sequence; and 28S ribosomal RNA gene, partial sequence	95.9	100	KT389889
Synedropsis hyperborea	AeN707-94	Fragilariaceae SB-2012 strain MALINA_FT42.3PG3 28S ribosomal RNA gene, partial sequence	98.9	87.87	JQ995394
		Synedropsis hyperboreoides strain 5-15 large subunit ribosomal RNA gene, partial sequence	98.6	100	AF417685
		Fragilariaceae SB-2012 strain RCC2519 28S ribosomal RNA gene, partial sequence	98.1	91	JQ995462

Table S13: *Alignment of the partial 28S rRNA genetic sequences included in the phylogenetic tree.*

>AB430658.1-_Bolidomonas_pacifica
AATTAAGCATATAATTAAGCGGAGGAAAAGAAACTAACCA-
GGATTCCCCTAGTAAGGGCGACTGAAGCGGGAAGAGCTCAAAATGTGAATCTAATAGCCTT----------
AGCTGGCTGTTCGAATTGTGGTCTACAGATTTGGATTTGGAGCGCGCGGCGGGATAAGTCCATTGGAACATGGCGGCAG
AGAGGGTGAGACCCCCGTTCATGCCTTCC--
GCGTCAACCTTAACATTCCTTATCAATGAGTCGAGTTGCTTGGGATTGCAGCTCAAAGTGGGTGGTAAATTCCATCTAAAG
CTAAATATTGGTGGGAGACCGATAGCGAACAAGTACCGTGAGGGAAAGATGCAAAGAACTTTGAAAAGAGAGTTAAAG
AGTACCTGAAATTGCTGAAAGGGAAGCGAAGGAAACCAGTGTC-
GAGTTTGTGCATATTACTGGCGCCTAGTGGCGTCAG---
GCCGTGTGCTTACTCGGGTCAGTATCGGTTTACATCTGGGGTGAAAC----------GGTTGCCTGCGTT---------
TTGCGCGGCTTCTCCGACTC-CGGTAAGACCGAGGCCAGTCTCGCAAGAGCTCGTGATA-
CTGACGAAATGGTTTTCTTTACCCCGTCTTGAAACCGGGAACCAA----------

> AeN706-04_Nitzschia_frigida
--TTAAGCATATAATTAAGCGGAGGAAAAGAAACTAACCA-
GGATTCCCTCAGTAAGGGCGACTGAAGCGGGAAGTGCTCAGGATGTGAATCTGCGCTA----------
TGCGCCGAATTGTGGTCTGTAGAC----
GGTGGCGCTACTAGCCGGGCCAAGTCCCTTGGAAAAGGGCAGCTGAGAGGGTGAGACTCCCGTCC--GCCCGGC---------
TGGGTGAGCTACTAGTCAACGAGTCGAGTTGTTTGGGATTGCAGCTCAAAGTGGGTGGTAAATTCCATCTAAAGCTAAAT
ATTGGTGGGAGACCGATAGCGTACAAGTACCGTGAGGGAAAGATGCAAAGAACTTTGAAAAGAGAGTTAAAGAGTACC
TGAAATTGCTGAAAGGGAAGCGAAGGAAACCAGTGTT--
TGCTCGGTCATATTTCCCTGGCCGCTTGCGGCTTGGGCGCTGTG-
TCCGGCTTGTGTTGTTCTTGGTTGGGACCCTTGGAAGAGCGCAGAGGGAGTTGA----------
CCTCTGTTGCTAGCATT-GGTCCTGACTGAGG----------
AGGACGAAATGGTTTTCTTTACCCCGTCTTGAAACACGGACCAAGG---------

>AeN706-17_Nitzschia_sp.
AATTAAGCATATAATTAAGCGGAGGAAAAGAAACTAACCA-
GGATTCCCTCAGTAAGGGCGACTGAAGCGGGAAGTGCTCAGGATGTGAATCTGCGCTA----------
TGCGCCGAATTGTGGTCTGTAGAC----
GGTGGCGCTACTAGCCGGGCCAAGTCCCTTGGAAAAGGGCAGCTGAGAGGGTGAGACTCCCGTCC--GCCCGGC---------
TGGGTGAGCTACTAGTCAACGAGTCGAGTTGTTTGGGATTGCAGCTCAAAGTGGGTGGTAAATTCCATCTAAAGCTAAAT
ATTGGTGGGAGACCGATAGCGTACAAGTACCGTGAGGGAAAGATGCAAAGAACTTTGAAAAGAGAGTTAAAGAGTACC
TGAAATTGCTGAAAGGGAAGCGAAGGAAACCAGTGTT--
TGCTCGGTCATATTTCCCTGGCCGCTTGCGGCTTGGGCGCTGTG-
TCCGGCTTGTGTTGTTCTTGGTTGGGACCCTTGGAAGAGCGCAGAGGGAGTTGA----------
CCTCTGTTGCTAGCATT-GGTCCTGACTGAGG----------
AGGACGAAATGGTTTTCTTTACCCCGTCTTGAAACACGGACCAAGG---------

>AF417667-_Nitzschia_lecointei
ATTTAAGCATATAATTAAGCGGAGGAAAAGAAACTAACCA-
GGATTCCCTCAGTAAGGGCGACTGAAGCGGGATGTGCTCAGGATGTGAATCTGCGCTA----------
TGCGCCGAATTGTGGTCTGTAGAC----
GGTGGCGCTACCAGCCGGGCTAAGTCCCTTGGAACAGGGCAGCTGAGAGGGTGAGACTCCCGTCC--GCCTGGC---------
AGGGTGAGCTATCAGTCAACGAGTCGAGTTGTTTGGGATTGCAGCTCAAAGTGGGTGGTAAATTCCATCTAAAGCTAAAT
ATTGGTGGGAGACCGATAGCGTACAAGTACCGTGAGGGAAAGATGCAAAGAACTTTGAAAAGAGAGTTAAAGAGTACC
TGAAATTGCTGAAAGGGAAGCGAAGGAAACCAGTGTT--
TGCCTGGTCATATTTCCCTGGCCGCTTGCGGCTTGGGCGCTGTG-
TCCGGCTTGTGTTGTGCTTGGTTGGAACCTTTGGAAGAGCGCAGAGGGAGTTGA----------
CCTTTGTTGCTAGCAGT-GGTTTTGACTGAGC----------
AGGACGAAATGGTTTTCTTTACCCCGTCTTGAAACACGGACCAAGGAG-------

>KX839237_Nitzschia_sp.
-ATTAAGCATATAATTAAGCGGAGGAAAAGAAACTAACCA-
GGATTCCCCCAGTAAGGGCGACTGAAGCGGGAAGTGCTCAGGATGTGAATCTGCGCTG----------
TGCGCCGAATTGTGGTCTGTAGAC----
GGTGGCGCTACTAGCCGGGCCAAGTCCCTTGGAAAAGGGCAGCTGAGAGGGTGAGACTCCCGTCC--GCCTGGC---------
AAGGTGAGCTACCAGTCGACGAGTCGAGTTGTTTGGGATTGCAGCTCAAAGTGGGTGGTAAATTCCATCTAAAGCTAAAT
ATTGGTGGGAGACCGATAGCGTACAAGTACCGTGAGGGAAAGATGCAAAGAACTTTGAAAAGAGAGTTAAAGAGTACC
TGAAATTGCTGAAAGGGAAGCGAAGGAAACCAGTGTT--
GGCTCAGTCATATTTCCCTGGCCGCTGGCGGCTTGGGCGCTGTG-
TCTGGCTTGTGTTGTGCTTGGTTGGATCCTTTGGAAGAGCTCGGAGGGAGTTGA----------
CCTCCGCTGCTAGCACT-GGATCCGACCGAGC----------
AGGACGAAATGGTTTTCTTTACCCCGTCTTGAAACACGGACCAAGGAG-------

>AeN707-42__Nitzschia_laevissima
AATTAAGCATATAATTAAGCGGAGGAAAAGAAACTAACCA-
GGATTCCCCCAGTAAGGGCGACTGAAGCGGGATGTGCTCAGGATGTGAATCTGCGCTTT----------
TGCGCCGAATTGTGGTCTGTAGAC----
GGTGGCGCTACCAGCCGGGCCAAGTCCCTTGGAACAGGGCAGCTGAGAGGGTGAGACTCCCGTCC--GCCTGGC---------
AGGGTAAGCTACTAGTCAACGAGTCGAGTTGTTTGGGATTGCAGCTCAAAGCGGGTGGTAAATTCCATCTAAAGCTAAAT
ATTGGTGGGAGACCGATAGCGTACAAGTACCGTGAGGGAAAGATGCAAAGAACTTTGAAAAGAGAGTTAAAGAGTACC
TGAAATTGCTGAAAGGGAAGCGAAGGAAACCAGTGTT--
TGCTCAGTCATATTTCCCTGGCCGCTTGCGGCTTGGGCGCTGTG-
TCTGGCTTGTGTTGTGTTTGGTTGGGTCTTTTGGAAGAGCATTGAGGGAGTTGA----------
CCTCGATTGCTAGCACT-GGACCCGACTGAGC----------
AGGACGAAATGGTTTTCTTTACCCCGTCTTGAAACACGGACCAAGG---------

>KX839245_Nitzschia_frustulum
-----TACATATAATTAAGCGGAGGAAAAGAAACTAACTA-
GGATTCCCTCAGTAAGGGCGACTGAAGCGGGAAGTGCTCAGGATGTGAATCTGCGCTTT----------
TGCGCCGAATTGTGGTCTGTAGAC----
GGTGGCGTTACTGGCCGGGCCAAGTCCCTTGGAAAAGGGCAGCTGAGAGGGTGACACTCCCGTCC--GCCCGGC---------
CGTGTGAGCTGCTAGTCAACGAGTCGAGTTGTTTGGGATTGCAGCTCAAAGTGGGTGGTAAATTCCATCTAAAGCTAAAT
ATTGGTGGGAGACCGATAGCGTACAAGTACCGTGAGGGAAAGATGCAAAGAACTTTGAAAAGAGAGTTAAAGAGTACC
TGAAATTGCTGAAAGGGAAGCGAAGGAAACCAGTGTT--
TGCCTGGTCATATTTCCCTGGCCGCTTGCGGCTTGGGCGCTGTG-
TCCGGCTTTTGTTGTTCTTGGTTGGGACCTTTGGAAGAGCGCGTAAGGAGTTGA----------
CTTGCGTTGCTAGCGCT-GGTCCTGACTGAGG----------
AGGACGAAATGGTTTTCTTTACCCCGTCTTGAAACACGGACCAAGGAG-------

>KT390088_Nitzschia_cf._pusilla
ATTTAAGCATATAATTAAGCGGAGGAAAAGAAACTAACCA-
GGATTCCCCTAGTAAGGGCGACTGAAGCGGGATCTGCTCAGGATGTGAATCTGCGCCTT----------
AGAAGCGCCGAATTGTGGTCTGTAGAC----
AGTGGCATTACCAGCCGGGCCAAGTCCCTTGGAACAGGGCAGCTGAGAGGGTGAGACTCCCGTTC--GCCTGGC---------
AGGATGAGCTACTAGTCAACGAGTCGAGTTGTTTGGGATTGCAGCTCAAAGCGGGTGGTAAATTCCATCTAAAGCTAAAT
ATTGGTGGGAGACCGATAGCGTACAAGTACCGTGAGGGAAAGATGCAAAGAACTTTGAAAAGAGAGTTAAAGAGTACC
TGAAATTGCTGAAAGGGAAGCGAAGGAAACCAGTGTT--
GGCTTGGTCATATTTCCCTGTCCGCTTGCGGTTTGGGCGCTGTG-
TCCGGCTTGTGTTGTTCTTGGTTGGTACTTTTGGAAGAGCGCAGTGAGAGTTGA----------
TCTCTGTTGCTAGCATT-GGTACTGACTGAGG----------
AGGACGAAATGGTTTTCTTTACCCCGTCTTGAAACACGGACCAAGGAG-------

>MN725814_Nitzschia_linearis
ATTTAAGCATATAATTAAGCGGAGGAAAAGAAACTAACCA-
GGATTCCCCCAGTAACGGCGAGTGAAGCGGGAAATGCTCAGGATGTGAATCTGCGCTTT----------
TGCGCCGAGTTGTGGTCTGTCGAC----
GGTGACACTACCAGCCGGGCCAAGTTCCTTGGAAAAGGACAGCTGAGAGGGTGAGACTCCCGTCC--GCCCGGT---------
AGGGTGAGTTGCCAGTCTTCGAGTCGAGTTGTTTGGGATTGCAGCTCTAAGTGGGTGGTAAATTCCATCTAAAGCTAAAT
ATTGGTGGGAGACCGATAGCGTACAAGTACCGTGAGGGAAAGATGCAAAGAACTTTGAAAAGAGAGTTAAAGAGTACC
TGAAACCGCTGAAAGGGAAGCGAAGGAAACCAGTGTT--
TGCCTGGTCATATTTCCCTGGCCGCTTGCGGCTTGGGCGCTGTG-
TCCGGCTTGAGTTGTGCTTGGTTGCGGCCCTTGGAAGAGCGCAGAGGGAGTTGA----------
CCTCTGTTGCTAGCATTGGGCCTTGACTGAGT----------
AGGACGAAATGGTTTTCTTTACCCCGTCTTGAAACACGGACCAAGGAG-------

>JQ995420.1_Pseudo-nitzschia_granii
----------CAGGATGTGAATCTGCGCTTT----------
TAAGGCGCCGAATTGTGGTCTGTAGAC----
TTTGATGTTATCTGCCGGGCCAAGTTCCTTGGAAAAGGACAGCTGAGAGGGTGAGACTCCCGTCC--GCCTGGT---------
AGAATGAATCATGTGTCAACGAGTCGAGTTGTTTGGGATTGCAGCTCTAATTTGGTGGTAAATTCCATCTAAAGCTAAATA
TTGGTGGGAGACCGATAGCGTACAAGTACCGTGAGGGAAAGATGCAAAGAACTTTGAAAAGAGAGTTAAAGAGTACCT
GAAATTGCTGAAACGGAAGCGAAGGAAACCAGTGTT--
TGTTGGTTCATATTTCCCTGACCACTTGTGGTTTGGGCGCTGTGAGCCTGCGTGGGTTTGTTTTGATTGATCCCTTTGGAAG
AGCGCAGACAGAGTTGA----------TGTCTGTTGCTAGCACT-GGGTTTGATTGATG----------
CAGACGAAATGGTTTTCTTTACCCCGTCTTGAAACACGGACCAAGGAGTCTAACA

>KU212806.1_Pseudo-nitzschia_arctica
----------TGAAGCGGGACTAGCTCAGGATGTGAATCTGCGCTCT----------
----TATGGCGCCGAATTGTGGTCTGTAGAC----
TTTGACGTTATTTGCCGGGCCAAGTTCCTTGGAAAAGGACAGCTGAGAGGGTGAGACTCCCGTCC--GCCTGGT---------
AGAATGAGTCATGTGTCAACGAGTCGAGTTGTTTGGGATTGCAGCTCTAATTTGGTGGTAAATTCCATCTAAAGCTAAATA
TTGGTGGGAGACCGATAGCGTACAAGTACCGTGAGGGAAAGATGCAAAGAACTTTGAAAAGAGAGTTAAAGAGTACCT
GAAATTGCTGAAACGGAAGCGAAGGAAACCAGTGTT--
TGTTGGTTCATATTTCCCTGGCCACTTGTGGTTTGGGCGCTGTGAGCTTGCGTGGGTTTGTTTTGATTGATCCCTTTGGAAG
AGCGCAGACAGAGTTGA----------TGTCTGTTGCTAGCACT-GGGTTTGATTGATG----------
CAGACGAAATGGTTTTCTTTACCCCGTCTTGAAACACGGACCAAGGAGTCTAACA

>AM710588.1_Achnanthidium_minutissimum

TAATTAAGCGGAGGAAAAGAAACTAACTAGGGATTCCCTCAGTAAGGGCGACTGAAGCGGGAATAGCTCATCTTGTGAA
TCTGCGCTT----------TGCGCCGAATTGTGGTCTAGAGAC----
TTTTGCATTACTGGCCGGGCCAAGTCCTCTGGAATGAGGCAGCTGAGAGGGTGACACTCCCGTCC--GCCTGGC---------
CTCTTGAGCAATT-
GTCCACGAGTCGAGTTGTTTGGGATTGCAGCTCAAAGCGGGTGGTAAATTCCATCTAAGGCTAAATATTGGTGGGAGACC
GATAGCGTACAAGTACCGTGAGGGAAAGATGCAAAGAACTTTGAAAAGAGAGTTAAAGAGTACCTGAAATTGCTGAAAC
GGAAGCGAAGGAAACCAGTGTC--AGCTGCGTCATACTTCCCCGCTCGCTTGCGGTCGGGGCGCTGTG-GCCAGCAT-
TGTCAGGCTTGGCTGGATTGGCCGGAACCGCGTACAGGGAGTTGA----------CCTGTGCATGTCGCGGT-
CGATCCGACTGAGG----------TTGGCGAAATGGTTTTCTTTACCCCG----------

>AeN707-94_Synedropsis_hyperborea
GGATTCCCTCAGTAAGGGCGACTGAAGCGGGAATAGCTCGAACCGAA----------
GAATTGTGGTGTG---------
TTTGCGTTACTTGCTCGGCCAAAGTCCCTTGGAACAGGGCAGCGTAGAGGGTGAGACTCCCGTTT--GGCTGTG---------
CTTTTGAGCTTAC-
ATGATGGAGTCGAGTTGTTTGGGATTGCAGCTCAAAGTGGGTGGTAAATTCCATCGAAAGCTAAATATTGGTGGGAGAC
CGATAGCGTACAAGTACCGTGAGGGAAAGATGCAAAGAACTTTGAAAAGAGAGTTAAAGAGTACCTGAAATTGCTGAAA
TGGAAGCGAAGGAAACCAGTGTC--GTGCTTGTCATATTTCTGTCACTGCTTGCGGTGGCGGCGCTGTGG--
CTGCACTGGTCAGGGTTGGTTCTGGT----------CTGGTACAATTCGTGCT-
GGCTGGGACTGAGTT----------CTGTCGAAATGGTTTTCTTTACCCCGTCTTGAAACACGGACCAAGGA--------

>JQ995434_Fragilariaceae_strain
----------GGGCGACTGAAGCGGGAATAGCTCGAACCGAA----------
----------GAATTGTGGTGTG---------
TTTGCGTTACTTGCTCGGCCAAAGTCCCTTGGAACAGGGCAGCGTAGAGGGTGAGACTCCCGTTT--GGCTGTG---------
CTTTTGAGCTTAC-
ATGATGGAGTCGAGTTGTTTGGGATTGCAGCTCAAAGTGGGTGGTAAATTCCATCGAAAGCTAAATATTGGTGGGAGAC
CGATAGCGTACAAGTACCGTGAGGGAAAGATGCAAAGAACTTTGAAAAGAGAGTTAAAGAGTACCTGAAATTGCTGAAA
TGGAAGCGAAGGAAACCAGTGTC--GTGCTTGTCATATTTCTGTCACTGCTTGCGGTGGCGGCGCTGTGG--
CTGCACTGGTCAGGGTTGGTTCTGGT----------CTGGTACAATTCGTGCT-
GGCTGGGACTGAGTT----------CTGTCGAAATGGTTTTCTTTACCCCGTCTTGAAACACGGACCAAGGAG-------

>JQ995463_Fragilariaceae_strain
----------TAAGGGCGACTGAAGCGGGAATAGCTCGAACCGAA----------
----------GAATTGTGGTGTG---------
TTTGCGTTACTTGCTCGGCCAAAGTCCCTTGGAACAGGGCAGCGTAGAGGGTGAGACTCCCGTTT--GGCTGTG---------
CTTTTGAGCTTAC-
ATGATGGAGTCGAGTTGTTTGGGATTGCAGCTCAAAGTGGGTGGTAAATTCCATCGAAAGCTAAATATTGGTGGGAGAC
CGATAGCGTACAAGTACCGTGAGGGAAAGATGCAAAGAACTTTGAAAAGAGAGTTAAAGAGTACCTGAAATTGCTGAAA
TGGAAGCGAAGGAAACCAGTGTC--GTGCTTGTCATATTTCTGTCACTGCTTGCGGTGGCGGCGCTGTGG--
CTGCACTGGTCAGGGTTGGTTCTGGT----------CTGGTACAATTCGTGCT-
GGCTGGGACTGAGTT----------CTGTCGAAATGGTTTTCTTTACCCCGTCTTGAAACACGGACCAAGGAG-------

>JQ995400_Fragilariaceae_strain
----------AAGCGGGAATAGCTCGAACCGAA----------
----AATTGTGGTGTG---------
TTTGCGTTACTTGCTCGGCCAAAGTCCCTTGGAACAGGGCAGCGTAGAGGGTGAGACTCCCGTTT--GGCTGTG---------
CTTTTGAGCTTAC-
ATGATGGAGTCGAGTTGTTTGGGATTGCAGCTCAAAGTGGGTGGTAAATTCCATCGAAAGCTAAATATTGGTGGGAGAC
CGATAGCGTACAAGTACCGTGAGGGAAAGATGCAAAGAACTTTGAAAAGAGAGTTAAAGAGTACCTGAAATTGCTGAAA
TGGAAGCGAAGGAAACCAGTGTC--GTGCTTGTCATATTTCTGTCACTGCTTGCGGTGGCGGCGCTGTGG--
CTGCACTGGTCAGGGTTGGTTCTGGT----------CTGGTACAATTCGTGCT-
GGCTGGGACTGAGTT----------CTGTCCAAATGGTTTTCTTTACCCCGTCTTGAAACACGGACCAAGGAG-------

>JQ995460_Fragilariaceae_strain
----------CGGGAATAGCTCGAACCGAA----------
GAATTGTGGTGTG---------
TTTGCGTTACTTGCTCGGCCAAAGTCCCTTGGAACAGGGCAGCGTAGAGGGTGAGACTCCCGTTT--GGCTGTG---------
CTTTTGAGCTTAC-
ATGATGGAGTCGAGTTGTTTGGGATTGCAGCTCAAAGTGGGTGGTAAATTCCATCGAAAGCTAAATATTGGTGGGAGAC
CGATAGCGTACAAGTACCGTGAGGGAAAGATGCAAAGAACTTTGAAAAGAGAGTTAAAGAGTACCTGAAATTGCTGAAA
TGGAAGCGAAGGAAACCAGTGTC--GTGCTTGTCATATTTCTGTGACCGCTTGCGGTTACGGCGCTGTGG--
CTGCACTGGTCAGGGTTGGTTCTGGT----------ACGGTACAATTCGTGCT-
GTCTGGGACCGAGTT----------CTGTCGAAATGGTTTTCTTTACCCCGTCTTGAAACACGGACCAAGGAG-------

>AeN707-15_Chaetoceros_gelidus
----------ACTA-
TGATTCCCTCAGTAAGGGCGACTGAAGCGGGAAGAGCTCATTCTGTGAATCTGTATACTAT----------
TTTTGGTATACCGAGTTGTGGAATATAGAAGCA-
CATCAGTTCGAGTTCTGGTCTAAGTCTCTTGGAAAAGAGCAGCTTAGAGGGTGACACTCCCGTTCTTGGCTAGA--
ACTCAAACTTTAGCATGTGGTTTCGACGAGTCGAGTTGCTTGGGATTGCAGCTCAAAGTTGGTGGTAAATTCCATCTAAAG
CTAAATATCGGTGGGAGACCGATAGCGTACAAGTACCGTGAGGGAAAGATGCAAAGAACTTTGAAAAAAGAGTTAAAG
AGTACCTGAAATTGCTGAAATGGAAGCGAAGGAAACCAGTGCC-
GTTCTATACCATTTTTCTGTTCTTGCTTGCGAGAATAGCGCTGTGGTTTAGTACAGGCCAGCGTGAGTTTGAG--
CCGAAGGAAGCAGCTTTGCAGGAGGCAGCACAATTT-CTGTGCGATTACTGCTTAGTTTTGCTTC-
GGCTTGGACTGAGGCTAGTCACT--TGTGCTCGTGACG-
CTGGCGAAATGGTTTTCTTTACCCCGTCTTGAAACACGGACCAAGGA--------

>HE573580.1_Chaetoceros_socialis
----------CTA-
TGATTCCCTCAGTAAGGGCGACTGAAGCGGGAAGAGCTCATTCTGTGAATCTGTATACTAT----------
TTTTGGTATACCGAGTTGTGGAATATAGAAGCA-
CATCAGTTCGAGTTCTGGTCTAAGTCTCTTGGAAAAGAGCAGCTTAGAGGGTGACACTCCCGTTCTTGGCTAGA--
ACTCAAACTTTAGCATGTGGTTTCGACGAGTCGAGTTGCTTGGGATTGCAGCTCAAAGTTGGTGGTAAATTCCATCTAAAG
CTAAATATCGGTGGGAGACCGATAGCGTACAAGTACCGTGAGGGAAAGATGCAAAGAACTTTGAAAAAAGAGTTAAAG
AGTACCTGAAATTGCTGAAATGGAAGCGAAGGAAACCAGTGCC-
GTTCTATACCATTTTTCTGTTCTTGCTTGCGAGAATAGCGCTGTGGTTTAGTACAGGCCAGCGTGAGTTTGAG--
CCGAAGGAAGCAGCTTTGCAGGAGGCAGCACAATTT-CTGTGCGATTACTGCTTAGTTTTGCTTC-
GGCTTGGACTGAGGCTAGTCACT--TGTGCTCGTGACG-
CTGGCGAAATGGTTTTCTTTACCCCGTCTTGAAACACGGACCAAGGAGTCTAACA

>JQ995409.1_Chaetoceros_socialis

TCCCTCAGTAAGGGCGACTGAAGCGGGAAGAGCTCATTCTGTGAATCTGTATACTAT----------
TTTTGGTATACCGAGTTGTGGAATATAGAAGCA-
CATCAGTTCGAGTTCTGGTCTAAGTCTCTTGGAAAAGAGCAGCTTAGAGGGTGACACTCCCGTTCTTGGCTAGA--
ACTCAAACTTTAGCATGTGGTTTCGACGAGTCGAGTTGCTTGGGATTGCAGCTCAAAGTTGGTGGTAAATTCCATCTAAAG
CTAAATATCGGTGGGAGACCGATAGCGTACAAGTACCGTGAGGGAAAGATGCAAAGAACTTTGAAAAAAGAGTTAAAG
AGTACCTGAAATTGCTGAAATGGAAGCGAAGGAAACCAGTGCC-
GTTCTATACCATTTTTCTGTTCTTGCTTGCGAGAATAGCGCTGTGGTTTAGTACAGGCCAGCGTGAGTTTGAG--
CCGAAGGAAGCAGCTTTGCAGGAGGCAGCACAATTT-CTGTGCGATTACTGCTTAGTTTTGCTTC-
GGCTTGGACTGAGGCTAGTCACT--TGTGCTCGTGACG-
CTGGCGAAATGGTTTTCTTTACCCCGTCTTGAAACACGGACCAAGGAGTCTAACA

>JQ995435_Chaetoceros_socialis
----------AGCGGGAAGAGCTCATTCTGTGAATCTGTATACTAT----------
TTTTGGTATACCGAGTTGTGGAATATAGAAGCA-
CATCAGTTCGAGTTCTGGTCTAAGTCTCTTGGAAAAGAGCAGCTTAGAGGGTGACACTCCCGTTCTTGGCTAGA--
ACTCAAACTTTAGCATGTGGTTTCGACGAGTCGAGTTGCTTGGGATTGCAGCTCAAAGTTGGTGGTAAATTCCATCTAAAG
CTAAATATCGGTGGGAGACCGATAGCGTACAAGTACCGTGAGGGAAAGATGCAAAGAACTTTGAAAAAAGAGTTAAAG
AGTACCTGAAATTGCTGAAATGGAAGCGAAGGAAACCAGTGCC-
GTTCTATACCATTTTTCTGTTCTTGCTTGCGAGAATAGCGCTGTGGTTTAGTACAGGCCAGCGTGAGTTTGAG--
CCGAAGGAAGCAGCTTTGCAGGAGGCAGCACAATTT-CTGTGCGATTACTGCTTAGTTTTGCTTC-
GGCTTGGACTGAGGCTAGTCACT--TGTGCTCGTGACG-
CTGGCGAAATGGTTTTCTTTACCCCGTCTTGAAACACGGACCAAGGAG-------

>JQ995446_Chaetoceros_gelidus

CCCTCAGTAAGGGCGACTGAAGCGGGAAGAGCTCATTCTGTGAATCTGTATACTAT----------
TTTTGGTATACCGAGTTGTGGAATATAGAAGCA-
CATCAGTTCGAGTTCTGGTCTAAGTCTCTTGGAAAAGAGCAGCTTAGAGGGTGACACTCCCGTTCTTGGCTAGA--
ACTCAAACTTTAGCATGTGGTTTCGACGAGTCGAGTTGCTTGGGATTGCAGCTCAAAGTTGGTGGTAAATTCCATCTAAAG
CTAAATATCGGTGGGAGACCGATAGCGTACAAGTACCGTGAGGGAAAGATGCAAAGAACTTTGAAAAAAGAGTTAAAG
AGTACCTGAAATTGCTGAAATGGAAGCGAAGGAAACCAGTGCC-
GTTCTATACCATTTTTCTGTTCTTGCTTGCGAGAATAGCGCTGTGGTTTAGTACAGGCCAGCGTGAGTTTGAG--
CCGAAGGAAGCAGCTTTGCAGGAGGCAGCACAATTT-CTGTGCGATTACTGCTTAGTTTTGCTTC-
GGCTTGGACTGAGGCTAGTCACT--TGTGCTCGTGACG-
CTGGCGAAATGGTTTTCTTTACCCCGTCTTGAAACACGGACCAAGGAG-------

>KF219704_Chaetoceros_gelidus
----------AAGGGCGACTGAAGCGGGAAGAGCTCATTCTGTGAATCTGTATACTAT----
----------TTTTGGTATACCGAGTTGTGGAATATAGAAGCA-
CATCAGTTCGAGTTCTGGTCTAAGTCTCTTGGAAAAGAGCAGCTTAGAGGGTGACACTCCCGTTCTTGGCTAGA--
ACTCAAACTTTAGCATGTGGTTTCGACGAGTCGAGTTGCTTGGGATTGCAGCTCAAAGTTGGTGGTAAATTCCATCTAAAG
CTAAATATCGGTGGGAGACCGATAGCGTACAAGTACCGTGAGGGAAAGATGCAAAGAACTTTGAAAAAAGAGTTAAAG
AGTACCTGAAATTGCTGAAATGGAAGCGAAGGAAACCAGTGCC-
GTTCTATACCATTTTTCTGTTCTTGCTTGCGAGAATAGCGCTGTGGTTTAGTACAGGCCAGCGTGAGTTTGAG--
CCGAAGGAAGCAGCTTTGCAGGAGGCAGCACAATTT-CTGTGCGATTACTGCTTAGTTTTGCTTC-
GGCTTGGACTGAGGCTAGTCACT--TGTGCTCGTGACG-
CTGGCGAAATGGTTTTCTTTACCCCGTCTTGAAACACGGACCAAGGAG-------

>JQ995458.1_Chaetoceros_cf._neogracilis
----------CGGGAACAGCTCATTCTGTGAATCTCTGCTTC----------
--GGCAGCGAGTTGTGG------
AAAGGCATGTCAGCTAAGCTACTGGTCTAAGTCTCTTGGAAAAGAGCGCTTGAAAGGGTGACAGCCCCGTCTTTGACTGG
TTAGCTGTGGCTTTAGCACATGTTTTATACGAGTCGAGTTGCTTGGGATTGCAGCTCTAAGTGGGTGGTAAATTCCATCTA
AAGCTAAATATTGGTGGGACACCGATAGCGTACAAGTACCGTGAGGGAAAGATGCAAAGAACTTTGAAAAGAGAGTTAA
AGAGTACCTGAAATTGCTGAAATGGAAGCGAAGGAAACCAGTGCC-
ATTCTTCACTATTTTTCTGTTCCTACTTGTGGGAATAGCGCTGTGGTGTTGAATAGGCCAGCGTGGGTTTGTA--
CCGGGGGGATAACACTCATCAGAAGGCAGCTAGATTT-CCTAGCGATTGCTGTTGAGCTGTGCTCT-
GGTACAGACTGAGGCTAGTCACT--TGTGCTCGTGACG-
CTGGCGAAATGGTTTTCTTCACCCCGTCTTGAAACACGGACCAAGGAGTCTAACA

>DQ512395.1-_Porosira_glacialis_

ATACACCTAGTAAGGGCGACTGAACAGTGTGAAGCTCACCGTGTGAATCTGTGTAACCTT---GACTCCGGTC-
TTTTGGTGCACCGAATTGTGGTCTGAAGAAGTATTGTCGGTTGCAGTCCCGGACCAAGTCCCTTGGAAAAGGGCAGCTGA
GAGGGTGAGACTCCCGTTCTTGTCTGGGAACTGTGTGCCATGGCACATGCTTTCAACGAGTCGTGTTGATTGGGATTTCA
GCACAAATTCTGTGGTAAATGCCACATAAAGCTAAATATTGGTGGGAGACCGATAGCGCACAAGTACCGTGAGGGAAAG
ATGCAAAGAACTTTGAAAAGAGAGTTAAAGAGTACCTGAAATTGCTGAAAGGGAAGCGAAGGAAACCAGTGCCGTAGT
GTTGTCATACTTCCCCTTCTGCTTGCGGATGGGGCGCTGTGACAGTACGTGGATCAGCATCAACTTTAC-
CTTGGACCAAATGGGTGATTGGTAGACAGCCCCTTTCGAGGGGCCAGTGCTAGTCATTTCTGGTCT-
GAGCGAGGTTGAGGTCAGTCATTC-TGTGCTCGTGATG-CTGAT----------

>JQ995468.1_Porosira_sp.

GGCGACTGAACAGTGTGAAGCTCACCGTGTGAATCTGTGTAACCCATTTGACTCCGGTCTTTTGGGTGCACCGAATTGTG
GTCTGAAGAAGTATTGTCGGTTGCAGTCCCGGACCAAGTCCCTTGGAAAAGGGCAGCTGAGAGGGTGAGACTCCCGTTC
TTGTCTGGGAACTGTGTGCCATGGCACATGCTTTCAACGAGTCGTGTTGATTGGGATTTCAGCACAAATTCTGTGGTAAAT
GCCACATAAAGCTAAATATTGGTGGGAGACCGATAGCGCACAAGTACCGTGAGGGAAAGATGCAAAGAACTTTGAAAAG
AGAGTTAAAGAGTACCTGAAATTGCTGAAAGGGAAGCGAAGGAAACCAGTGCCGTAGTGTTGTCATACTTCCCCTTCTGC
TTGCGGATGGGGCGCTGTGACAGTACGTGGATCAGCATCAACTTTAC-
CTTGGACCAAATGGGTGATTGGTAGACAGCCCCTTTCGAGGGGCCAGTGCTAGTCATTTCTGGTCT-
GAGCGAGGTTGAGGTCAGTCATTC-TGTGCTCGTGATG-
CTGATGAAATGGTTTTCTTTACCCCGTCTTGAAACACGGACCAAGGAGTCTAAGA

>DQ512433_Thalassiosira_rotula

CTAGTAACGGCGAGTGAAGCGGGAAGAGCTCACCATGTGAATCTGTGTAACCGG----------
AAACGGTGCACCGAATTGTGGTCTGGAGAAGTACTGTCGGCCGTGTTCCCGGGCCAAGTCTCTTGGAAAAGGGCAGCTG
AGAGGGTGAAACTCCCGTTCTTGCCTGGGAACATTGCGCTTTGGCATATACTTTCTACGAGTCGAGTTGCTTGGGATTGCA
GCTCAAATTTGGTGGTAAATTCCATCTAAAGCTAAATATTGGTGGGATACCGATAGTGCACAAGTACCGTGAGGGAAAGA
TGCAAAGAACTTTGAAAAGAGAGTTAAAGAGTACCTGAAATTGTTGAAAGGGAAGCGAAGGAAACCAGTGCCGAAGCTT
AGTCATACTTCTCTTACTACTTGTGGTAAGGGCGCTGTGGCTTTGCGTGGGTCAGCATCGGCTCTTTGCCTGGGATATATC
TTCAGTAGGTAGACGACCTCTTCG--GAGGTGAGTGCCTATTGTTGCTATTCC-GGGTTGGGCTGAGGTCAGTCACTC-
TGTGCTCGTGATG-CTG----------

>EF423391_Thalassiosira_rotula
----------CTAACAA-
GGATTCCCCTAGTAACGGCGAGTGAAGCGGGAAGAGCTCACCATGTGAATCTGTGTAACCGG----------
AAACGGTGCACCGAATTGTGGTCTGGAGAAGTACTGTCGGCCGTGTTCCCGGGCCAAGTCTCTTGGAAAAGGGCAGCTG
AGAGGGTGAAACTCCCGTTCTTGCCTGGGAACATTGCGCTTTGGCATATACTTTCTACGAGTCGAGTTGCTTGGGATTGCA
GCTCAAATTTGGTGGTAAATTCCATCTAAAGCTAAATATTGGTGGGATACCGATAGTGCACAAGTACCGTGAGGGAAAGA
TGCAAAGAACTTTGAAAAGAGAGTTAAAGAGTACCTGAAATTGTTGAAAGGGAAGCGAAGGAAACCAGTGCCGAAGCTT
AGTCATACTTCTCTTACTACTTGTGGTAAGGGCGCTGTGGCTTTGCGTGGGTCAGCATCGGCTCTTTGCCTGGGATATATC
TTCAGTAGGTAGACGACCTCTTYG--GAGGTGAGTGCCTATTGTTGCTATTCC-GGGTTGGGCTGAGGTCAGTCACTC-
TGTGCTYGTGATG-CTGGCAAAATGGTTTTCTTTACCCCGTCTTGAAACACGGACCAAGGAG-------

>HE492-07_Thalassiosira_gravida
----AAGCATATAATTAAGCGGAGGAAAAGAAACTAACAA-
GGATTCCCCTAGTAACGGCGAGTGAAGCGGGATGAGCTCACCATGTGAATCTGTGTAACCGG----------
AAACGGTGCACCGAATTGTGGTCTGGAGAAGTACTGTCGGCCGTGTTCCCGGGCCAAGTCTCTTGGAAAAGGGCAGCTG
AGAGGGTGAAACTCCCGTTCTTGCCTGGGAACATTGCGCTTTGGCATATACTTTCTACGAGTCGAGTTGCTTGGGATTGCA
GCTCAAATTTGGTGGTAAATTCCATCTAAAGCTAAATATTGGTGGGATACCGATAGTGCACAAGTACCGTGAGGGAAAGA
TGCAAAGAACTTTGAAAAGAGAGTTAAAGAGTACCTGAAATTGTTGAAAGGGAAGCGAAGGAAACCAGTGCCGAAGCTT
AGTCATACTTCTCTTACTACTTGTGGTAAGGGCGCTGTGGCTTTGCGTGGGTCAGCATCGGCTCTTTGCCTGGGGTATATC
TTCAGTAGGTAGACGACCTCTTCG--GAGGTGAGTGCCTATTTTTGTTATTCC-GGGTTGGGCTGAGGTCAGTCACTC-
TGTGCTCGTGATG-CTGGCAAAATGGTTTTCTTTACCCCGTCTTGAA----------

>JQ995402_Thalassiosira_rotula
----------CGAGTGAAGCGGGATGAGCTCACCATGTGAATCTGTGTAACCGG----------
AAACGGTGCACCGAATTGTGGTCTGGAGAAGTACTGTCGGCCGTGTTCCCGGGCCAAGTCTCTTGGAAAAGGGCAGCTG
AGAGGGTGAAACTCCCGTTCTTGCCTGGGAACATTGCGCTTTGGCATATACTTTCTACGAGTCGAGTTGCTTGGGATTGCA
GCTCAAATTTGGTGGTAAATTCCATCTAAAGCTAAATATTGGTGGGATACCGATAGTGCACAAGTACCGTGAGGGAAAGA
TGCAAAGAACTTTGAAAAGAGAGTTAAAGAGTACCTGAAATTGTTGAAAGGGAAGCGAAGGAAACCAGTGCCGAAGCTT
AGTCATACTTCTCTTACTACTTGTGGTAAGGGCGCTGTGGCTTTGCGTGGGTCAGCATCGGCTCTTTGCCTGGGGTATATC
TTCAGTAGGTAGACGACCTCTTCG--GAGGTGAGTGCCTATTTTTGTTATTCC-GGGTTGGGCTGAGGTCAGTCACTC-
TGTGCTCGTGATG-CTGGCAAAATGGTTTTCTTTACCCCGTCTTGAAACACGGACCAAGGAG-------

>JQ995414_Thalassosira_gravida
----------CGGGATGAGCTCACCATGTGAATCTGTGTAACCGG----------
AAACGGTGCACCGAATTGTGGTCTGGAGAAGTACTGTCGGCCGTGTTCCCGGGCCAAGTCTCTTGGAAAAGGGCAGCTG
AGAGGGTGAAACTCCCGTTCTTGCCTGGGAACATTGCGCTTTGGCATATACTTTCTACGAGTCGAGTTGCTTGGGATTGCA
GCTCAAATTTGGTGGTAAATTCCATCTAAAGCTAAATATTGGTGGGATACCGATAGTGCACAAGTACCGTGAGGGAAAGA
TGCAAAGAACTTTGAAAAGAGAGTTAAAGAGTACCTGAAATTGTTGAAAGGGAAGCGAAGGAAACCAGTGCCGAAGCTT
AGTCATACTTCTCTTACTACTTGTGGTAAGGGCGCTGTGGCTTTGCGTGGGTCAGCATCGGCTCTTTGCCTGGGGTATATC
TTCAGTAGGTAGACGACCTCTTCG--GAGGTGAGTGCCTATTTTTGTTATTCC-GGGTTGGGCTGAGGTCAGTCACTC-
TGTGCTCGTGATG-CTGGCAAAATGGTTTTCTTTACCCCGTCTTGAAACACGGACCAAGGAG-------

>JQ995408.1_Shionodiscus_bioculatus
----------AGAGCTCACCATGTGAATCTGTGTAACCCG----------
CAAGGGTGCACCGAATTGTGGTCTGGAGAAGTATTGTCGGCCGTGTTCTCGGGCCAAGTCTCTTGGAAAAGGGCAGCTG
AGAGGGTGAAACTCCCGTTCTTGCCTGAGAACATTGCGCCTTGGCATATGCTTTCTACGAGTCGAGTTGCTTGGGATTGCA
GCTCAAATTTGGTGGTAAATTCCATCTAAAGCTAAATATTGGTGGGATACCGATAGTGCACAAGTACCGTGAGGGAAAGA
TGCAAAGAACTTTGAAAAGAGAGTTAAAGAGTACCTGAAATTGTTGAAAGGGAAGCGAAGGAAACCAGTGCCGAAGCTT
ATTCATACTTCTCTTGCTACTTGTGGTAAGGGCGCTGTGGATTTGCATGGGTCAGCATCGGCTCTTCGCCTGGGATATATC
TTTAGTGGGTAGACGACCTCTTCG--GAGGTGAGTGCCCATTATTGCTATTCT-GGGTTGGGCTGAGGTCAGTCACTC-
TGTGCTCGTGATG-CTGGCAAAATGGTTTTCTTTACCCCGTCTTGAAACACGGACCAAGGAGTCTAACA

>KT692948.1_Bacterosira_constricta
ATTTAAGCATATAATTAAGCGGAGGAAAAGAAACTAACAA-
GGATTCCCCTAGTAACGGCGAGTGAAGCGGGAAGAGCTCACCATGTGAATCTGTGTAACCCG----------
CAAGGGTGCACCGAATTGTGGTCTGGAGAAGTATTGTCGGCCGAATTTCCGGGCCAAGTCTCTTGGAAAAGGGCAGCTG
AGAGGGTGAAACTCCCGTTCTTGCCTGGAAATTTTGCGCCTTGGCATATGCTTTCTATGAGTCGAGTTGCTTGGGATTGCA
GCTCAAATTTGGTGGTAAATTCCATCTAAAGCTAAATATTGGTGGGATACCGATAGTGCACAAGTACCGTGAGGGAAAGA
TGCAAAGAACTTTGAAAAGAGAGTTAAAGAGTACCTGAAATTGTTGAAAGGGAAGCGAAGGAAACCAGTGCCGAAGCTT
AGTCATATTTCTCTTGCTACTTGTGGCAAGGGCGCTGTGGCTTTGCATGGGTCAGCATCGACTCTTCGCCTGGGGTAAATC
TTCGGTTGGTAGACGGCCCTATTA-TGGGGTGAGTGCCTTCCGTTGCTATCCT-GGGTTGGGTCGAGGTCAGTCACTC-
TGTGCTCGTGATG-CTGGCAAAATGGTTTTCTTTACCCCGTCTTGAAACACGGACCAAGGAGTCTAACA

>JQ995428.1_Thalassiosira_nordenskioeldii
----------GTGAACCGGGAAGAGCTCACCATGTGAATCTGCGTAACCTT----------
----C--
GGGTGCGCCGAATTGTGGTCTGGAGAAGTATTGTCGGCCGAGTTTCCGGGCCAAGTCTCTTGGAAAAGGGCAGCTGAGA
GGGTGAAACTCCCGTTCTTGCCTGGAAACTTTGTGTCATGGCACATGCTTTCTACGAGTCGAGTTGCTTGGGATTGCAGCT
CAAATTTGGTGGTAAATTCCATCTAAAGCTAAATATTGGTGGGATACCGATAGTGCACAAGTACCGTGAGGGAAAGATGC
AAAGAACTTTGAAAAGAGAGTTAAAGAGTACCTGAAATTGTCAAAAGGGAAGCGAAGGAAACCAGTGCCGAAGCTTTGT
CATACTTCTCTTGCTACTTGTGGTAAGGGCGCTGTGGCATTGCGTGGGTCAGCATCGGCTCTTTGCCTGGGGTATATCTTC
GGTTGGTAGACGACACCTTCG--GGTGTGAGTGCCTTCTGTTGCTATCCT-GGGTGGGGCTGAGGTCAGTCACTC-
TGTGCTCGTGATG-CTGGCAAAATGGTTTTCTTTACCCCGTCTTGAAACACGGACCAAGGAGTCTAACA

>FR823449.1_Skeletonema_marinoi
-----AGCATATAATTAAGCGGAGGAAAAGAAACTAACAA-
GGATTCCCCTAGTAACGGCGAGTGAAGCGGGATGAGCTCACCATGTGAATCTGCGCAACCTG----------
CAAAGGTGCGCCGAATTGTGGTCTGAAGAAGTATTGTCGGCCGCGAATCCGGGCCAAGTCTCTTGGAAAAGGGCAGCTG
AGAGGGTGAAACTCCCGTTCTTGCCTGGAATCGTTGCGCTCTGGCACATGCTTTCTACGAGTCGAGTTGCTTGGGATTGCA
GCTCAAATTTGGTGGTAAATTCCATCTAAAGCTAAATATTGGTGTGACACCGATAGTGTACAAGTACCGTGAGGGAAAGA
TGCAAAGAACTTTGAAAAGAGAGTTAAAGAGTACCTGAAATTGTTAAAAGGGAAGCGAAGGAAACCAGTGTA-
AAGCGAAGCCATTCTTCCTAAGCCACTTGTGGTTTGGGCGCTGTGGTTAGCTGT--ACTAATTCTGGGCTTGA-
TCTGGGGCAAACGTTTAGTGAGTAGACGACTCTTC----GGAGTGAGTGCTCACTTTTCATATCCT-
GGGTCGGGCTGAGGTCAGTCACTC-
TGTGCTCGTGATGAATTAGAAAATGGTTTTCTTTACCCCGTCTTGAAACACGGACCAAGGAGTCTAACA

>LC258389.1_Skeletonema_menzelii
ATTTAAGCATATAATTAAGCGGAGGAAAAGAAACTAACAA-
GGATTCCCCTAGTAACGGCGAGTGAAGCGGGATGAGCTCACCATGTGAATCTGCGCAACCAG----------
CAATGGTGCGCCGAATTGTGGTCTGAAGAAGTATTGTCGGCCGCGAATCCGGGCCAAGTCTCTTGGAAAAGGGCAGCTG
AGAGGGTGAAACTCCCGTTCTTGCCTGGATTTGTTGCGCTCTGGCACATGCTTTCTACGAGTCGAGTTGCTTGGGATTGCA
GCTCAAATTTGGTGGTAAATTCCATCTAAAGCTAAATATTGGTGGGACACCGATAGTGTACAAGTACCGTGAGGGAAAGA
TGCAAAGAACTTTGAAAAGAGAGTTAAAGAGTACCTGAAATTGTTAAAAGGGAAGCGAAGGAATCCAGTGTA-
AAGCGAAGCCATTCTTCTCAAGCCACTTGTGGTTTGGGCGCTGTGGTTAGCTGT--ACTAATTCTGGGCTTGA-
CTTGGGGCAAACGTTTAGTGAGTAGACGACCCTTC----GGGGTGAGTGCTCACTTTTCATGTTCT-
GGGTCGGGCTGAGGTCAGTCACTC-
TGTGCTCGTGATGAATTAGGAAATGGATTTCTTTACCCCGTCTTGAAACACGGACCAAGGAGTCTAACA

>JQ995412.1_Eucampia_groenlandica
----------TAGTAAGGGCGACTGAAGCAGGAAAAGCTCACCTTGTGAATCTATACACT----------
----
AGTTGTATCGAATTGTGGTCTGTAGAAGTATTGTCTGTCGCGGTCCTGGATTAAGTAGCCTGGAAAGGCTCAGCAGAGAG
GGTGAGACTCCCGTTCTTGTCTAGG-
ATCGTTGGCTTTAGCACATGCTTTCAACGAGTCGAGTTGTTTGGGATTGCAGCTCAAAGTGGGTGGTAAATTCCATCTAAA
GCTAAATACTGGCATGAGACCGATAGCGTACAAGTACCGTGAGGGAAAGATGCAAAGAACTTTGAAAAGAGAGTTAAAG
AGTACCTGAAATTGCTGAAAGGGAAGCGAAGGAAACCAGTGTC-
AGATTTGCCTGTATTTCCTCTATCTGTCAAGAGAGAGGCGCTGTGGGTATATCTGGGCCAGCATCTGTTTGAT--
TCTAAACAAATTGCTTGTAAGGAGGTAGGTTCTTCG--GAACCAATGACTTACTTGTGTTGTTTA-
GGATTGGACAGAGGACAGTCGTTA-TGCGATCGTGATG-
CTGGCAAAATGGTTTTCTTTACCCCGTCTTGAAACACGGACCAAGGAGTCTAACA

>JQ995430.1_Eucampia_groenlandica
----------CTAGTAAGGGCGACTGAAGCAGGAAAAGCTCACCTTGTGAATCTATACACT----------
AGTTGTATCGAATTGTGGTCTGTAGAAGTATTGTCTGTCGCGGTCCTGGATTAAGTAGCCTGGAAAGGCTCAGCAGAGAG
GGTGAGACTCCCGTTCTTGTCTAGG-
ATCGTTGGCTTTAGCACATGCTTTCAACGAGTCGAGTTGTTTGGGATTGCAGCTCAAAGTGGGTGGTAAATTCCATCTAAA
GCTAAATACTGGCATGAGACCGATAGCGTACAAGTACCGTGAGGGAAAGATGCAAAGAACTTTGAAAAGAGAGTTAAAG
AGTACCTGAAATTGCTGAAAGGGAAGCGAAGGAAACCAGTGTC-
AGATTTGCCTGTATTTCCTCTATCTGTCAAGAGAGAGGCGCTGTGGGTATATCTGGGCCAGCATCTGTTTGAT--
TCTAAACAAATTGCTTGTAAGGAGGTAGGTTCTTCG--GAACCAATGACTTACTTGTGTTGTTTA-
GGATTGGACAGAGGACAGTCGTTA-TGCGATCGTGATG-
CTGGCAAAATGGTTTTCTTTACCCCGTCTTGAAACACGGACCAAGGAGTCTAACA